NEW DEVELOPMENTS IN 1D LAKE MODELS: TREATMENT OF INTERNAL MOTIONS AND MIXING, BIOGEOCHEMISTRY OF GREENHOUSE GASES

Victor Stepanenko[1,2,3]

[1]*Lomonosov Moscow State University, Research Computing Center*
[2]*Lomonosov Moscow State University, Faculty of Geography*
[3]*Moscow Center of Fundamental and Applied Mathematics*

Brescia University, 21 May 2021

Lectures in Brescia

Tuesday 18/5/2021 13.45-15.30

"1D lake modeling: concepts, examples, applications"

This seminar is aimed at introducing e basic concepts of process-based modeling of lakes with emphasis on 1D models, pointing out capabilities and limitations, classical and new applications in limnology and climate sciences. Most examples are given for 1D LAKE model, developed in Moscow State University

Friday 21/5/2021 14.30-16.30

"New developments in 1D lake models: treatment of internal motions and mixing, biogeochemistry of greenhouse gases"

This lecture is devoted to specific novel extentions of classical 1D formulations implemented in LAKE model including treatment of basin-scale internal waves), throughflow in artificial reservoirs, sediment and in-water biogeochemistry of greenhouse gases. The prospects of new studies are outlined.

Outline

- General remarks on the lake physics
- Basics of 1D approach
- Basics on greenhouse gases in lakes
- Case studies with greenhouse gases modeling
- Modeling greenhouse gases in artificial reservoirs
- Internal gravitational and inertial waves in lakes
- Parameterizations of seiching in 1D models
- 1D vs 3D models
- 1½ D simulations of Lake Iseo seiching case

Vertical structure of a stratified lake

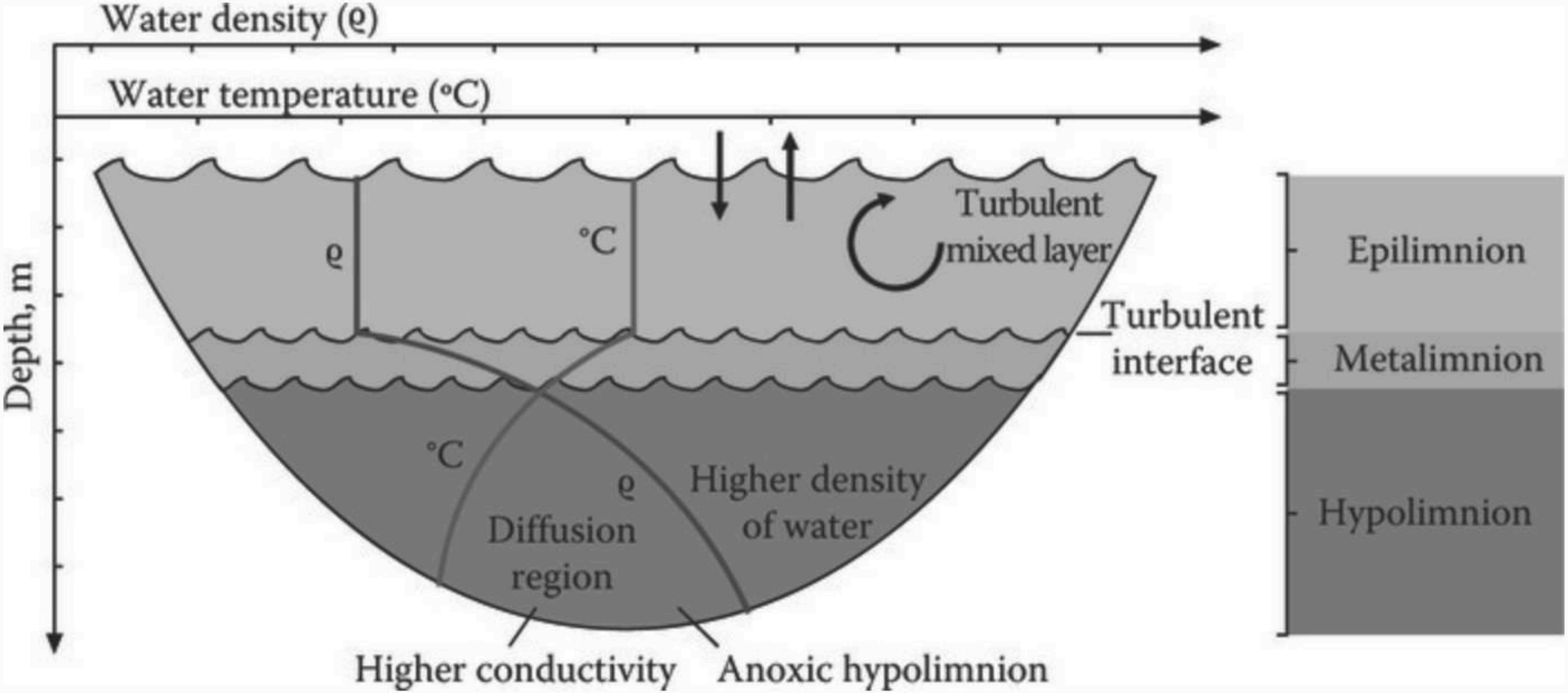

Figure 3.5 (See color insert.) Vertical structure of a stratified lake and its physical and chemical features (Original Degani and Tundisi 2011.).

Complex mixing processes in lakes

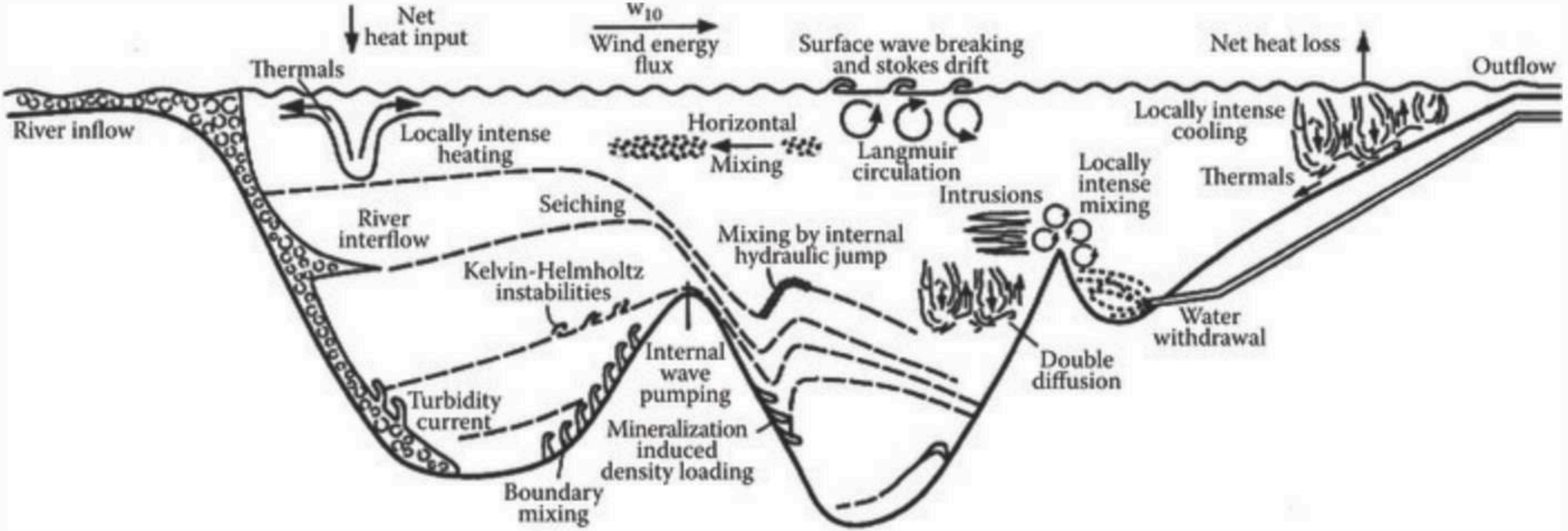

Figure 3.6 Complex mixing processes in lakes. (From Imboden, D.M. and Wuest, A., Mixing mechanisms in lakes, in: Lerman, A., Imboden, D., and Gat, J. (Eds.), Physics and Chemistry of Lakes, Springer-Verlag, Berlin, Germany, pp. 83–138, 1995.)

What is seiching?

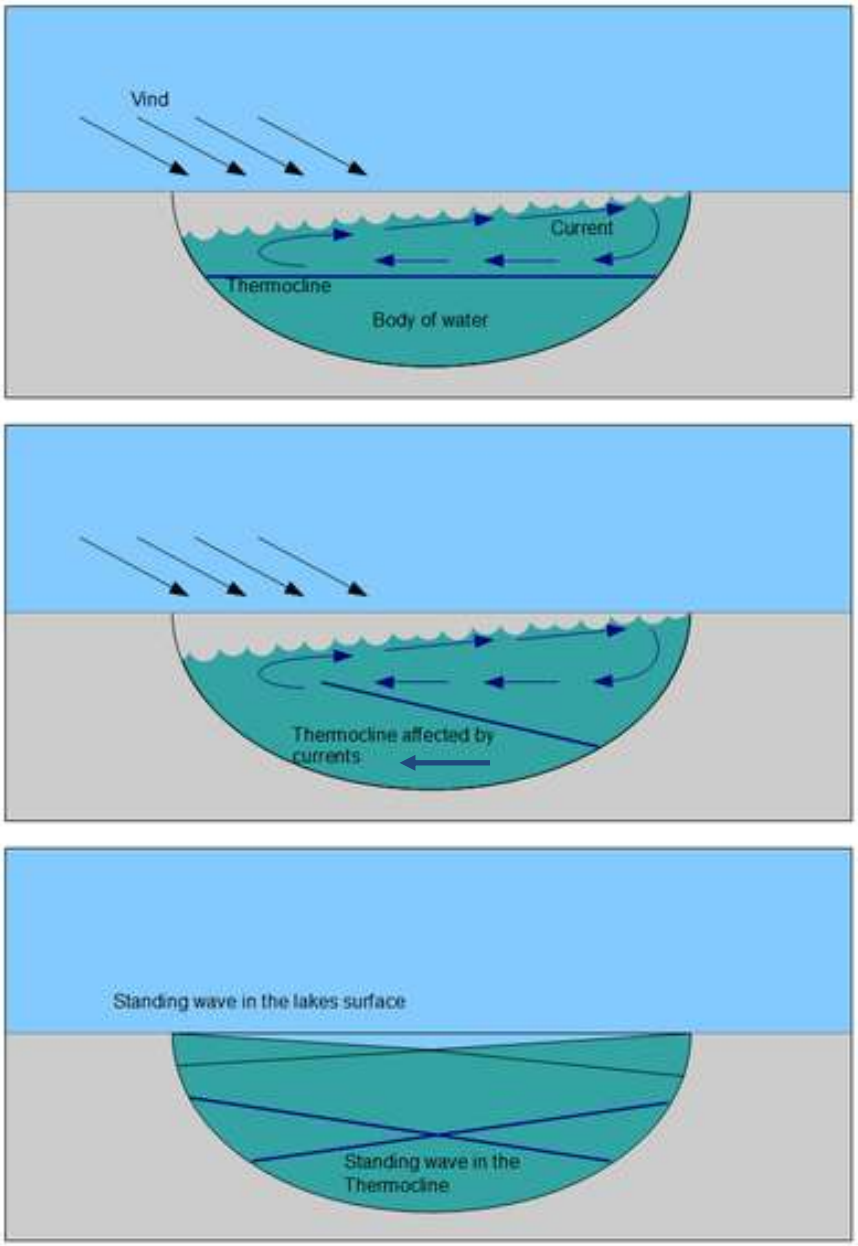

Boundary layers in lakes

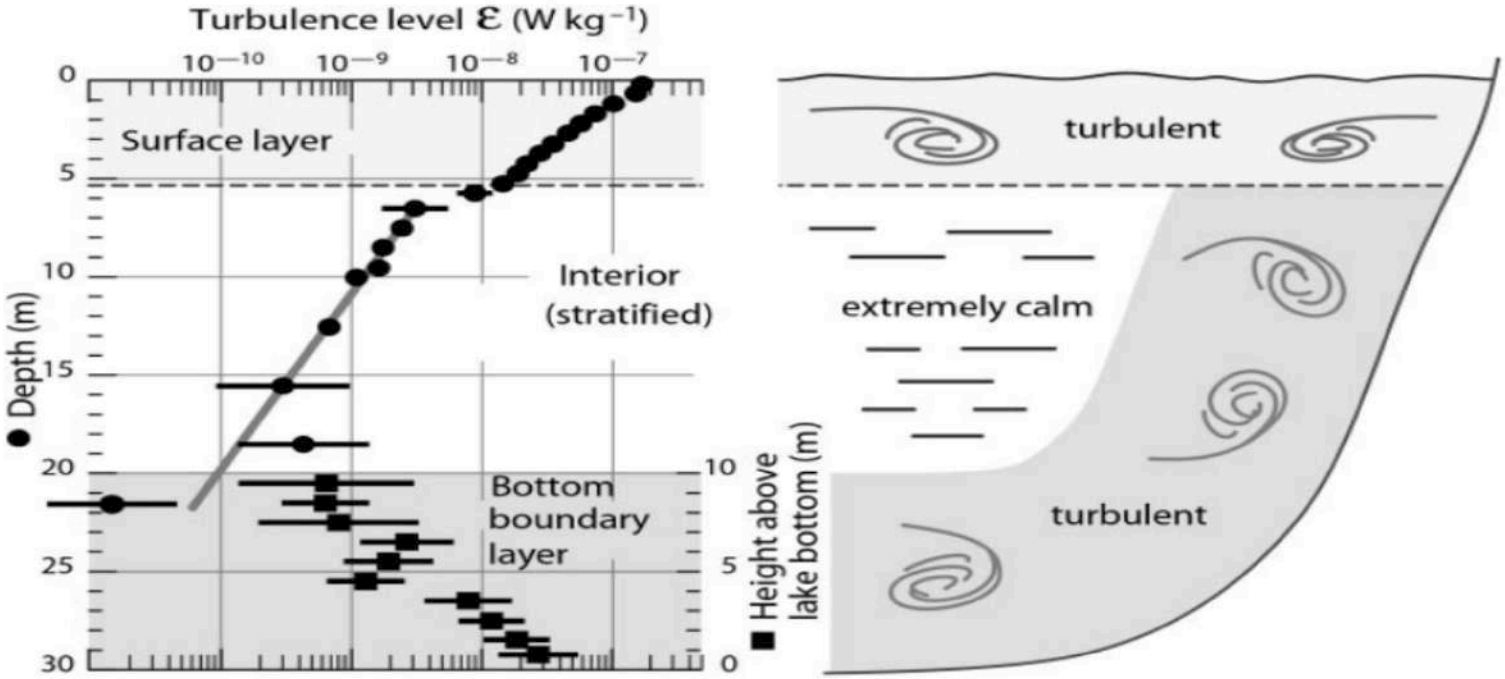

- the top mixed layer is eplimimnion: TKE is produced there by velocity shear caused by wind stress
- intermediate layer is metalimnion (thermocline): extremely stably stratified
- the lowest layer is hypolimnion: TKE is produced by velocity shears induced by internal lake motions (seiches, Kelvin and Poincare waves)

Wüest and Lorke 2003, Annu.Rev.Fluid Mech.

Hierarchy of lake models by dimensionality

- **3D models** (Reynolds equations in Boussinesq approximation)

$$\frac{\partial \overline{u}_i}{\partial t} + \frac{\partial \overline{u}_i \overline{u}_j}{\partial x_j} = -\frac{1}{\rho_0}\frac{\partial \bar{p}}{\partial x_i} - \delta_{i3} g \frac{\bar{\rho}}{\rho_0} - \frac{\partial \overline{u_i' u_j'}}{\partial x_j} - 2(\boldsymbol{\Omega} \times \overline{\boldsymbol{u}})_i + \nu \nabla^2 \overline{u}_i,$$

$$\frac{\partial \overline{u}_i}{\partial x_i} = 0,$$

$$\frac{\partial \bar{T}}{\partial t} + \frac{\partial \bar{T} \overline{u}_j}{\partial x_j} = -\frac{\partial \overline{T' u_j'}}{\partial x_j} - \frac{1}{\rho_o c_p}\frac{\partial \bar{F}_j}{\partial x_j}$$

- **2D models** – 3D equations are averaged in horizontal or vertical plane
- **1½ D models** – vertical transports are resolved, horizontal processes are resolved partially
- **1D models** – only vertical processes are simulated
- **½ D models** – vertical processes are simulated in simplified way (not explicitly)
- **0 D (bulk) models** – obsolete

LAKE model physics

- 1D heat and momentum equations
- $k - \epsilon$ turbulence closure
- Monin-Obukhov similarity for surface fluxes
- Beer-Lambert law for shortwave radiation attenuation
- Momentum flux partitioning between wave development and currents (Stepanenko et al., 2014)
- Soil heat and moisture transfer including phase transitions
- Multilayer snow and ice models

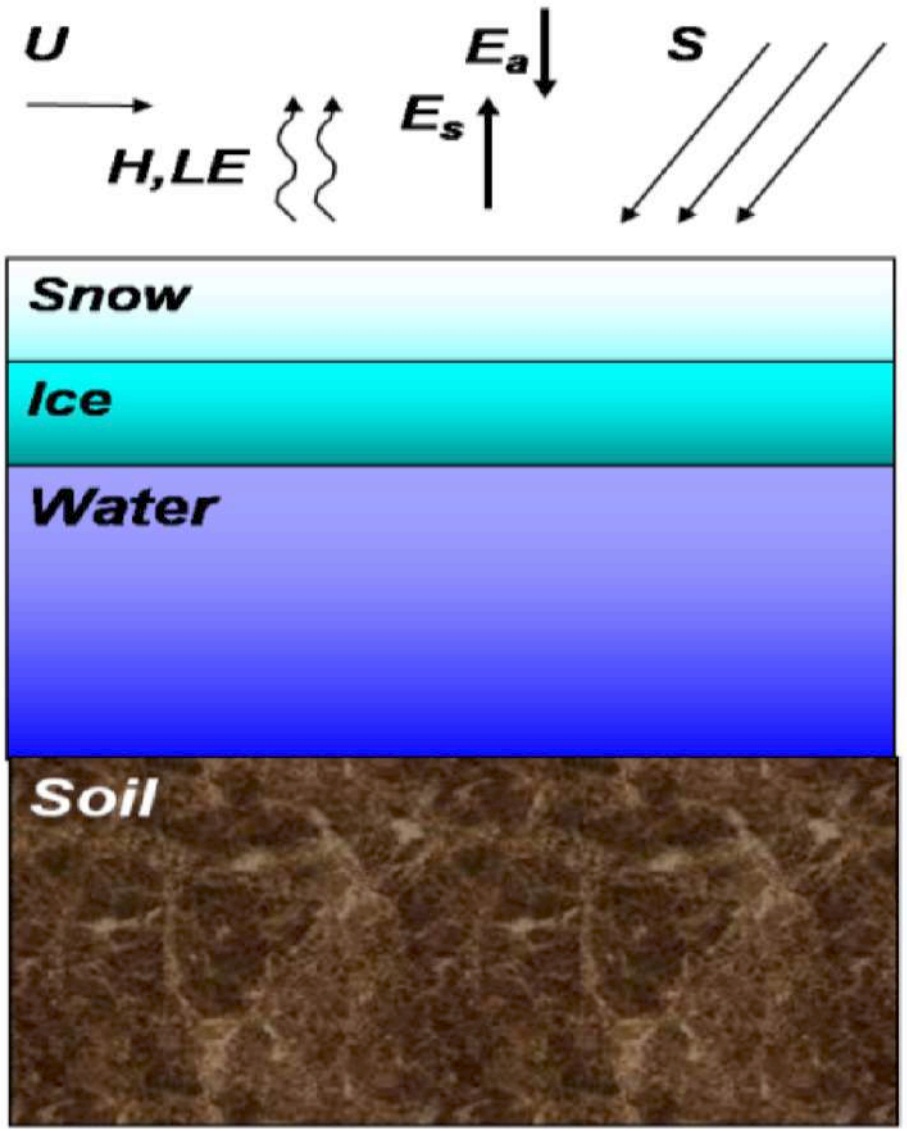

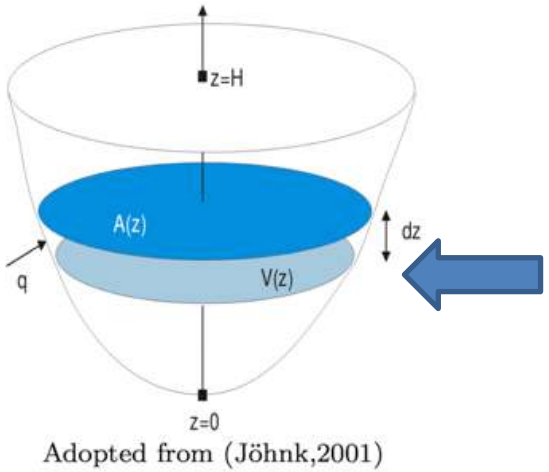

Adopted from (Jöhnk,2001)

A general procedure of horizontal averaging allows to take into account **heat and gas fluxes at the sloping bottom**

LAKE model

Velocity components and scalars in incompressible fluid are governed by equations of the form:

$$c\frac{\partial f}{\partial t} = -c\frac{\partial u_i f}{\partial x_i} - \frac{\partial F_i}{\partial x_i} + R_f(f, ...),$$

Avegaring over the horizontal cross-section $A(z)$:

$$\overline{f} = \frac{1}{A(z)} \int_{A(z)} f dx dy.$$

Assuming small slopes, $\overline{w} = 0$, yields:

$$c\frac{\partial \overline{f}}{\partial t} = \underbrace{-\frac{c}{A}\int_{\Gamma_{A(z)}} f(\mathbf{u_h}\cdot\mathbf{n})dl}_{\text{Inlets and outlets}} + \underbrace{\frac{1}{A}\frac{\partial}{\partial z}\left(Ak_f\frac{\partial \overline{f}}{\partial z}\right)}_{\text{Vertical diffusion}} -$$

$$\underbrace{-\frac{1}{A}\frac{\partial A\overline{F_{nz}}}{\partial z}}_{\text{Div. of non-diffusion flux}} \underbrace{+\frac{1}{A}\frac{dA}{dz}[F_{nz,b}(z) + F_{tz,b}(z)]}_{\text{Bottom flux}} \underbrace{+R_f(\overline{f}, ...)}_{\text{Sources}}.$$

Here, F_{tz} – vertical turbulent flux, F_{nz} – vertical non-turbulent flux of variable f.

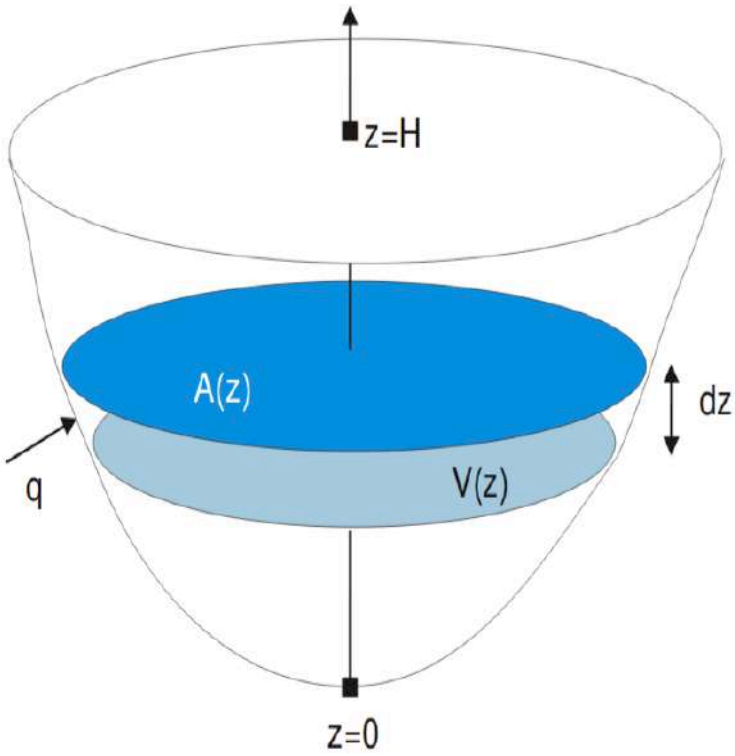

Adopted from (Jöhnk,2001)

1D equations for enclosed basins

Horizontally-averaged 3D equations for basic prognostic quantities:

$$c_w \rho_w \frac{\partial \overline{T}}{\partial t} = \cdots \frac{1}{A}\frac{\partial}{\partial z}\left(A\left(\lambda_m + c_w \rho_w \nu_T\right)\frac{\partial \overline{T}}{\partial z}\right) -$$

$$- \frac{1}{A}\frac{\partial A\overline{S}}{\partial z} + \frac{1}{A}\frac{dA}{dz}[S_b + F_{T,b}(z)], \quad \text{– heat conservation equation} \qquad (7)$$

$$\frac{\partial \overline{u}}{\partial t} = \cdots \overline{-\left(\frac{1}{\rho_w}\frac{\partial p}{\partial x}\right)} + \frac{1}{A}\frac{\partial}{\partial z}\left(A(\nu + \nu_m)\frac{\partial \overline{u}}{\partial z}\right) +$$

$$+ \frac{1}{A}\frac{dA}{dz}F_{u,b}(z) + f\overline{v}, \quad \text{– momentum equation for x-speed component} \qquad (8)$$

$$\frac{\partial \overline{v}}{\partial t} = \cdots \overline{-\left(\frac{1}{\rho_w}\frac{\partial p}{\partial y}\right)} + \frac{1}{A}\frac{\partial}{\partial z}\left(A(\nu + \nu_m)\frac{\partial \overline{v}}{\partial z}\right) +$$

$$+ \frac{1}{A}\frac{dA}{dz}F_{v,b}(z) - f\overline{u} \quad \text{– momentum equation for y-speed component} \qquad (9)$$

$1D^+$ framework

Traditional 1D model concept

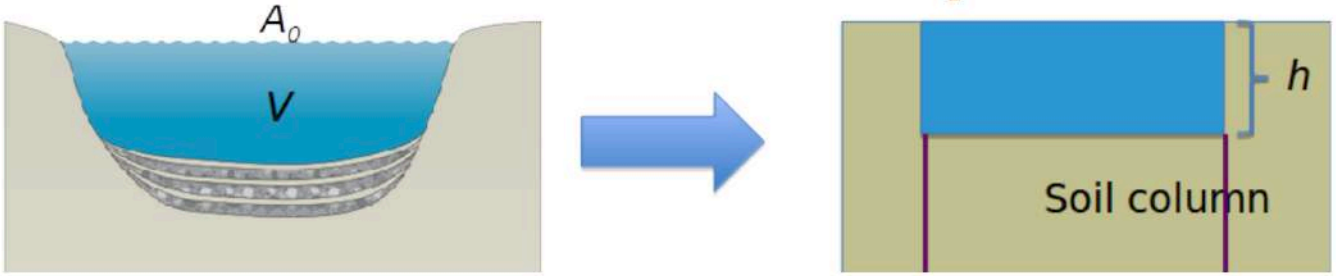

$1D^+$ model concept

- $1D^+$ model includes friction, heat and mass exchange at the lateral boundaries
- Heat, moisture and gas transfer are solved for each soil column independently

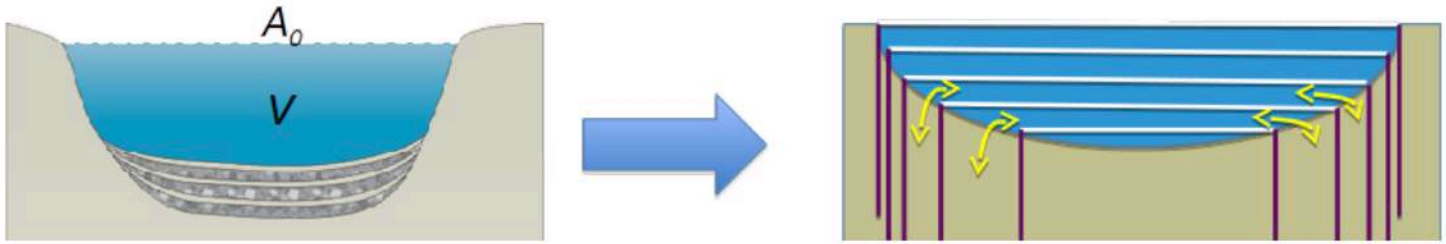

In $1D^+$ model horizontally averaged quantity f obeys the equation:

$$\frac{\partial f}{\partial t} = \frac{1}{A}\frac{\partial}{\partial z}\,A\,k_f\frac{\partial f}{\partial z} + F(z,t,f,A) + H_f\frac{1}{A}\frac{dA}{dz}.$$

Coupling heat transport in water and soil

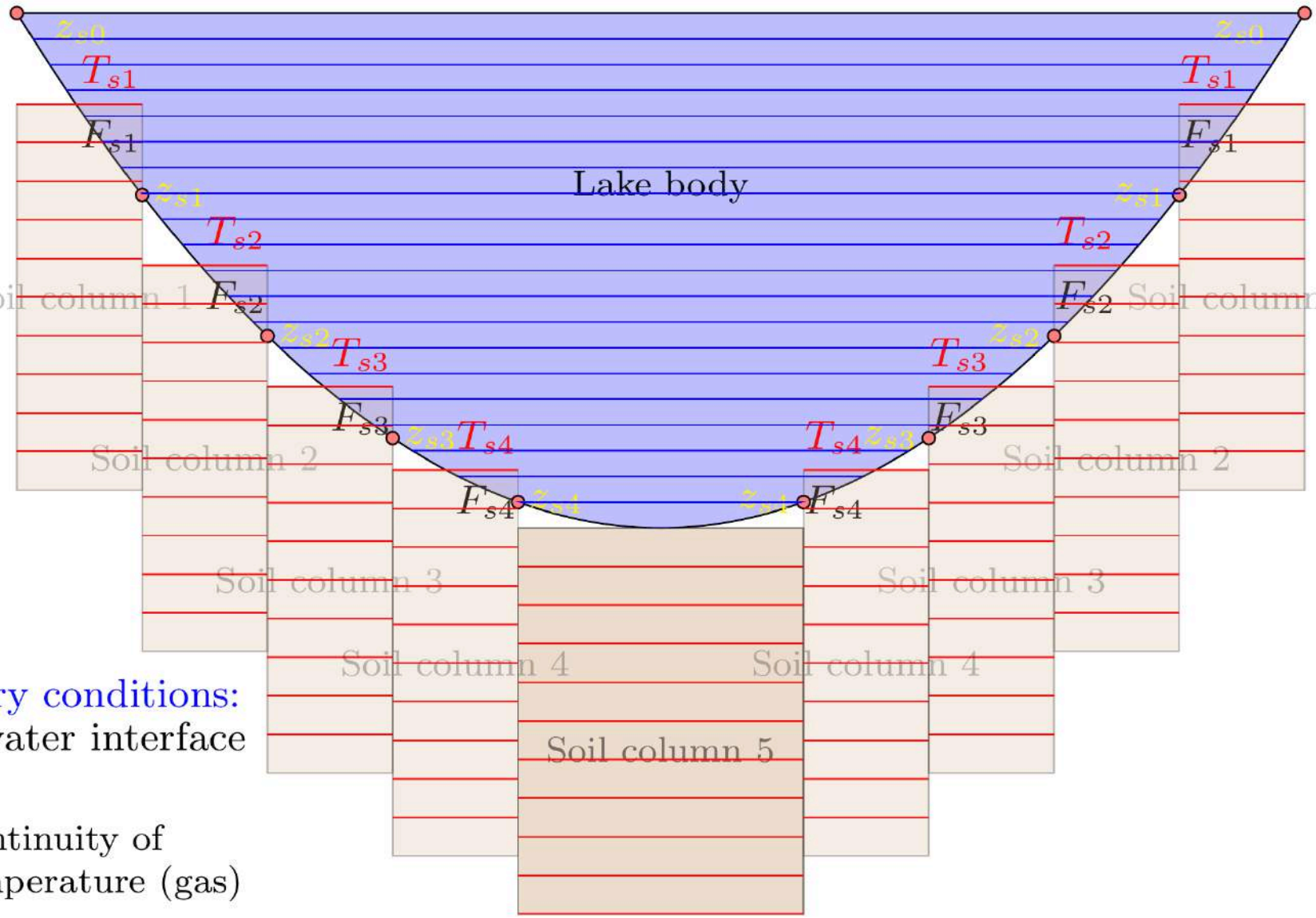

Boundary conditions:
at soil-water interface

- Continuity of temperature (gas)
- Continuity of flux

$k-\epsilon$ turbulence closure

$$\overline{w'\phi'} = -k_\phi \frac{\partial \bar{\phi}}{\partial z}$$

- counter-gradient effects missing

Kolmogorov formula (1942)

$$k_M = C_e \frac{E^2}{\varepsilon}, \qquad C_e = C_e(M,N)$$

$$k_T = k_S = C_{eT} \frac{E^2}{\varepsilon}, \quad C_{eT} = C_{eT}(M,N)$$

M – friction frequency,
N – Brunt-Vaisala frequency

stability functions

k-ε parameterization

$$\frac{\partial E}{\partial t} = \frac{\partial}{\partial z}\left(\nu + \frac{k_M}{\sigma_E}\right)\frac{\partial E}{\partial z} + P + B - \varepsilon$$

$$\frac{\partial \varepsilon}{\partial t} = \frac{\partial}{\partial z}\left(\nu + \frac{k_M}{\sigma_\varepsilon}\right)\frac{\partial \varepsilon}{\partial z} + \frac{\varepsilon}{E}\left(c_{1\varepsilon}P + c_{3\varepsilon}B - c_{2\varepsilon}\varepsilon\right)$$

Boundary conditions

$$-\frac{k_M}{\sigma_E}\frac{\partial E}{\partial z} = c_{we}\left(\frac{\tau_s}{\rho_w}\right)^{3/2}, \quad c_{we} \approx 100$$

$$-\frac{k_M}{\sigma_\varepsilon}\frac{\partial \varepsilon}{\partial z} = \left(C_e^0\right)^{3/4}\frac{k_M}{\sigma_\varepsilon}\frac{E^{3/2}}{\kappa\left(z'+z_0\right)^2}$$

The model of sediments

Soil heat and moisture transfer are governed by diffusion, gravity infiltration, runoff, root uptake and phase transitions:

$$\rho c \frac{\partial T}{\partial t} = \frac{\partial}{\partial x} \lambda_T \frac{\partial T}{\partial z} + \rho_d \left(L_i F_i - L_v F_v \right), T - \text{temperature}$$

$$\frac{\partial W}{\partial t} = \frac{\partial}{\partial z} \left[\lambda_W \left(\frac{\partial W}{\partial z} + \delta \frac{\partial T}{\partial z} \right) \right] + \frac{\partial \gamma}{\partial z} - F_i - F_v - R_f - R_r, W - \text{moisture}$$

$$\frac{\partial V}{\partial t} = \frac{\partial}{\partial z} \lambda_V \frac{\partial V}{\partial z} + F_v, V - \text{vapour}$$

$$\frac{\partial I}{\partial t} = F_i . I - \text{ice}$$

Thermal regime of sediments, including freezing/thawing is important for modeling biogeochemical processes, especially, CH4

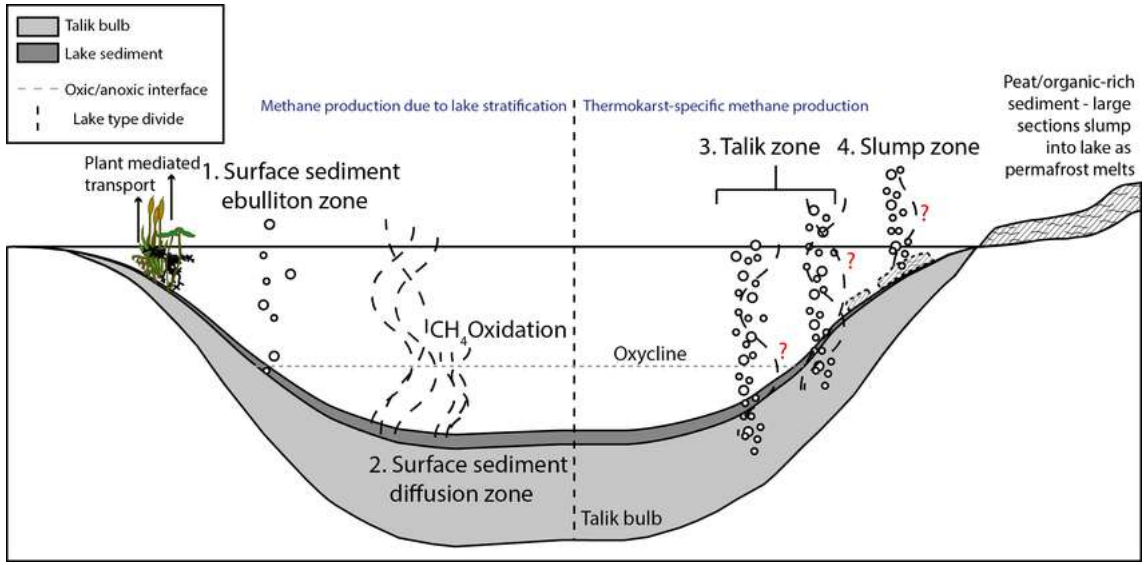

Lake-atmosphere continuum

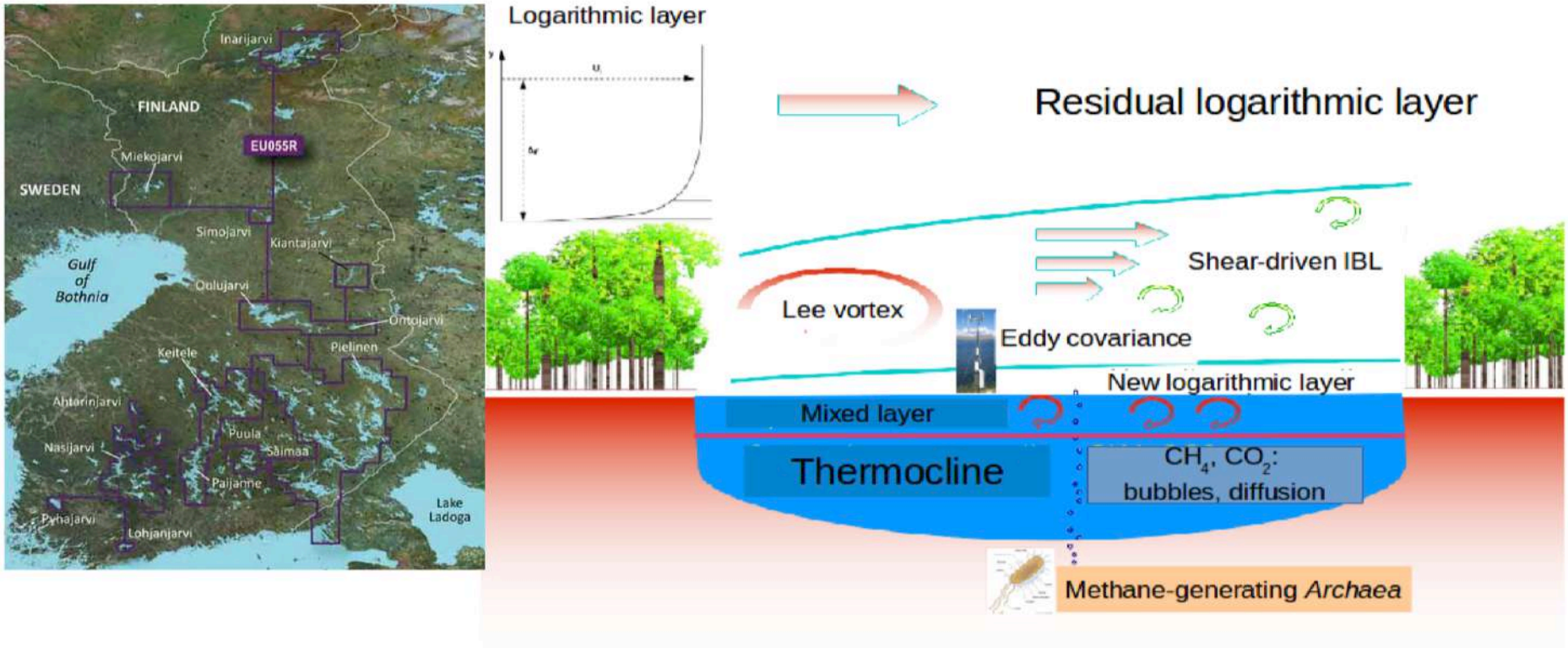

- Lakes are abundant in a number of regions, including Finland, Karelia, Siberia, Canada, China (famous for artificial reservoirs), **often surrounded by forested landscapes**
- Inland waters are currently included as **a separate tile** in many NWP and climate models, represented by 1D vertical heat transfer schemes
- **Efficient parameterizations** are needed to reproduce energy, momentum and gas exchange between “lake-forest” landscapes and the atmosphere
- **Highly-coupled problem** including in-lake and ABL processes

(Tranvik et al. 2009)

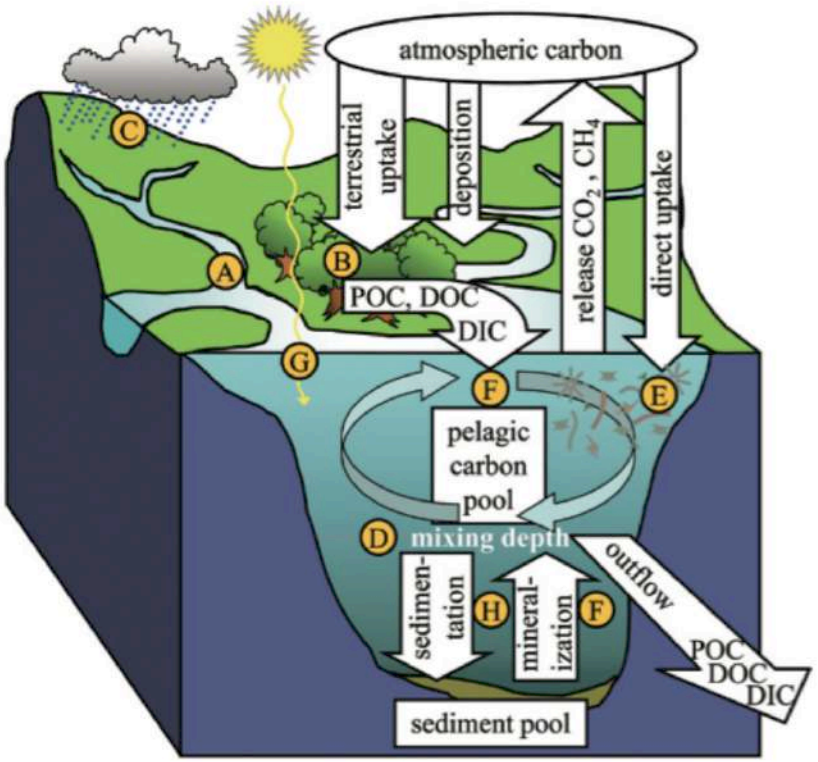

Fig. 2. Schematic diagram showing pathways of carbon cycling mediated by lakes and other continental waters. The letters correspond to rows in Table 1.

(Bastviken et al. 2011)

Latitude	Fluxes: Total open water Emiss.	n	CV	Ebullition Emiss.	n	CV	Diffusive Emiss.	n	CV	Stored Emiss.	n	CV	Area (km^2)
						Lakes							
>66°	6.8	17	72	6.4	17	74	0.7	60	37				288,318
>54°–66°	6.6	5	155	9.1	9	60	1.1	271	185	0.1	217	2649	1,533,084
25°–54°	31.6	15	127	15.8	15	177	4.8	33	277	3.7	36	125	1,330,264
<24°	26.6	29	51	22.2	28	54	3.1	29	97	21.3	1		585,536*
						Reservoirs							
>66°	0.2†												35,289
>54°–66°	1.0	24	176	1.8	2	140	0.2	4	93				161,352
25°–54°	0.7‡												116,922
<24°	18.1	11	87										186,437
						Rivers							
>66°	0.1	1											38,895
>54°–66°	0.2†												80,009
25°–54°	0.3	20	302										61,867
<24°	0.9‡												176,856
Sum open water	93.1	116		55.3	71		9.9	397		25.1	254		
Plant flux	10.2												
Sum all	103.3												

- Total freshwater methane emission is 104 Tg yr^{-1}, i.e. 50% of global wetland emission (177-284 Tg yr^{-1}, IPCC, 2013)
- greenhouse warming potentials from freshwater-originating CO_2 and CH_4 are roughly equal

CO_2 emissions by lakes and rivers

Raymond et al., 2013, Nature

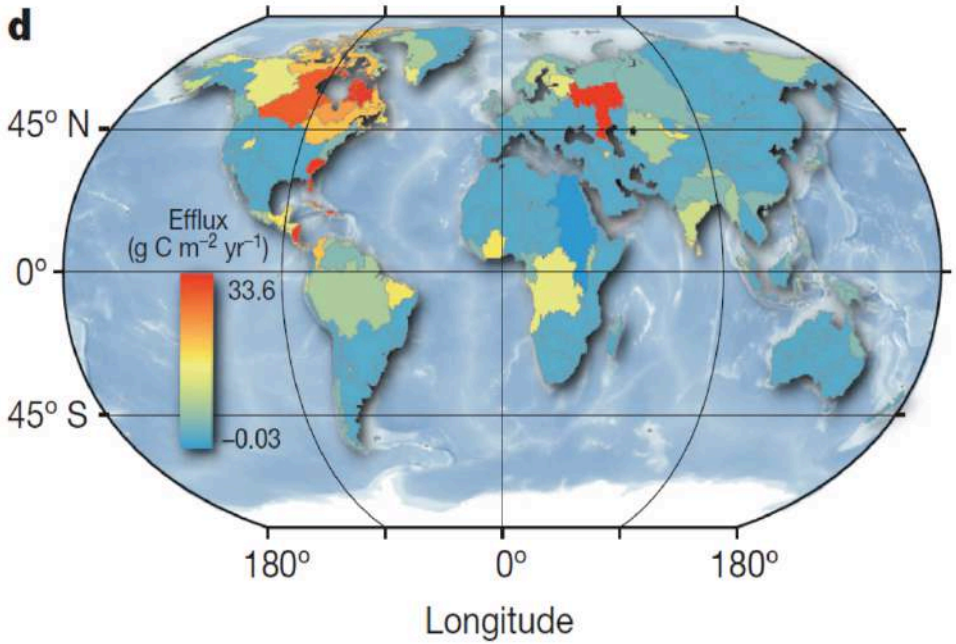

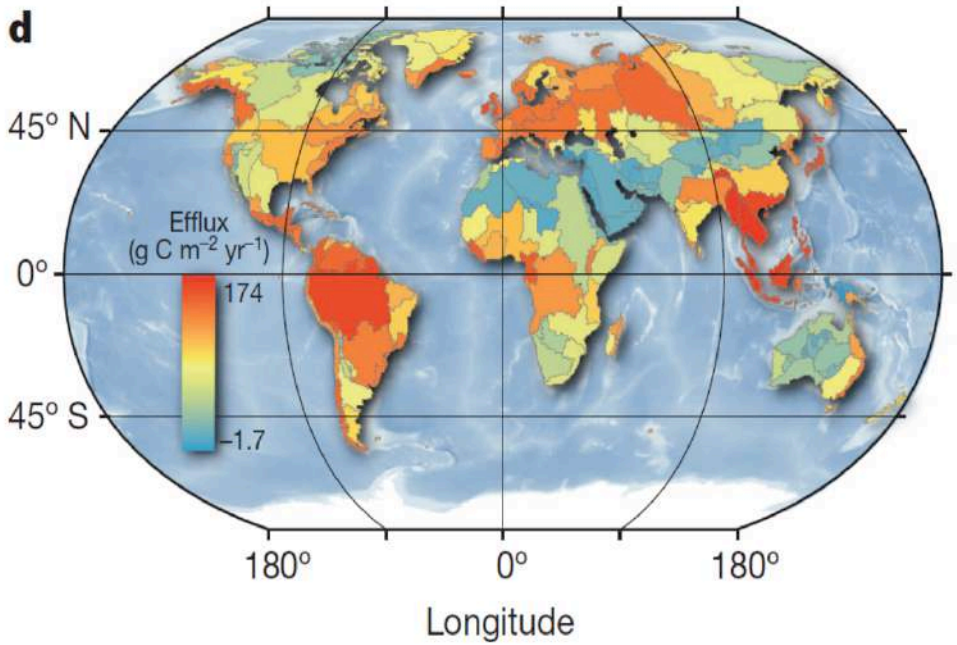

Lakes

Rivers

- global emission of CO_2 by freshwaters is 2.1 Pg C yr^{-1}
- lake emission is 0.3 Pg C yr^{-1}, river emissions is 1.8 Pg C yr^{-1}
- significant contribution of Volga hydropower reservoirs

Methane production, consumption, transport and emission in lakes

(Bastviken et al., 2004)

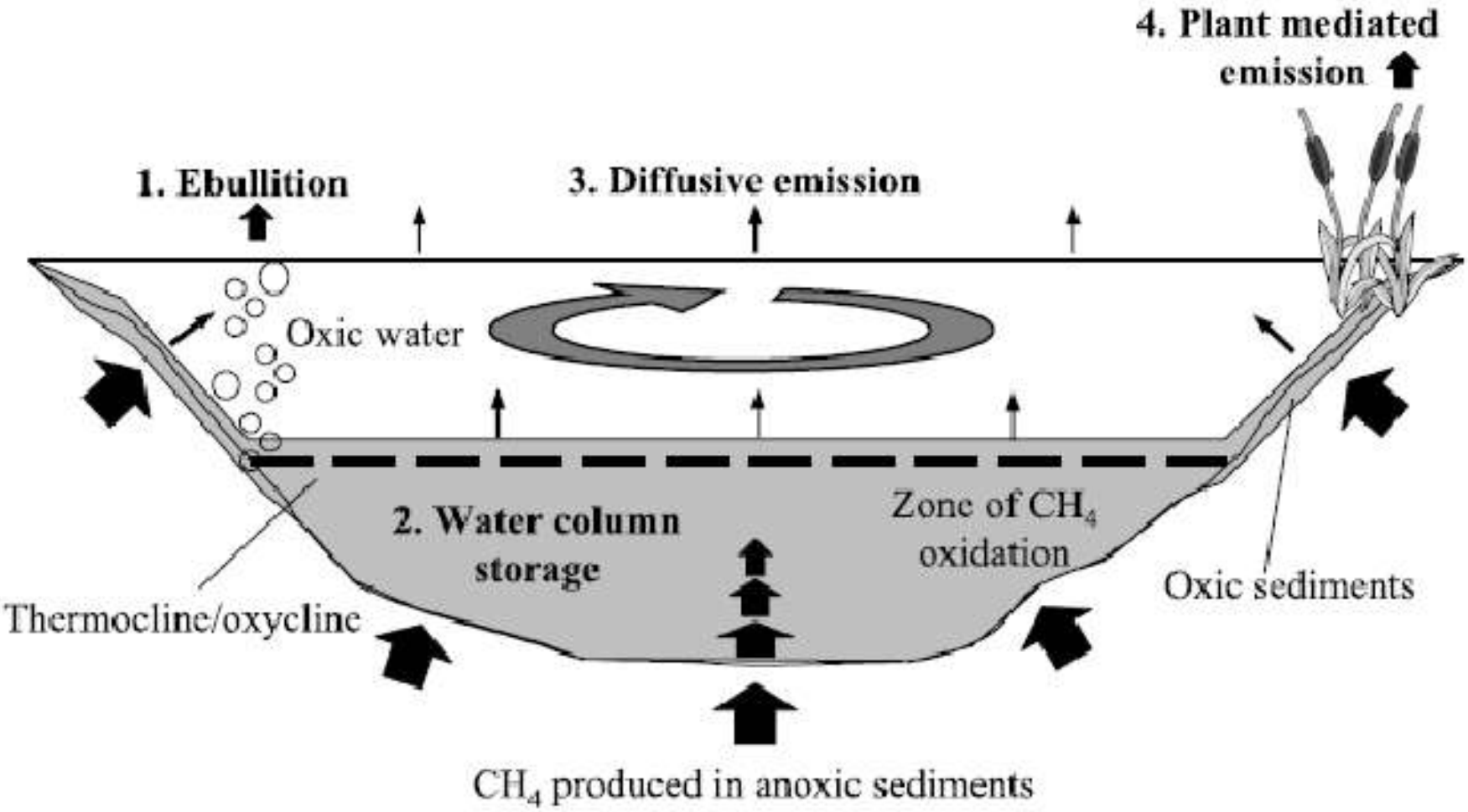

CH_4 and CO_2 production and vertical transport in a lake

Vertical gas transport mechanisms:

- Ebullition
- Surface mixed-layer turbulence → driven by wind forcing and surface heat balance
- Thermocline → very strong stratification with intermittent turbulence. Possible mixing mechanisms are K-H instability, nonlinear wave breaking, and marginal shear induced by seiches.
- Hypolimnion → governed by gravity currents and seiche-induced turbulence

Typical summer stratification in a temperate lake

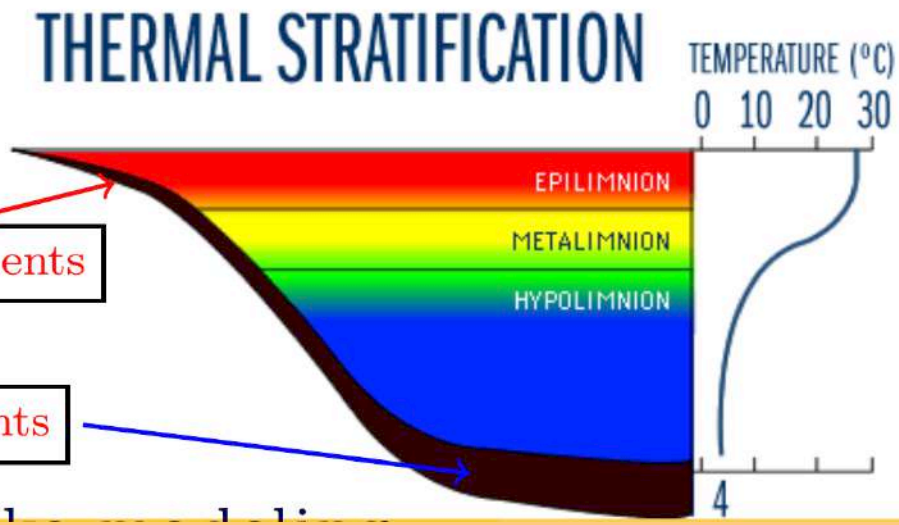

High CH_4 production in shallow sediments

Low CH_4 production in deep sediments

Biogeochemical interactions in the model

(Stepanenko et al., FAC, 2020)

- Photosynthesis, respiration and BOD are empirical functions of temperature, Chl-a and phosphorus
- Oxygen uptake by sediments (SOD) is controlled by O_2 concentration and temperature (Walker and Snodgrass, 1986)
- Methane production $\propto P_0 q_{10}^{T-T_0}$, P_0 is calibrated (Stepanenko et al., 2011)
- Methane oxidation follows Michaelis-Menthen equation

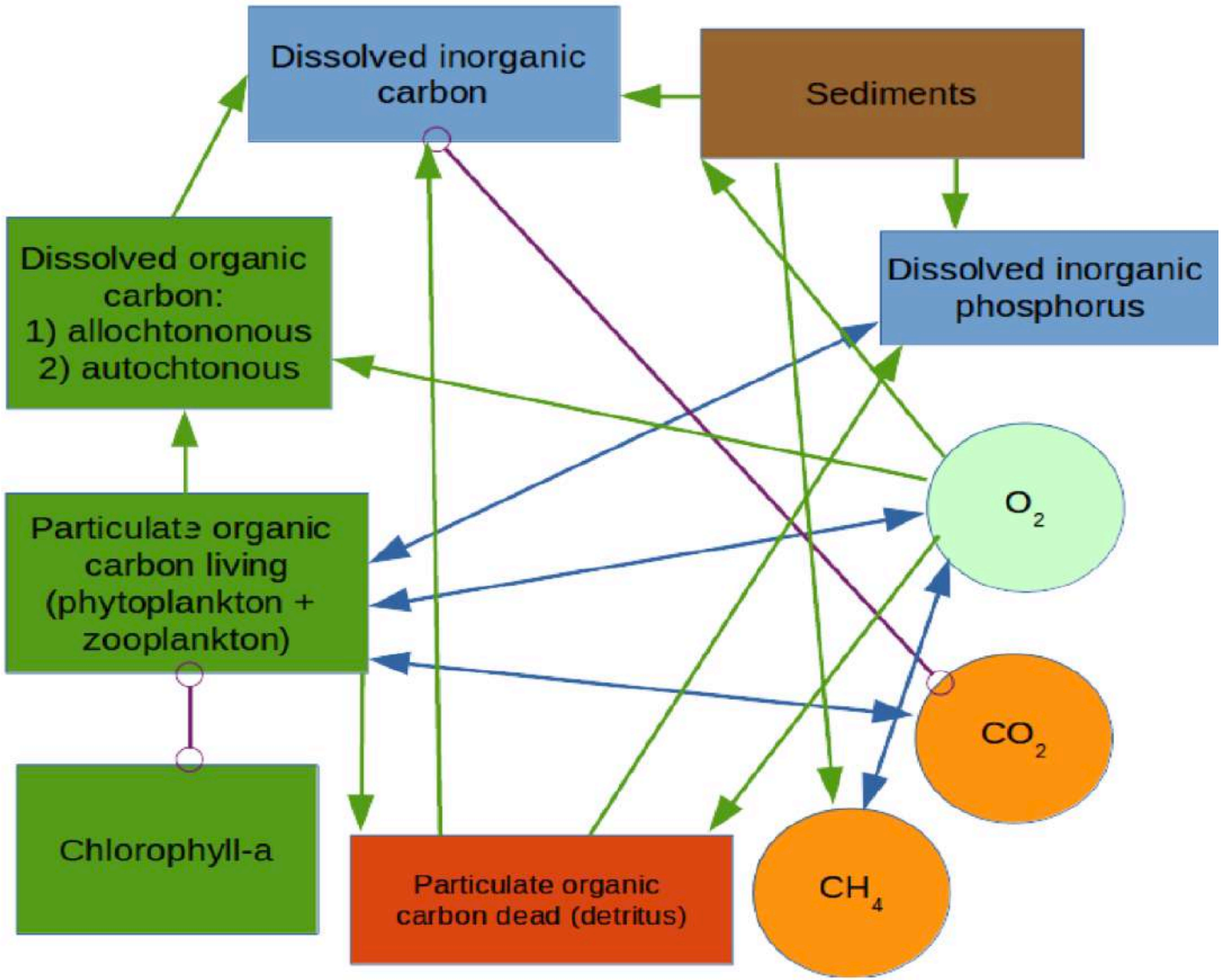

Bubble model

For shallow lakes (several meters), bubbles reach water surface not affected, for deeper lakes bubble dissolution has to be taken into account.

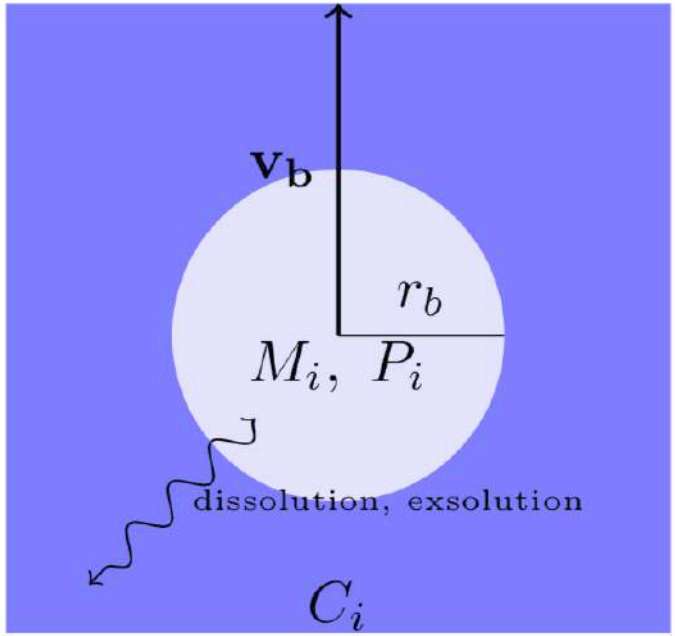

- Five gases are considered in a bubble: $CH_4,\ CO_2,\ O_2,\ N_2,\ Ar$
- Bubbles are composed of CH_4 and N_2 when they are emitted from sediments
- The velocity of bubble, v_b, is determined by balance between buoyancy and friction
- The molar quantity of i-th gas in a bubble, M_i, changes according to gas exchange equation (McGinnis et al.,

$$\frac{dM_i}{dt} = v_b \frac{\partial M_i}{\partial z} = -4\pi r_b^2 K_i (H_i(T) P_i - C_i).$$

- Gas exchange with solution is included in conservation equation for i-th gas :

$$\frac{\partial C_i}{\partial t} = \frac{1}{A}\frac{\partial}{\partial z} Ak \frac{\partial C_i}{\partial z} + \frac{1}{A}\frac{\partial AB_{C_i}}{\partial z} +$$

$$F(z,t,C_i,A) + (H_{C_i} - B_{C_i,b})\frac{1}{A}\frac{dA}{dz}.$$

Methane ebullition from different soil columns

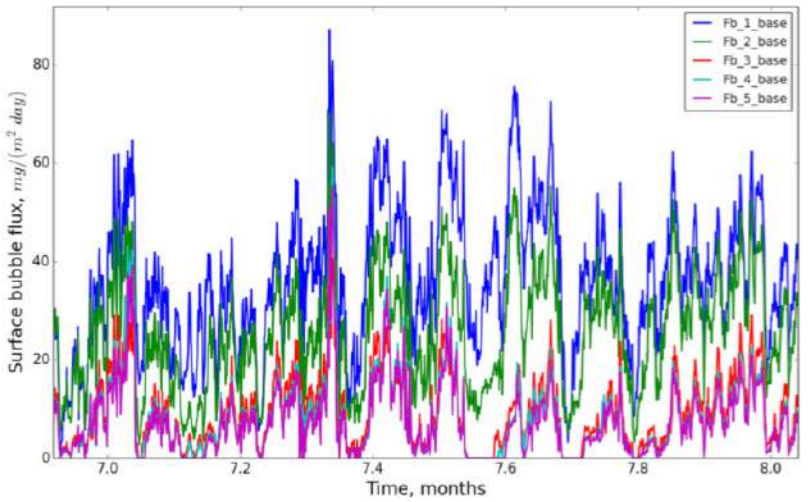

Kuivajärvi Lake (Finland)

- Mesotrophic, dimictic lake
- Area 0.62 km^2 (length 2.6 km, modal fetch 410 m)
- Altitude 142 m a.s.l.
- Maximal depth 13.2 m, average depth 6.4 m, deptl the point of measurements 12.5 m
- Catchment area 9.4 km^2

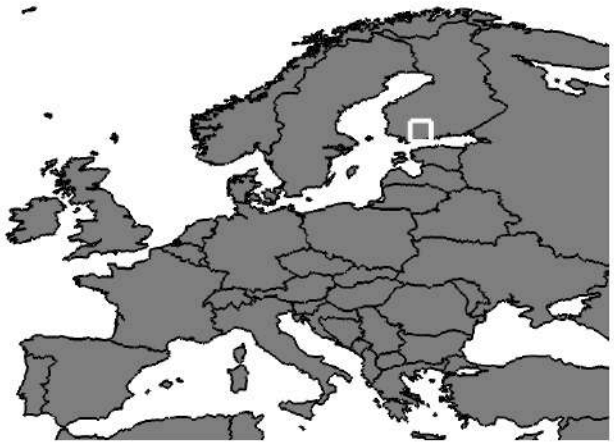

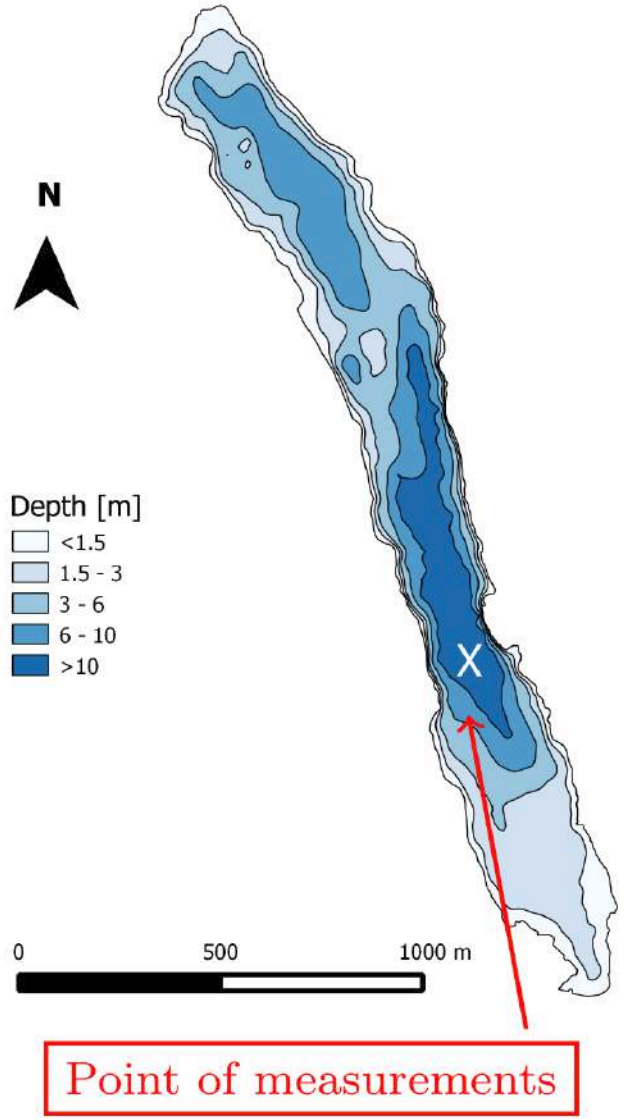

Measurements

- Conducted since 2009 by University of Helsinki
- Ultrasonic anemometer USA-1, Metek GmbH
- Enclosed-path infrared gas analyzers, LI-7200, LI-COR Inc.
- Four-way net radiometer (CNR-1)
- relative humidity at the height of 1.5 m (MP102H-530300, Rotronic AG)
- thermistor string of 16 Pt100 resistance thermometers (depths 0.2, 0.5, 1.0, 1.5, 2.0, 2.5, 3.0, 3.5, 4.0, 4.5, 5.0, 6.0, 7.0, 8.0, 10.0 and 12.0 m)
- Turbulent fluxes were calculated from 10 Hz raw data by EddyUH software

Measurement raft

Footprint of the raft measurements

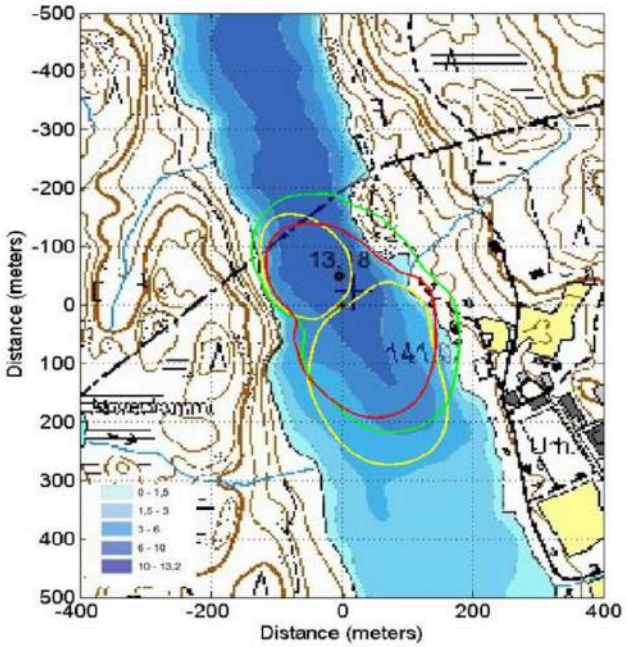

Water temperature

Measurements

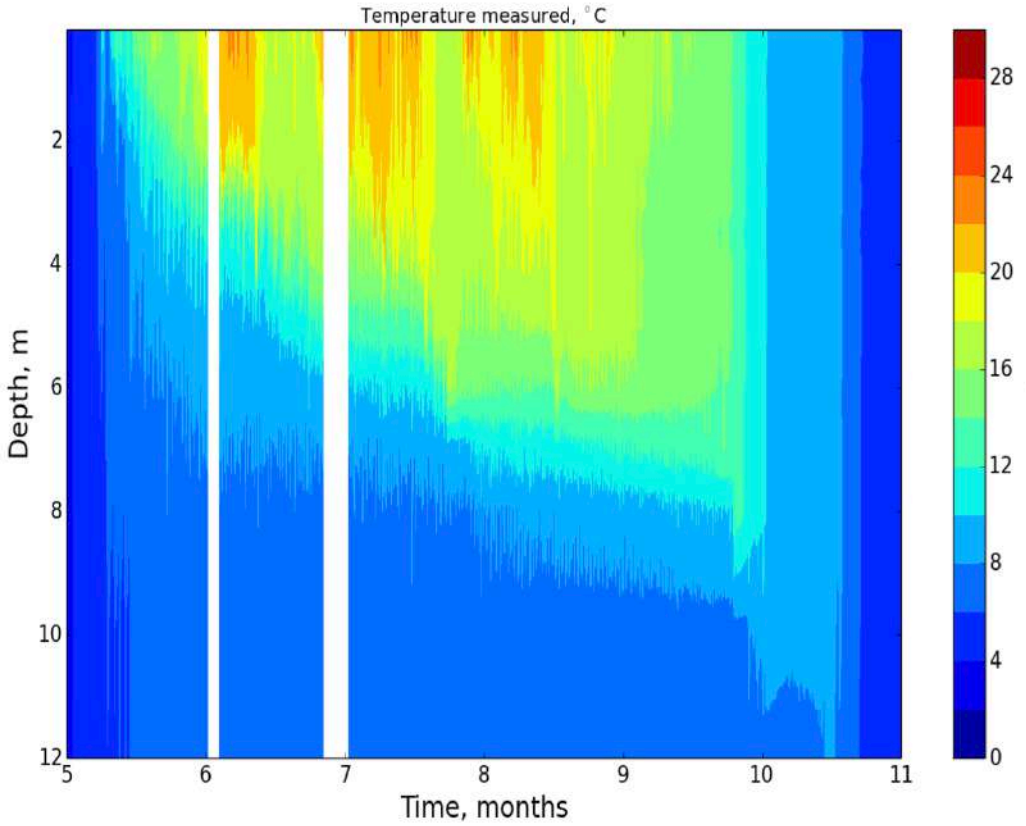

Model

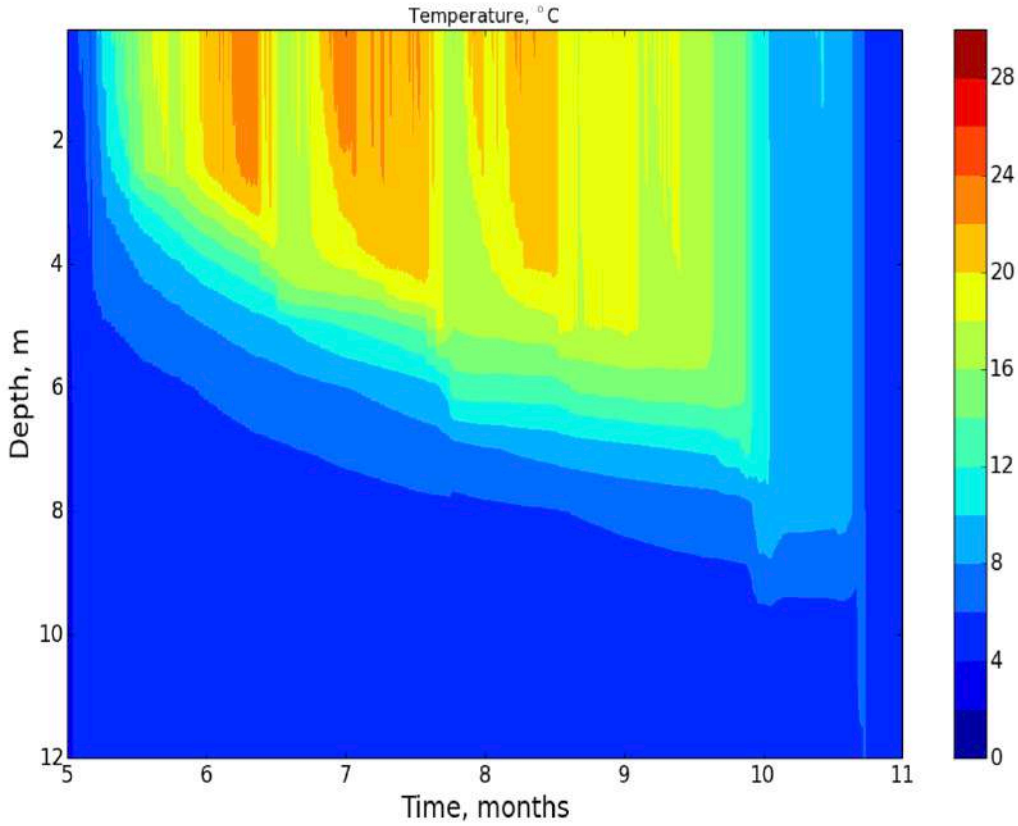

- Mixed layer depth and surface temperature (RMSE=1.54 ℃) are well reproduced
- Stratification strength in the thermocline is overestimated
- Model results lack frequent temperature oscillations in the thermocline

Thermocline thickness

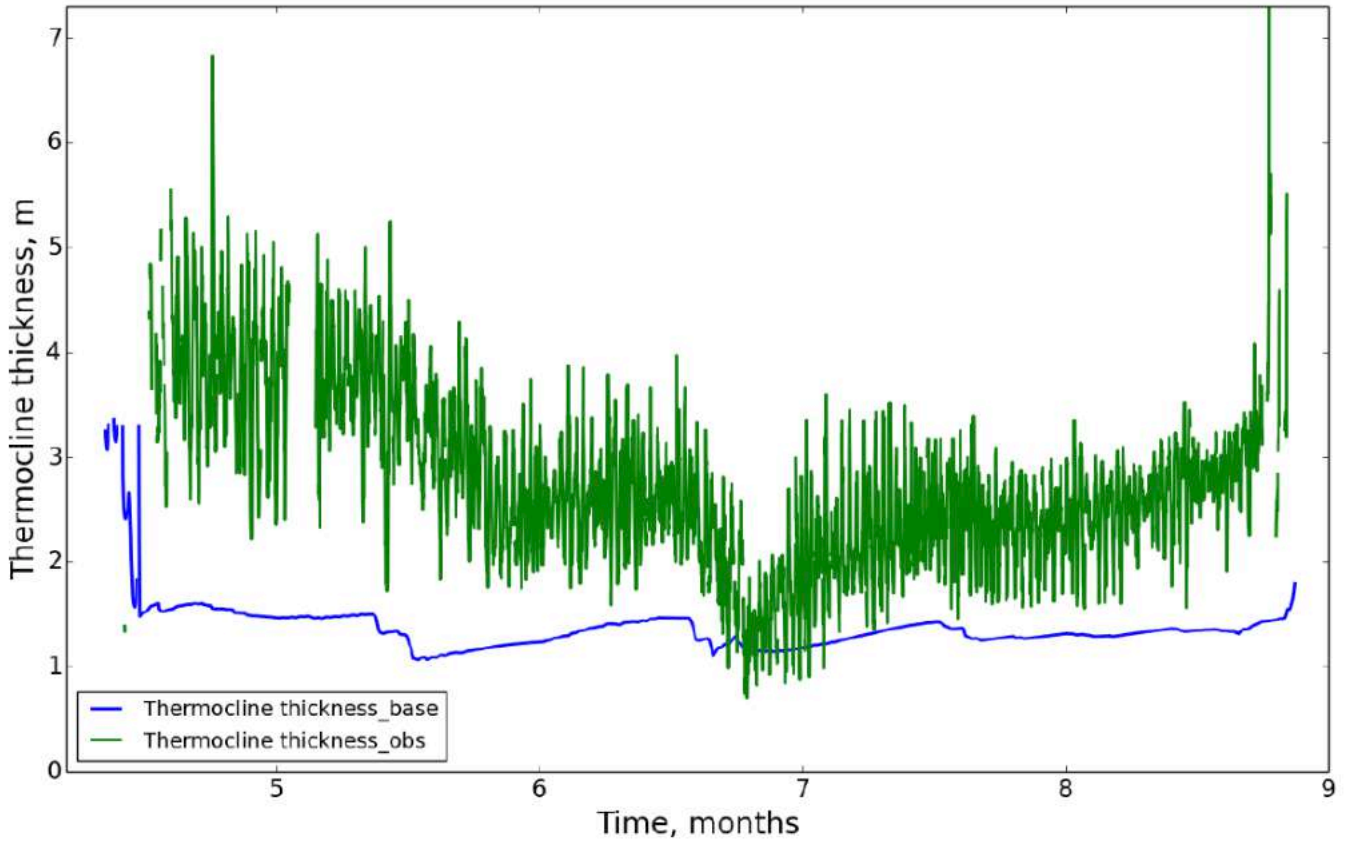

Thermocline thickness is defined as a depth difference between 8 ℃ and 14 ℃ isotherms

Oxygen

Stepanenko et al., Geosci. Mod. Dev., 2016

Measurements

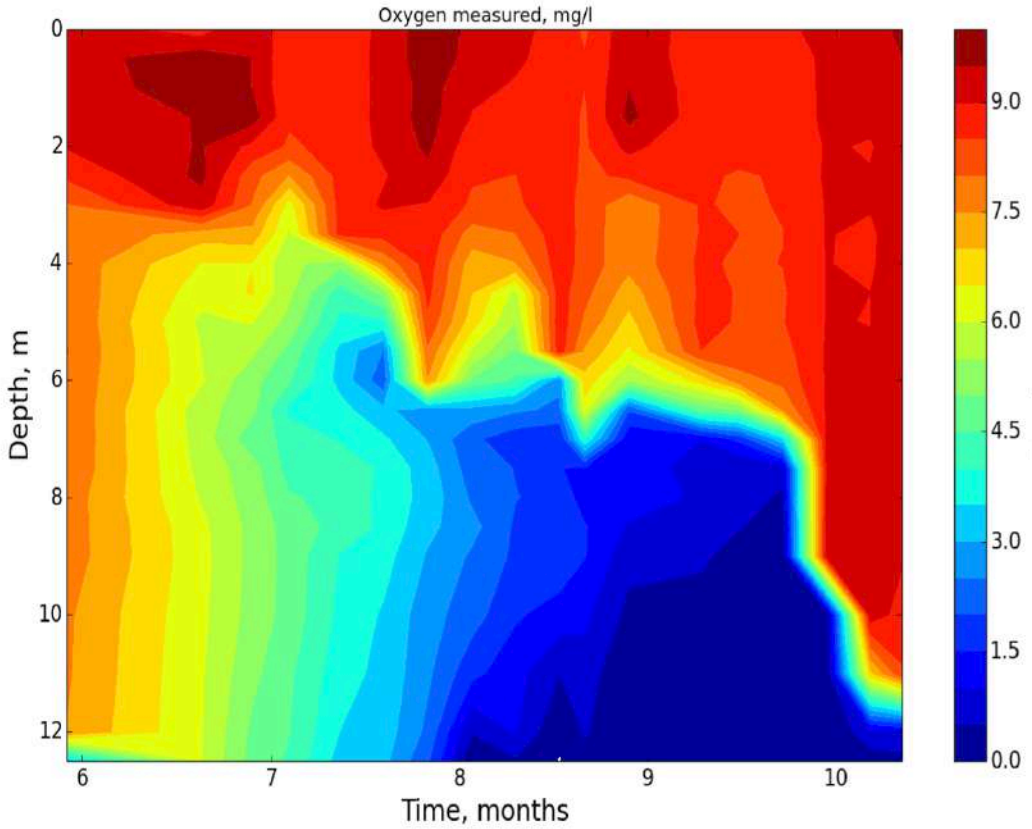

Model

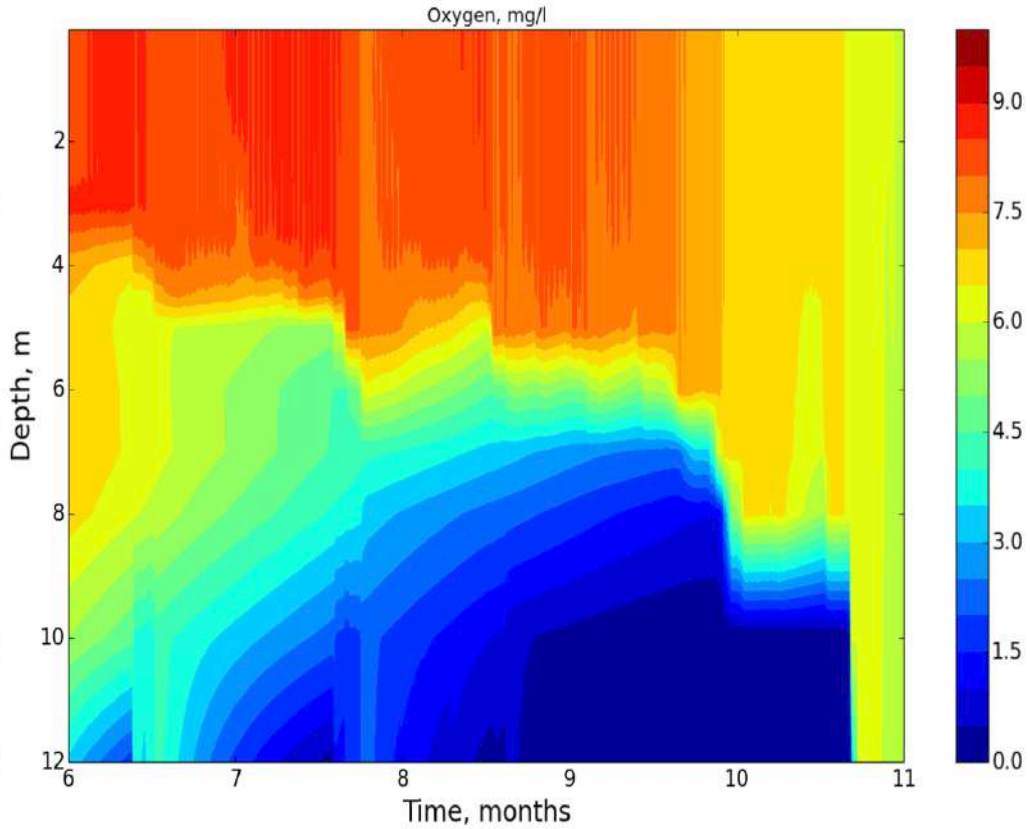

- Seasonal pattern is well captured: oxygen is produced in the mixed layer and consumed below
- Oxygen concentration in the mixed layer is underestimated by 1-1.5 mg/l, and more significantly during autumn overturn

Methane

Stepanenko et al., Geosci. Mod. Dev., 2016

Measurements

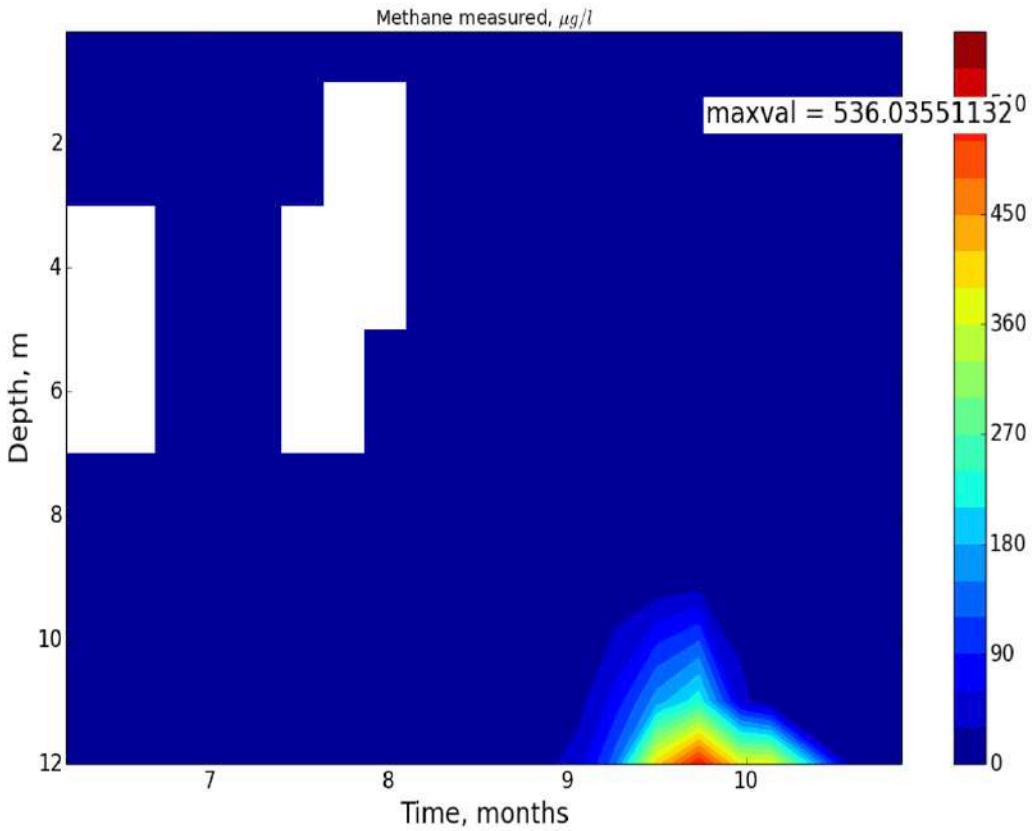

Model

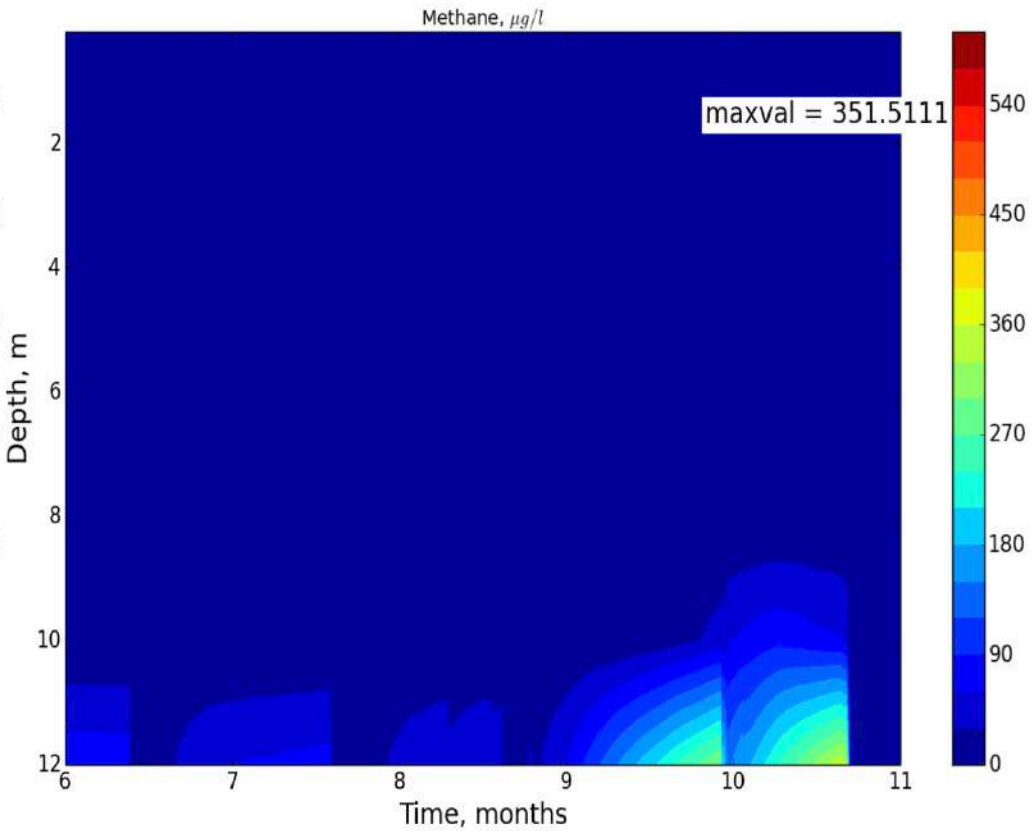

- Methane starts to accumulate near bottom in the late summer when oxygen concentration drops to low values
- Surface methane concentration is very small leading to negligible diffusive flux to the atmosphere, consistent with measurements

Carbon dioxide concentration

Stepanenko et al., Geosci. Mod. Dev., 2016

Measurements

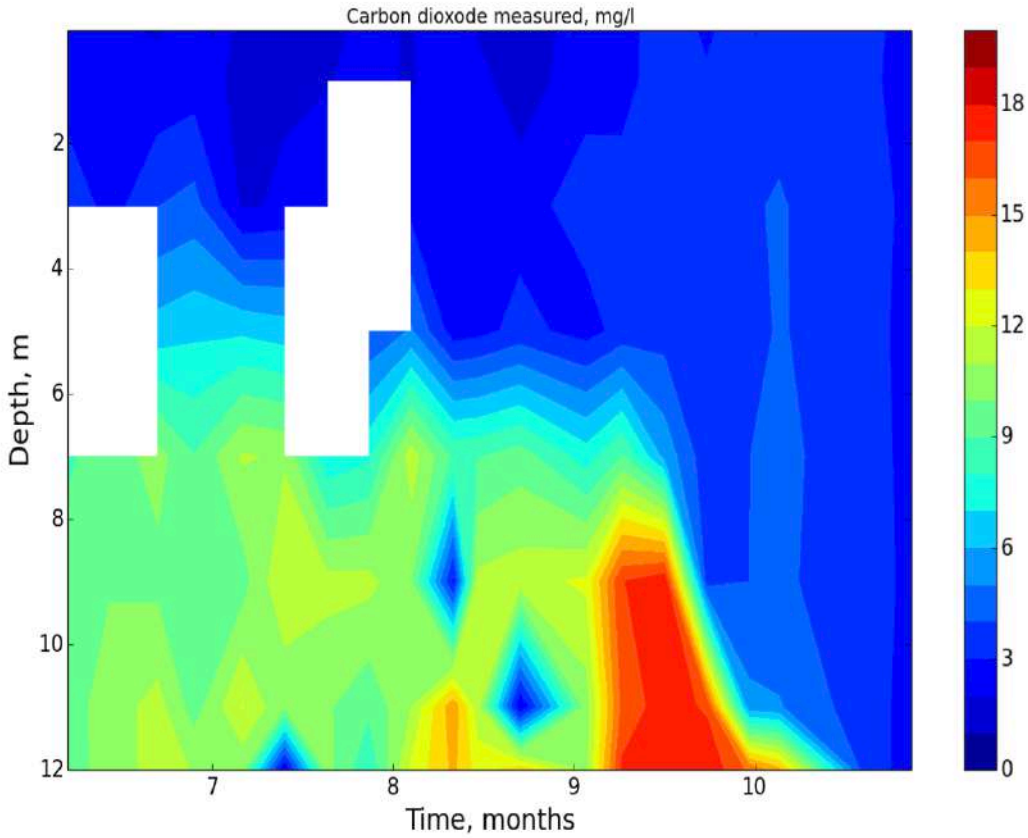

Model

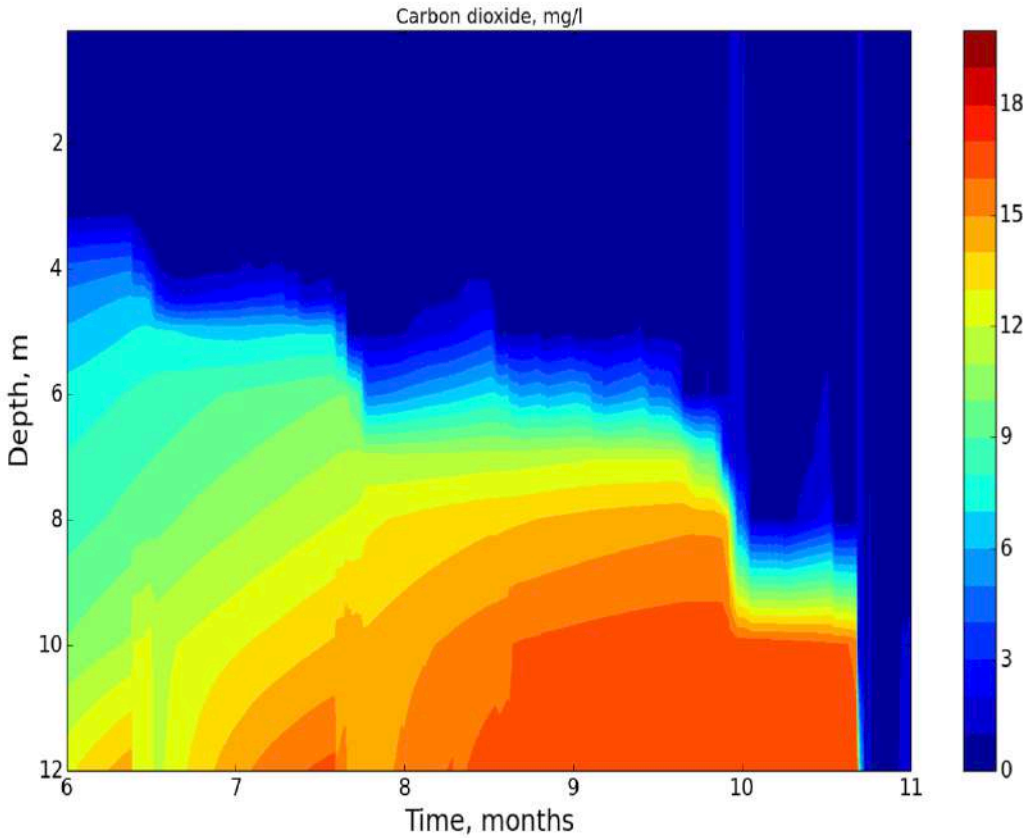

- Seasonal pattern is simulated realistically: carbon dioxide is consumed by photosynthesis in the mixed layer and produced in the thermocline and hypolimnion by aerobic organics decomposition
- Sudden CO_2 increase prior to autumn overturn is absent in the model

Further development: dissolved and particulate carbon

Adopting approach from Hanson et al., 2004

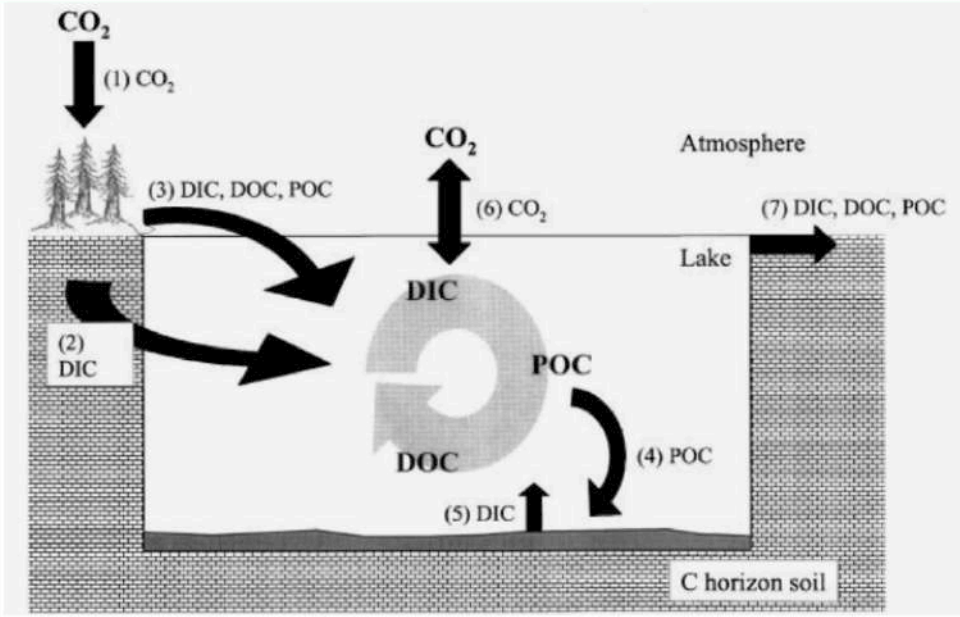

- The Hanson et al. model is reformulated to explicitly reproduce vertical distribution of DOC, POCL, POCD (instead of using mixed-layer and hypolimnion pools, as in original paper)
- The horizontal influx from catchment is included given the inlet measurement data

Extended biogeochemical model

$$\frac{\partial C_{CH_4}}{\partial t} = Dif_A(C_{CH_4}) + B_{CH_4} - O_{CH_4}, \quad (1)$$

$$\frac{\partial C_{O_2}}{\partial t} = \mathrm{Dif}_A(C_{O_2}) + B_{O_2} + P_{O_2} - R_{O_2} - D_{O_2} - S_{O_2} - O_{O_2}, \quad (2)$$

$$\frac{\partial C_{DIC}}{\partial t} = \mathrm{Dif}_A(C_{DIC}) + B_{CO_2} - P_{CO_2} + R_{CO_2} + D_{CO_2} + S_{CO_2} + O_{CO_2}, \quad (3)$$

$$\frac{\partial \rho_{DOC}}{\partial t} = \mathrm{Dif}(\rho_{DOC}) + E_{POCL} - D_{DOC}, \quad (4)$$

$$\frac{\partial \rho_{POCL}}{\partial t} = \mathrm{Dif}(\rho_{POCL}) + P_{POCL} - R_{POCL} - E_{POCL} - D_{h,POCL}, \quad (5)$$

$$\frac{\partial \rho_{POCD}}{\partial t} = \mathrm{Dif}(\rho_{POCD}) - \frac{w_g}{h}\frac{\partial \rho_{POCD}}{\partial \xi} - D_{POCD} + D_{h,POCL}. \quad (6)$$

Surface carbon dioxide concentration

Kuivajarvi Lake, June 2012 – December 2013

Measurements

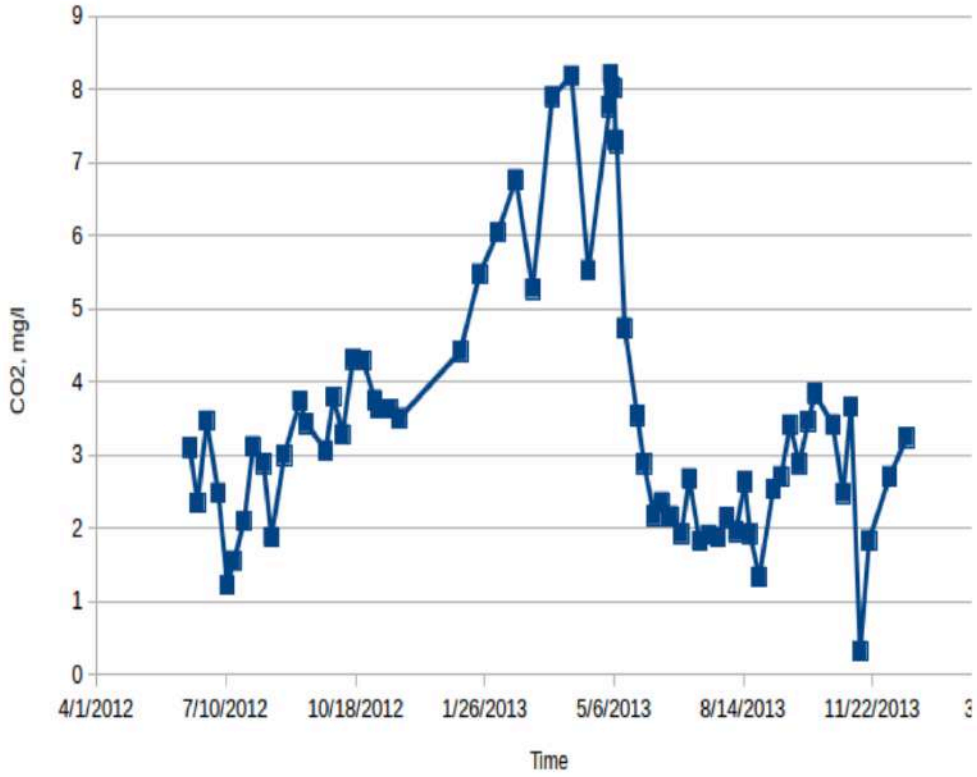

Model

Old carbon model, New carbon model,

New carbon model with NO inflow

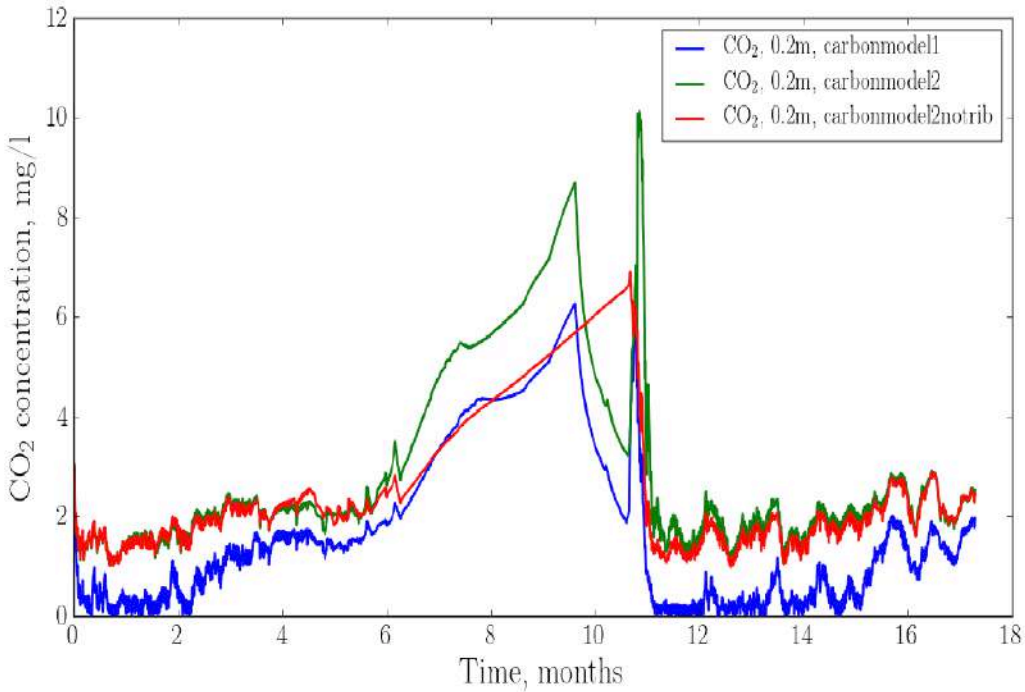

Surface CO_2 concentrations (~8 mg/l in winter, 2-3 mg/l in summer) are well captured by the model – dynamics of DOC and POC may be crucial to simulate lake-atmosphere CO_2 exchange

Gas transport through termocline

The concentration difference between epilimnion and hypolimnion may differ orders of magnitude. What are the trasnport mechanisms through metalimnion (thermocline)?

Internal seiches in Kuivajärvi

Temperature series at different depths

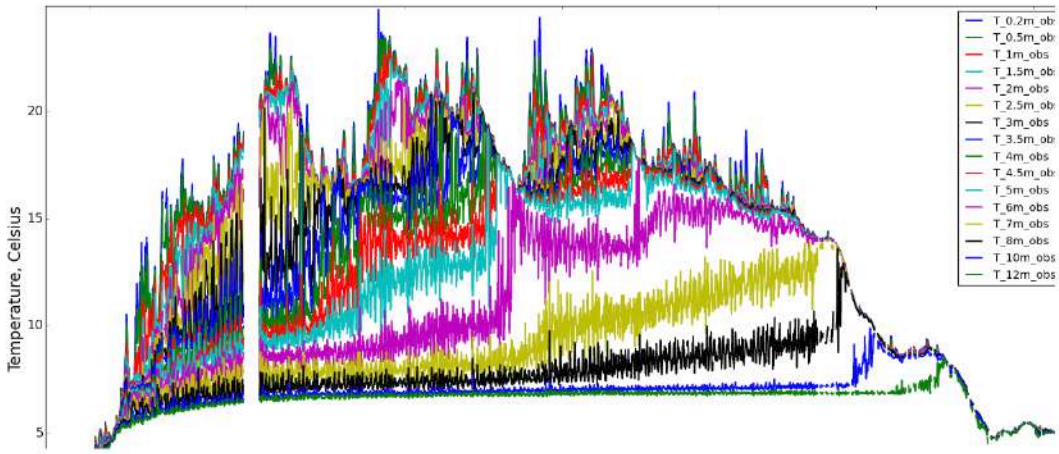

Power spectra of temperature fluctuations at three depths in the thermocline, maxima at $T \approx 3.9\ h$ and $T \approx 20.5\ h$

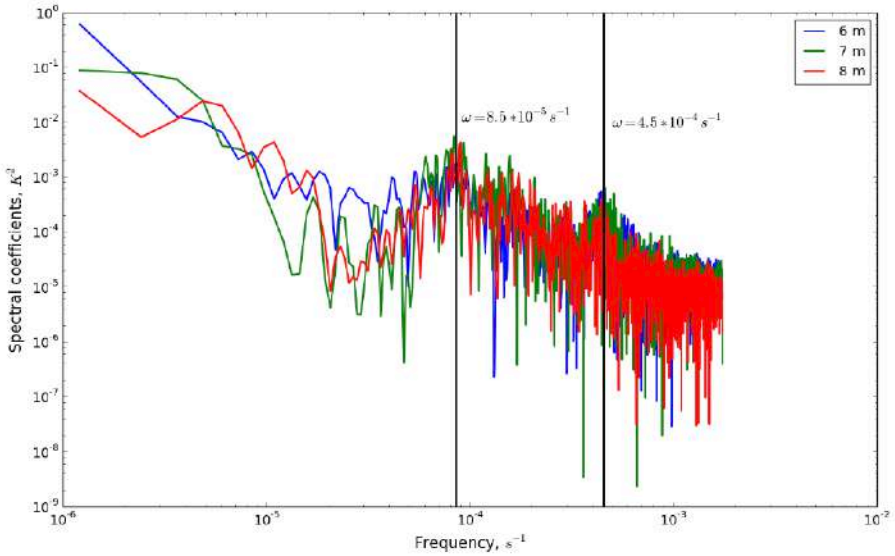

- Internal seiches are oscillations of thermocline after strong wind events.
- The periods of internal seiches may be calculated by linear theory (Münnich et al., 1992)

Seiche modes

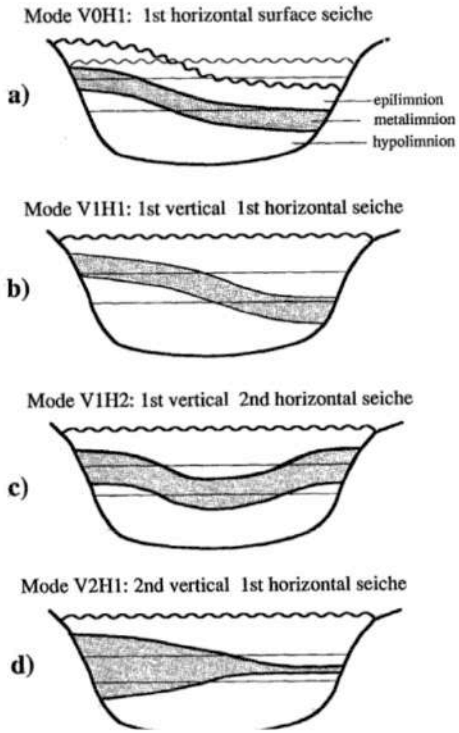

$$\frac{d^2W}{dz^2} + \left(\frac{N^2}{\omega^2} - 1\right) k^2 W = 0,\ W|_{z=0,H} = 0.$$

The Kuivajarvi stratification in June 2013 (N^2) and depth (12.5 m) yields $T \approx 6.5\ h$ for V1H1 mode and $T \approx 21.2h$ for V2H1.

Thermocline: does turbulence happens there?

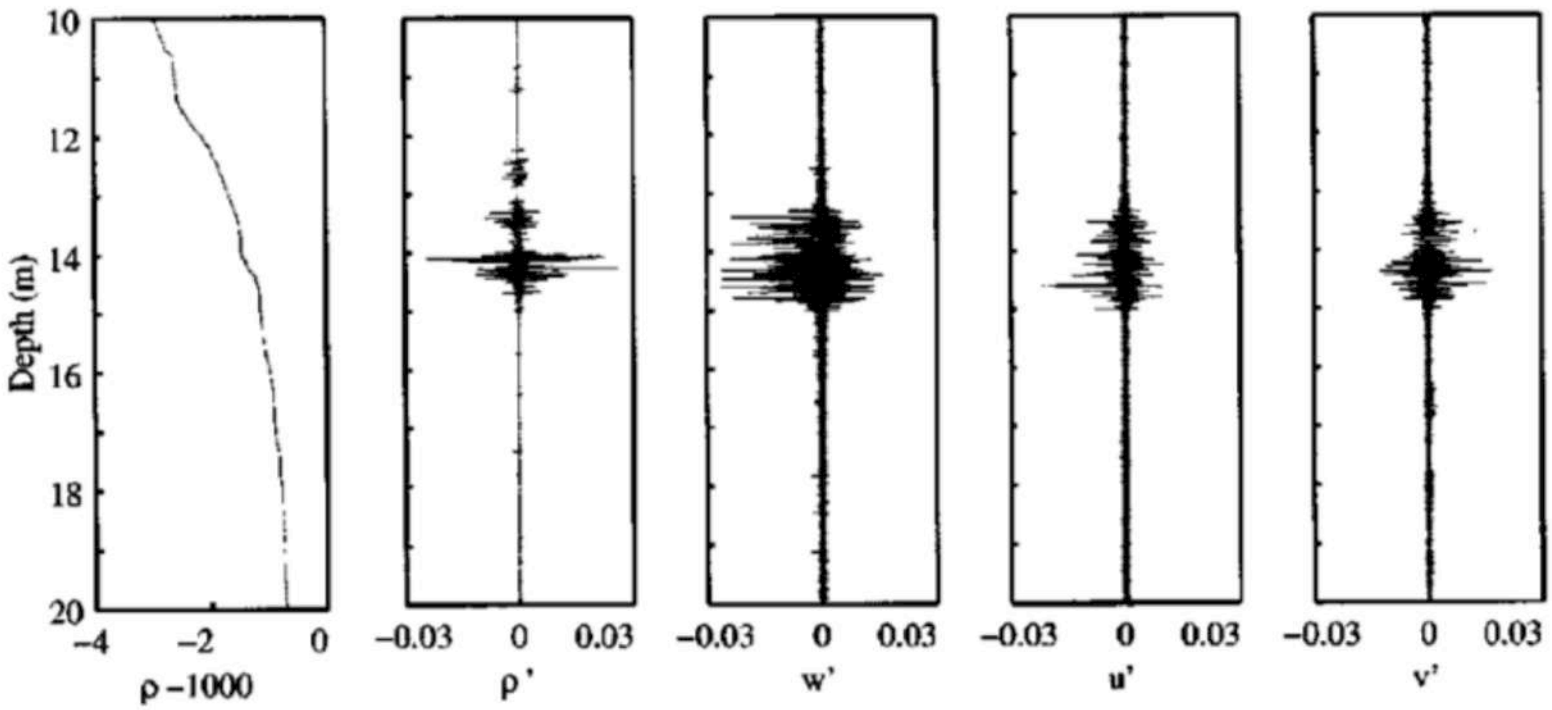

Saggio and Imberger, 2001

- measurement data tells us that, turbulence is either "almost absent", or demonstrates intermittent behaviour
- there is a long-standing research question, whether turbulence may exist in extremely stable stratification , e.g. in a form of "pre-turbulence" or few-mode regime (Zilitinkevich et al., 2013)

Model validation for Seida Lake

Guseva et al., Geogr. Env. Sust., 2016

Seida lake location

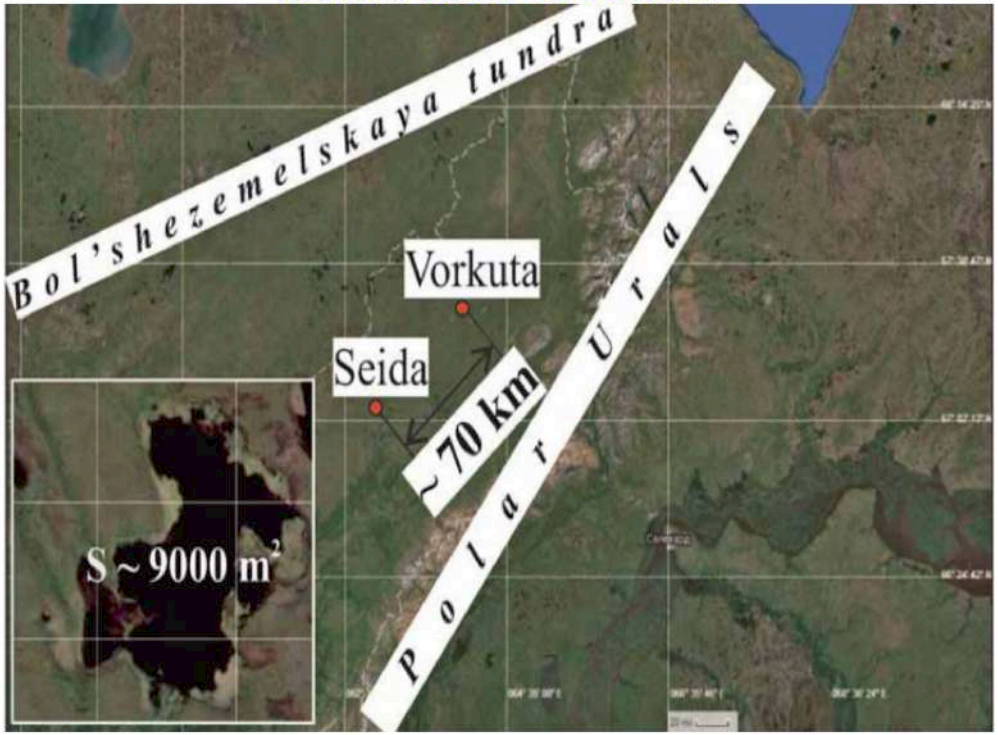

Bubble flux (starting from 01.07.2007)

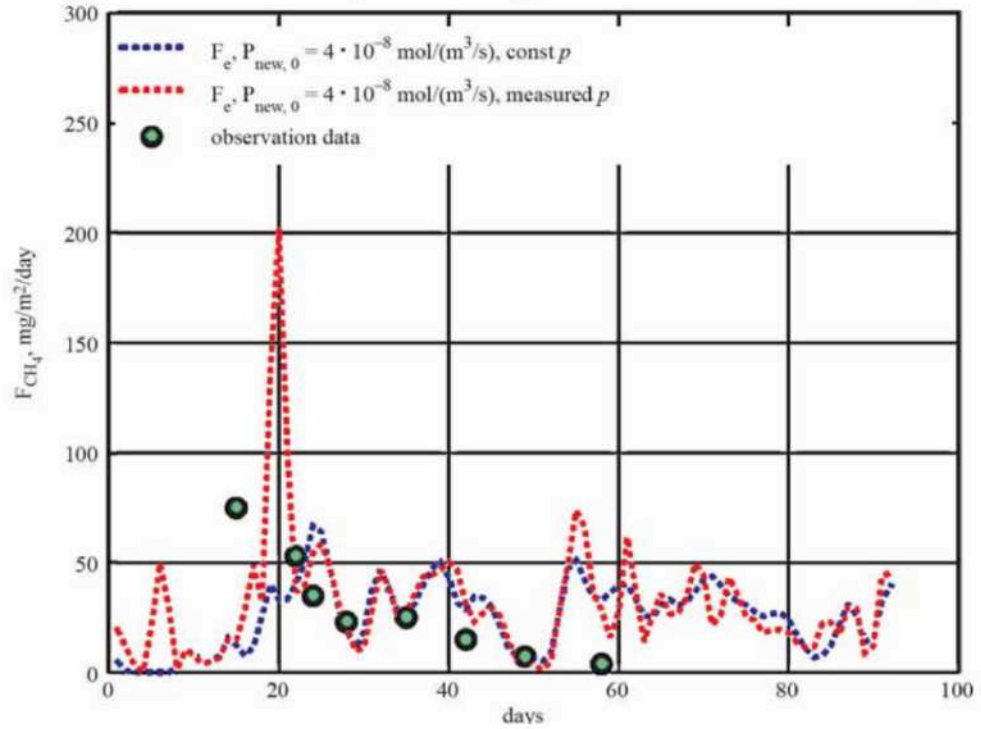

Table 3. Methane production rate constant $P_{new,0}$ in other studies

$P_{new,0}$ (mol · m^{-3} · s^{-1})	Source
$3.0 \cdot 10^{-8}$	Lake Kuivajärvi, Finland [Stepanenko et al., 2016]
$2.55 \cdot 10^{-8}$	Shuchi Lake, North Eastern Siberia, Russia [Stepanenko et al., 2011]
$8.3 \cdot 10^{-8} - 1.6 \cdot 10^{-7}$	High latitude wetlands [Walter & Heimann, 2000]
$4.0 \cdot 10^{-8}$	Lake at the Seida site, current study

Methane emission from Suwa Lake (Japan)

Simulations with LAKE by H.Iwata group in Nagano University

Lake sizes 3 km×4 km. Maximal depth 7 m.

Methane flux over the lake

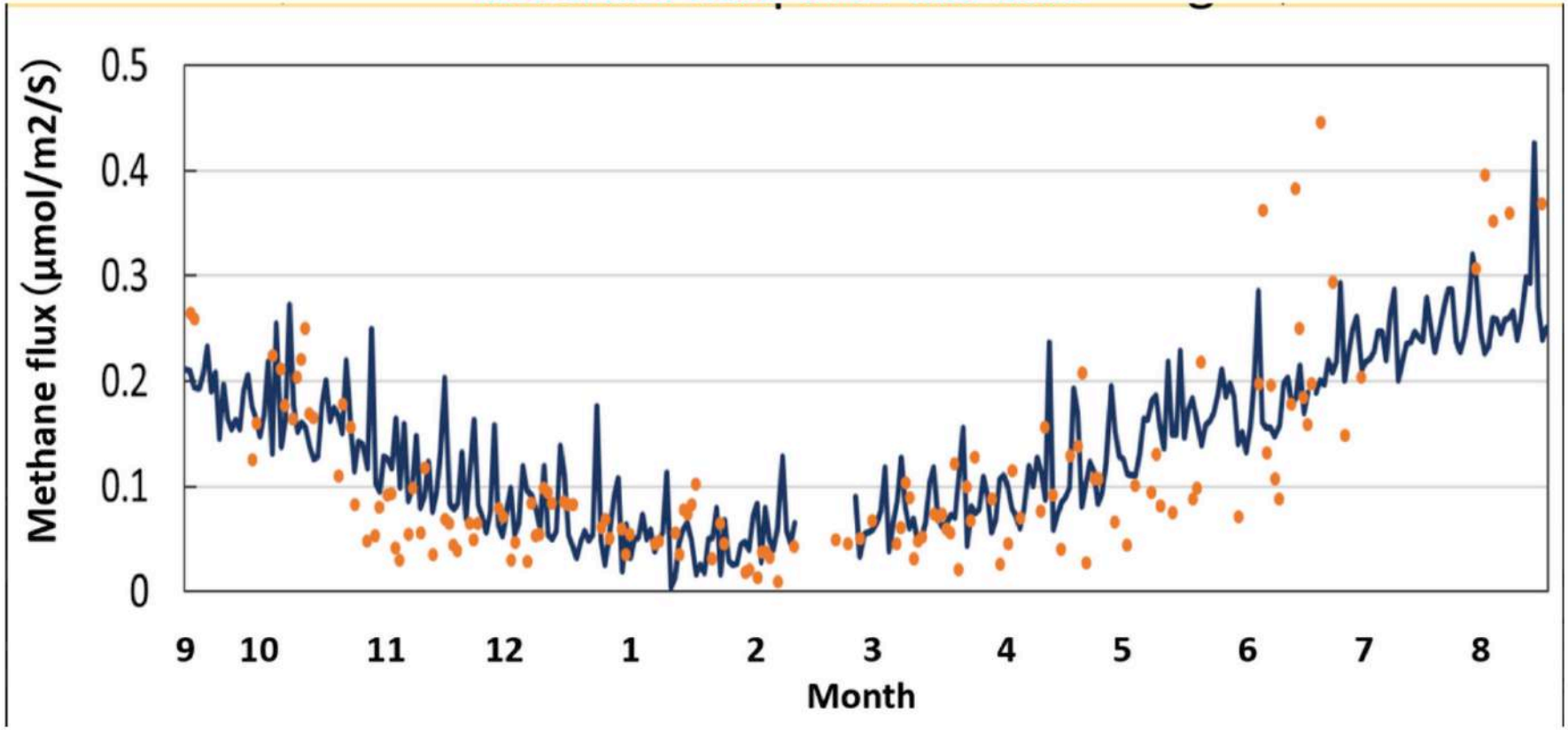

Methane production constant P_0 and maximal oxidation rate V_{max} are measured in lab.

Global estimates of GHGs from reservoirs

Hydropower is no more thought as greenhouse-gas-free energy source

Global synthesis of GHG emissions from artificial reservoirs (Deemer et al., 2016):

Table 1. The global surface area and GHG flux estimates from reservoirs compared with those of other freshwater ecosystems and other anthropogenic activities.

System Type	Surface Area ($\times 10^6$ km^2)	Annual teragrams (Tg) C or N (Tg per year)			Areal Rates (milligrams per square meter per day)			Annual CO_2 Equivalents (Tg CO_2 Eq per year)			
		CH_4-C	CO_2-C	N_2O-N	CH_4-C	CO_2-C	N_2O-N	CH_4	CO_2	N_2O	Total
All Reservoirs (This Study)	0.31[a]	13.3	36.8	0.03	120	330	0.30	606.5	134.9	31.7	773.1
All Reservoirs (Other Work)	0.51–1.5[b,c]	15–52.5[b,d]	272.7[b]	–	82–96	498	–	680–2380	1000	–	
Hydroelectric Reservoirs	0.34[e]	3–14[e,f]	48–82[e,f]	–	24–112	386–660	–	136–635	176–301	–	
Lakes	3.7–4.5[c,d,h]	53.7[d]	292[g]	–	40	216	–	2434	1071	–	
Ponds	0.15– 0.86[i]	12[i]	571[i]	–	27[i]	422[i]	–	544	2094	–	
Rivers	0.36–0.65[d,g]	1.1–20.1[d,j]	1800[g]	–	6–98[j]	7954	–	50–911	6600	–	
Wetlands	8.6–26.9[k]	106–198[k]	–	0.97[l]	15–63[k]	–	0.1–0.31	4805–8976		908	
Other Anthropogenic Emissions (2000s)	N.A.	248[m]	9200[m]	6.9[m]	–	–	–	11243	33733	6462	51438

Note: The values presented are mean estimates; the ranges of mean values are reported when there are multiple relevant models. In cases in which the areal rates are not referenced, they were derived from dividing annual teragrams (Tg) of C or N by the global surface-area estimate. The annual CO_2 equivalents were calculated by multiplying the mass-based flux (in units of Tg CH_4, CO_2 or N_2O per year) by the 100-year global warming potential of each gas (1 for CO_2, 34 for CH_4 and 298 for N_2O). [a] (Lehner et al. 2011). [b] (St. Louis et al. 2000). [c] (Downing and Duarte 2009). [d] (Bastviken et al. 2011) . [e] (Barros et al. 2011). [f] (Li and Zhang 2014). [g] (Raymond et al. 2013). [h] (Verpoorter et al. 2014). [i] (Holgerson and Raymond 2016). [j] (Stanley et al. 2016). [k] (Melton et al. 2013). [l] (Tian et al. 2015). [m] (Ciais et al. 2013).

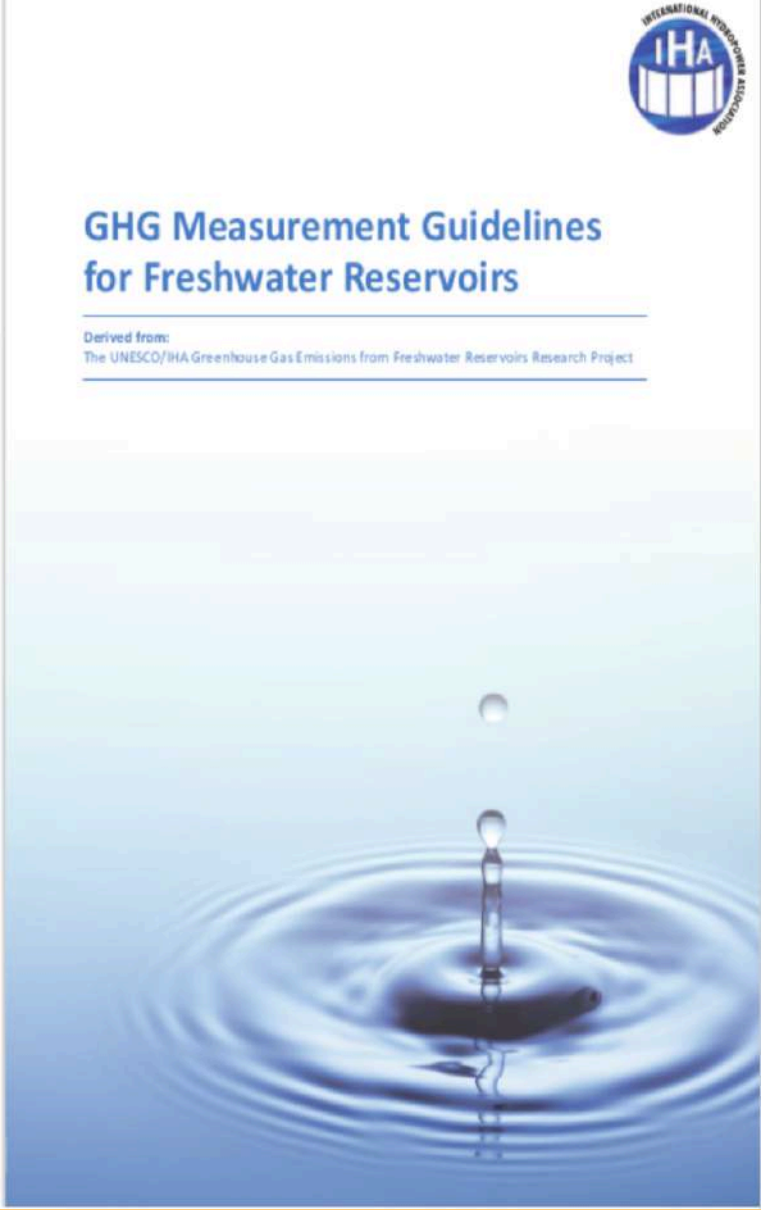

IPCC view on the problem

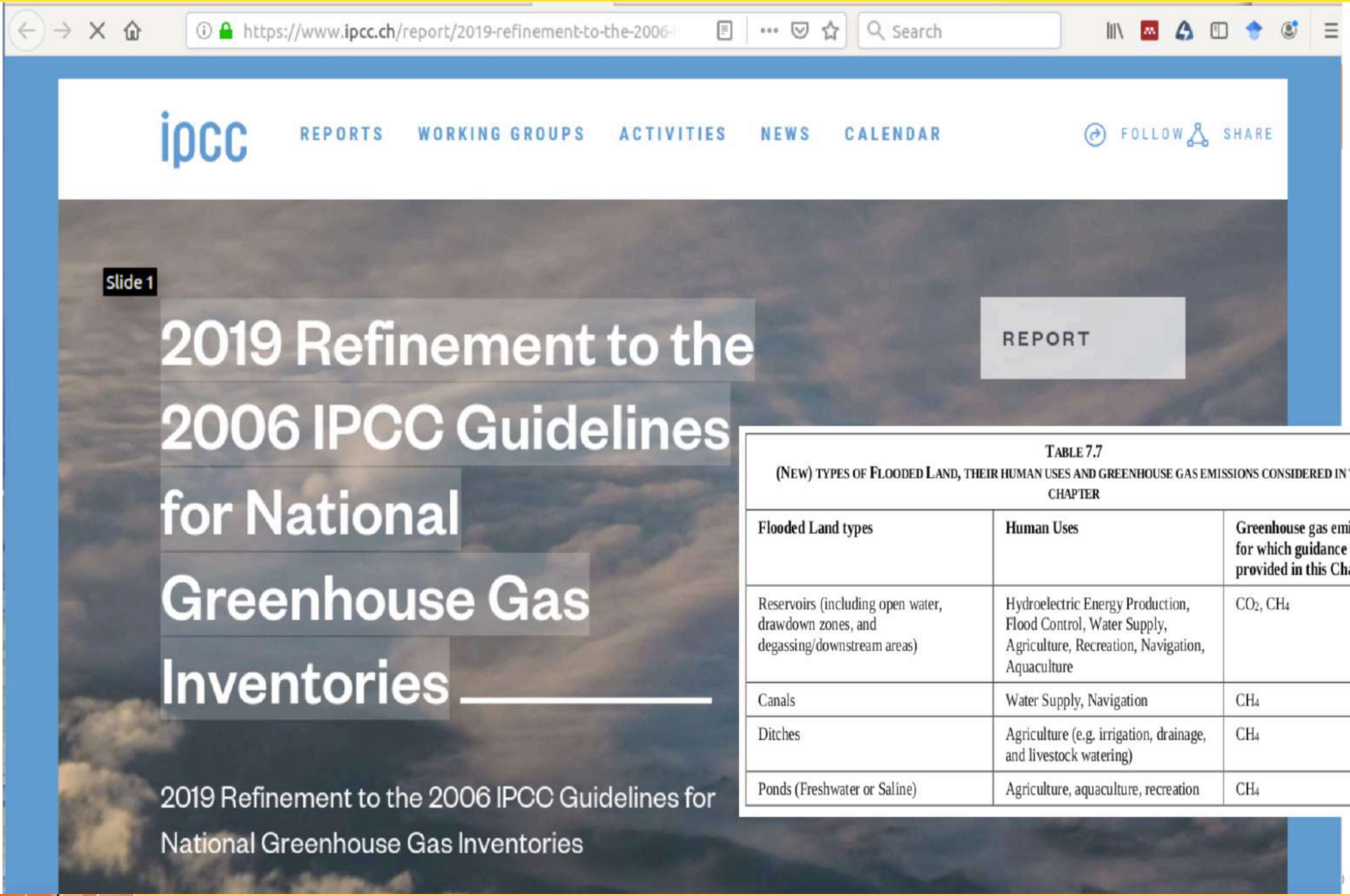

TABLE 7.7
(NEW) TYPES OF FLOODED LAND, THEIR HUMAN USES AND GREENHOUSE GAS EMISSIONS CONSIDERED IN THIS CHAPTER

Flooded Land types	Human Uses	Greenhouse gas emissions for which guidance is provided in this Chapter
Reservoirs (including open water, drawdown zones, and degassing/downstream areas)	Hydroelectric Energy Production, Flood Control, Water Supply, Agriculture, Recreation, Navigation, Aquaculture	CO_2, CH_4
Canals	Water Supply, Navigation	CH_4
Ditches	Agriculture (e.g. irrigation, drainage, and livestock watering)	CH_4
Ponds (Freshwater or Saline)	Agriculture, aquaculture, recreation	CH_4

Emission of greenhouse gases from reservoirs

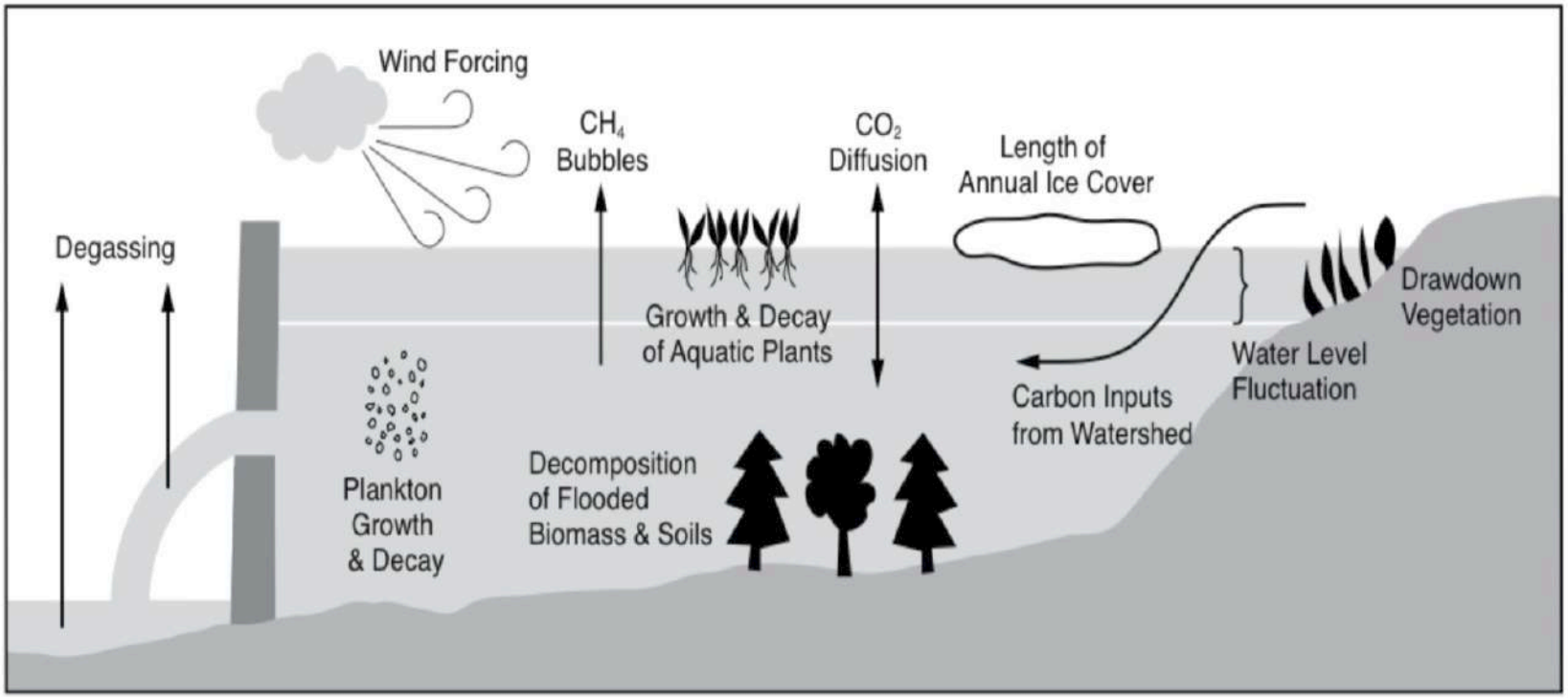

- Artificially flooded ecosystems are imposed to both aerobic (producing CO_2) and anaerobic (producing CH_4) degradation
- Compared to natural lakes there is an additional pathway of gases that is through turbines

Mozhayskoe reservoir

Depth of an impounded river bed

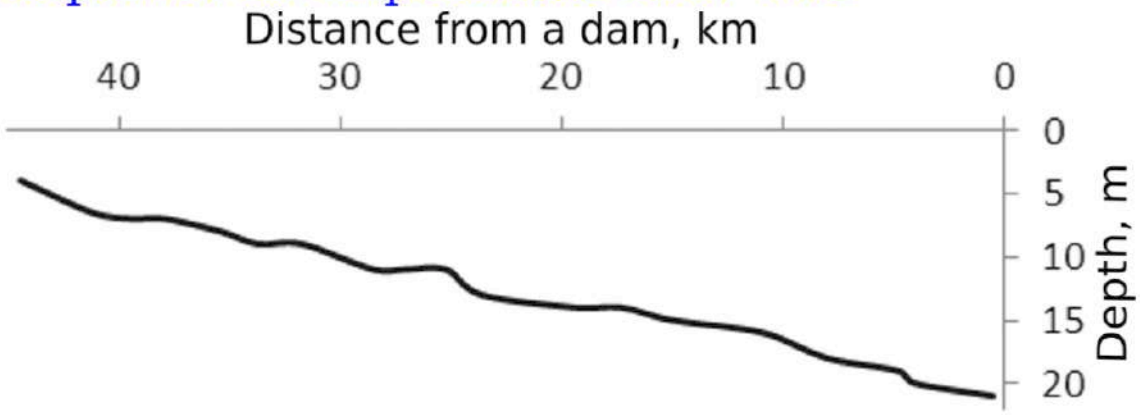

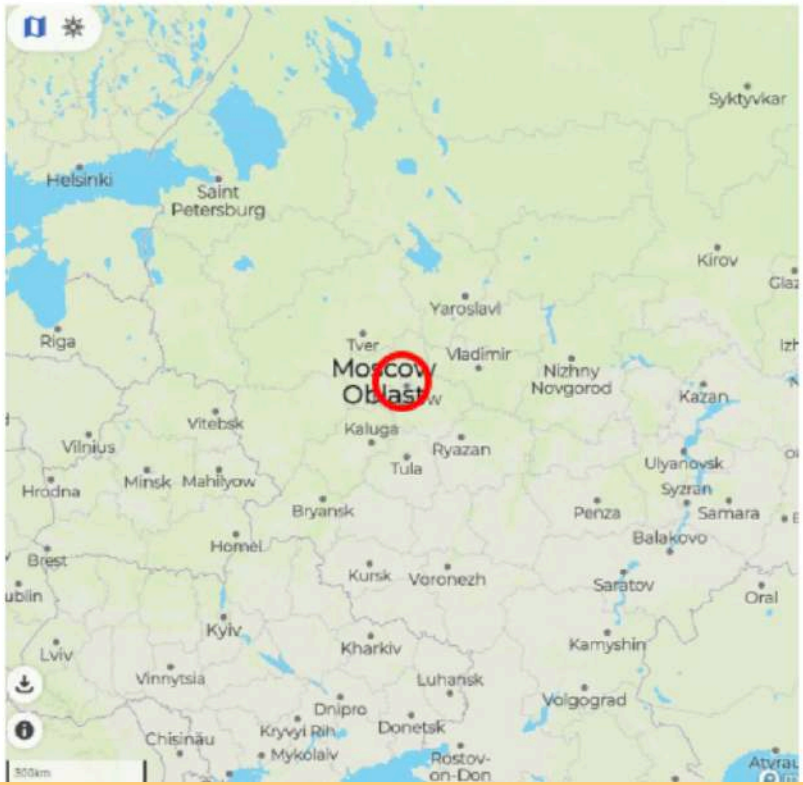

- length 47 km, width up to 3.5 km, max. depth 23 m
- water residence time 0.8 yr
- hydropower station and drinking water supply

Measurement data

- conventional meteorology from nearby Mozhayskoe station, corrected using empirical relations to on-lake conditions
- radiation fluxes from Zvenigorod station (IAP RAS)
- discharge data from a dam
- string of temperature loggers at the deep part (V) of reservoir
- whole-lake surveys of water temperature, dissolved oxygen, methane (headspace method)

Inflow, outflow and advection

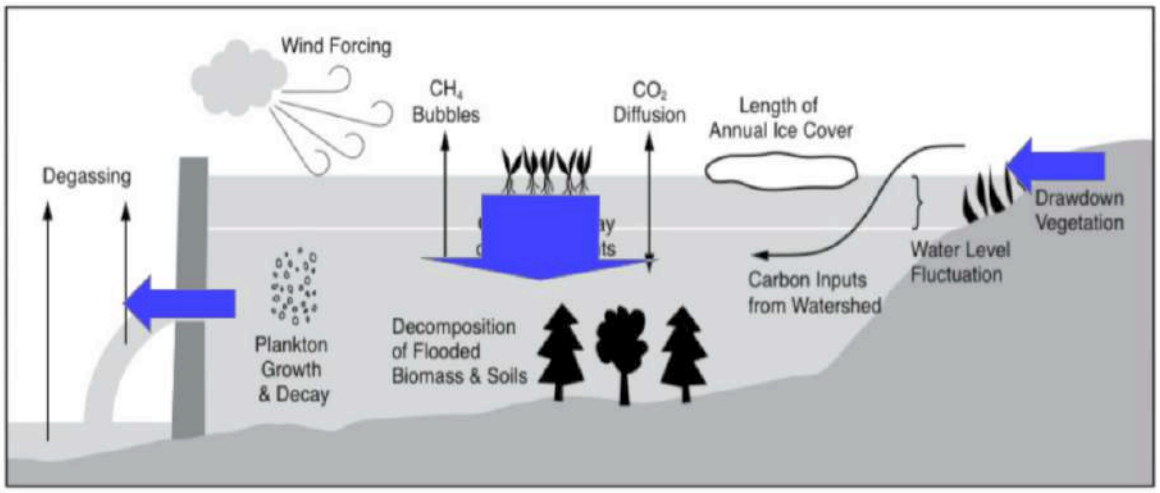

- Inflow and outflow are accounted for as source and sink of physical and biogeochemical variables
- The difference in the depth of water input and output leads to the large-scale water

Continuity equation allows to compute vertical speed w:

$$\frac{\partial \overline{w} A}{\partial z} = -\int_{\Gamma_{A(z)}} (\mathbf{u_h} \cdot \mathbf{n}) dl = \text{Inflow} - \text{Outflow}$$

Vertical advection is added to a balance equation of each scalar:

$$c\frac{\partial f}{\partial t} = -\frac{c}{A}\frac{\partial \overline{w} A \overline{f}}{\partial z} + \ldots$$

Mean vertical speed (m/day)

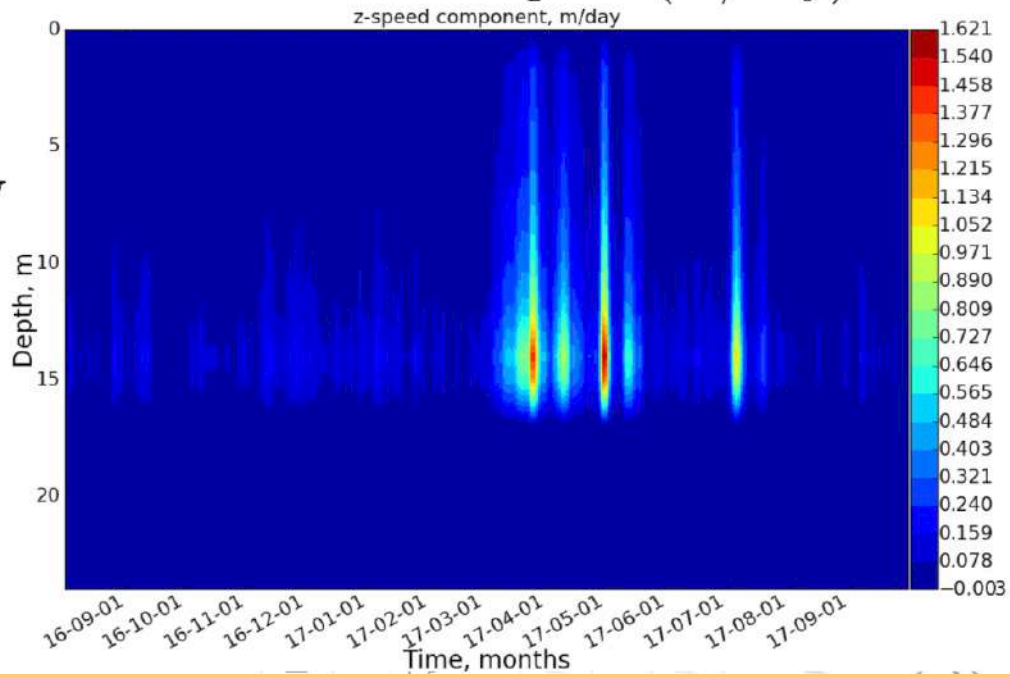

Temperature: effect of vertical advection

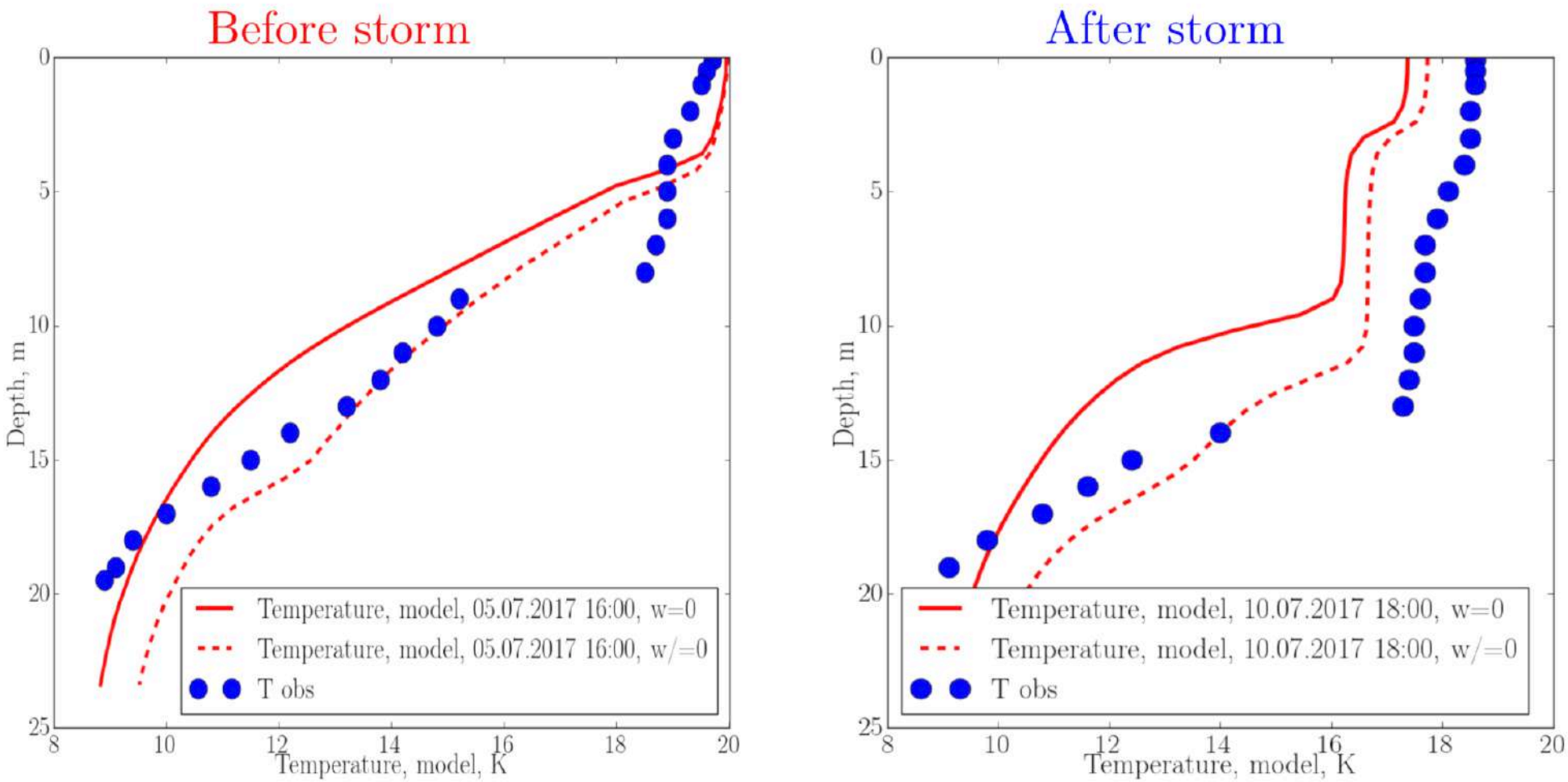

- High wind speeds (6-8 m/s) and rainfall persisted over 4 days, causing river discharge to reach 70 m^3/s (contrasting to 5-10 m^3/s before and after event)
- The mixed-layer deepening is much better reproduced when including vertical advection

Vertical distribution of temperature and methane in the Mozhaisk reservoir: summer 2017 *(Stepanenko et al., 2020)*

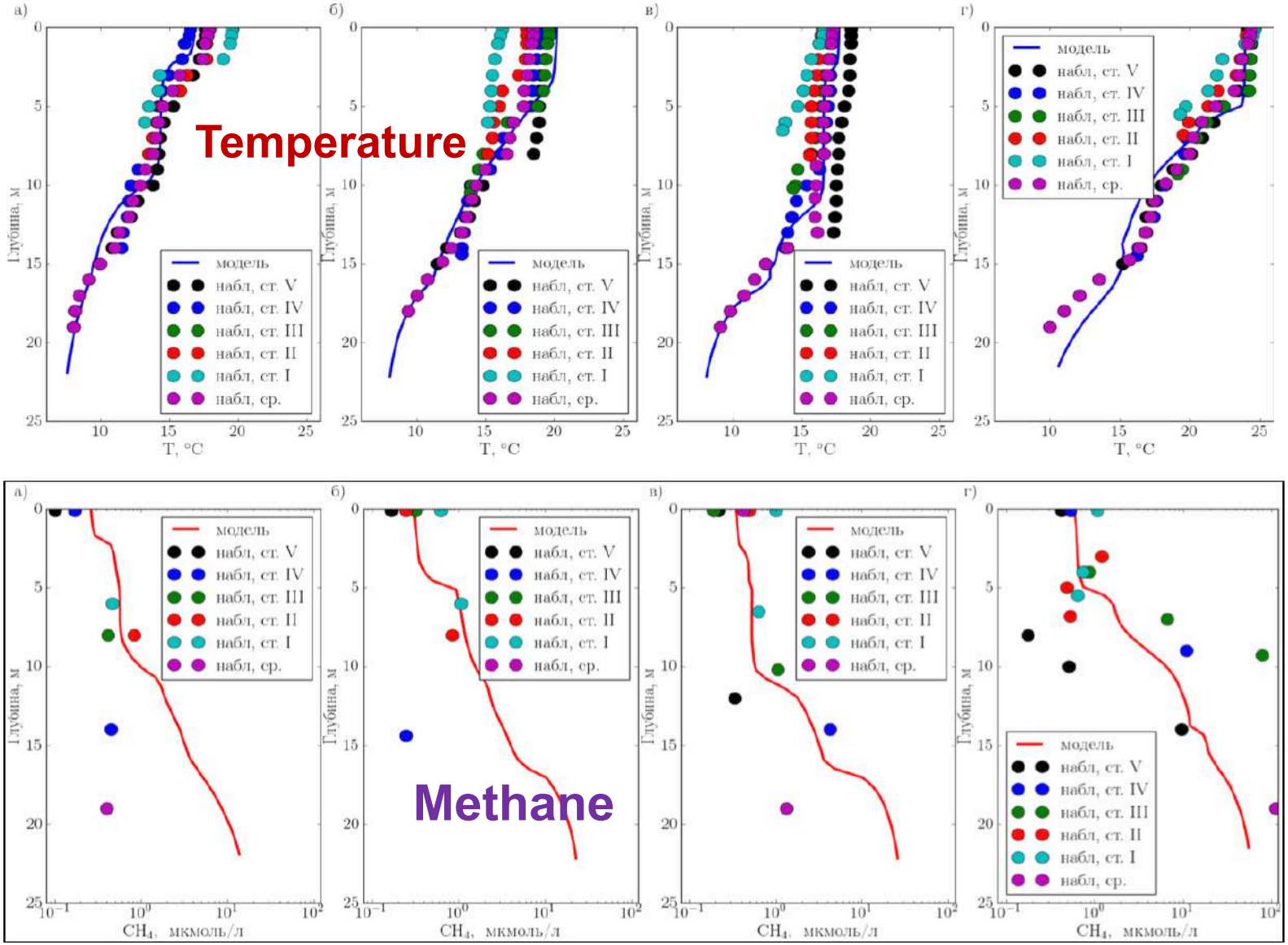

Results with Mozhayskoe reservoir

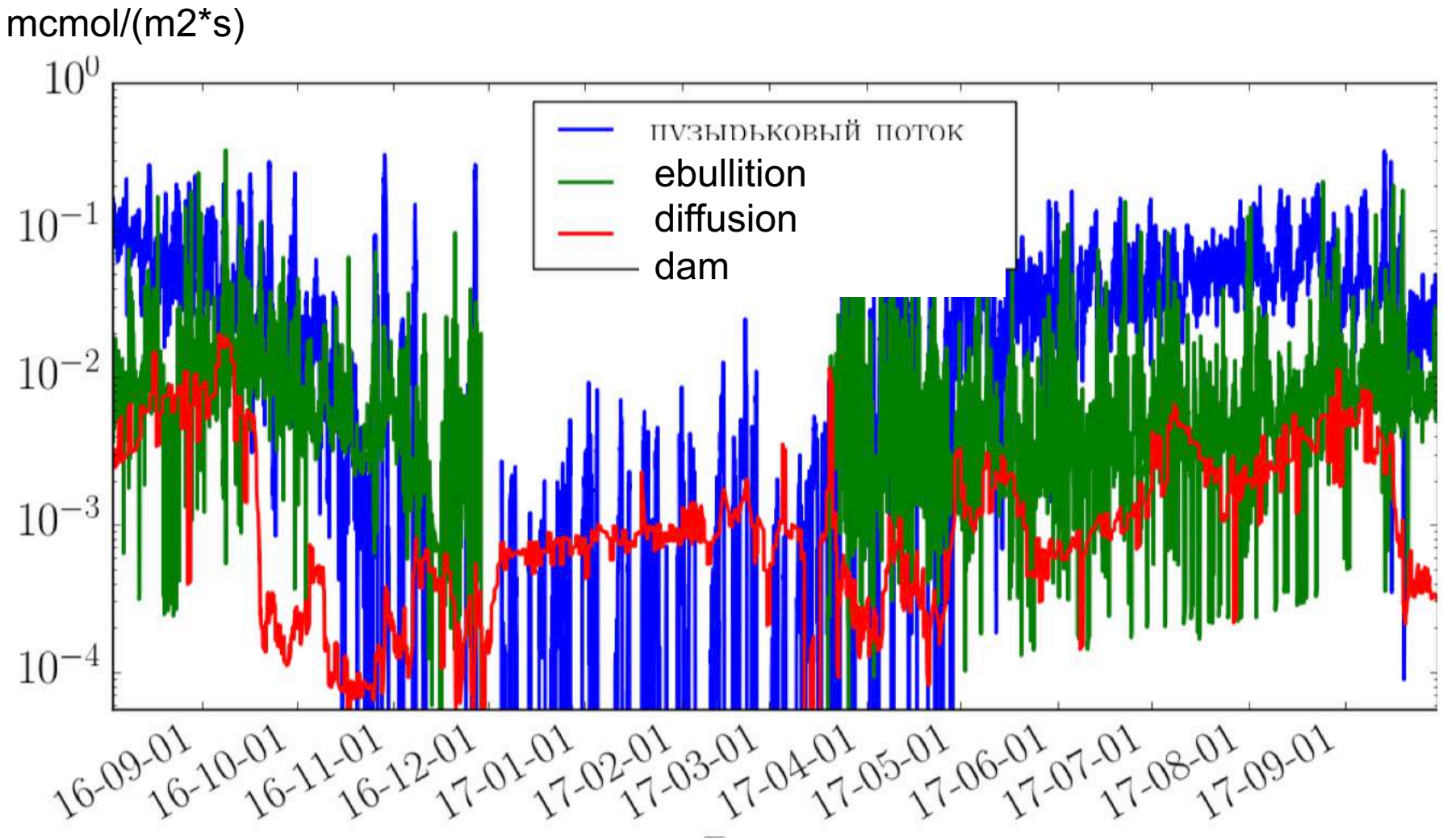

Total CH_4 flux from 1 August 2016 till 1 August 2017 is 570 Mt, where:
- ebullition 455 Mt/yr (80%),
- diffusion 87 Mr/yr (15%),
- dam flux 28 Mr/yr (5%).

ISIMIP project overview

climate projections
RCP scenarios from CMIP & CORDEX archives

Socio-economic input
SSP scenarios

Impact models global & regional

agriculture
biomes
coastal infrastructure
fisheries
agro-economics
water
Forests
health
energy
permafrost

- Synthesis of impacts at different levels of global warming
- Quantification of uncertainties
- Model improvement
- Cross-sectoral interactions
- Cross-scale intercomparison
- Focus topics (e.g. extreme events, adaptation)

Water (regional)
Valentina Krysanova
Fred Hattermann

Fisheries & Marine Ecosystems
Julia Blanchard (lead coordinator)

Energy Supply & Demand
Michelle van Vliet
Detlef van Vuuren
Victhalia Zapata Castillo

Regional Forests
Christopher Reyer

Permafrost
Anne Gädeke
Kirsten Thonicke
Eleanor Burke

Coastal Systems
Jochen Hinkel

Health
Veronika Huber (water-borne diseases and thermal stress)
Joacim Rocklöv (vector-borne diseases and malnutrition)

Lakes
Rafael Marce
Don Pierson
Malgorzata Golub
Wim Thiery

Global Biomes
Jinfeng Chang
Christopher Reyer

Agriculture Sector
Jonas Jägermeyr
Sam Rabin
Almut Arneth

Agro-economic Modelling
Hermann Lotze-Campen

Terrestrial Biodiversity
Thomas Hickler
Christian Hof

- Lakes regional
- Lakes global

ISIMIP3: lake methane sector

Requirements for the validation sites

VARIABLE NAME	*UNIT*	*RESOLUTION*	*COVERAGE*	*PRIORITY (1 is highest priority)*	*MANDATORY/ OPTIONAL*
LAKE TEMPERATURE (profiles)	K	daily or monthly	> 2 years	1	M
Total CH_4 flux to the atmosphere	mol/m^3	daily or monthly	> 2 years	1	M
Ebullition of CH_4	$mol/(m^2\ s)$	daily or monthly	> 2 years	2	O
Diffusive CH_4 flux	$mol/(m^2\ s)$	daily or monthly	> 2 years	2	O
CH_4 concentration (profiles)	mol/m^3	daily or monthly	> 2 years	2	M
Oxygen concentration (profiles)	mol/m^3	daily or monthly	> 2 years	3	O
C_{labile} (labile carbon density)	mol/m^3	daily or monthly	> 2 years	4	O
CO_2 concentration (profiles)	mol/m^3	daily or monthly	> 2 years	4	O
Total CO_2 flux to the atmosphere	mol/m^3	daily or monthly	> 2 years	4	O

Note that...

... 1D models do reproduce temperature profiles in many lakes well, but very few studies (if any) validated velocity and turbulence patterns produced by 1D models.

Internal seiche mixing parameterization in $k - \epsilon$ model

Goudsmit et al. 2002

- Shear production is generalized to include seiches $P = \nu_t M^2 + P_s$;
- TKE production by seiche-induced shear at lake's margins
  $P_s = -\frac{1 - C_{diss}\sqrt{C_{d,bot}}}{\rho_{w0} c A_b} \gamma \frac{1}{A} \frac{dA}{dz} N^2 E_s^{3/2}$, E_s - seiche energy;
- Seiche energy is derived from wind forcing: $\frac{dE_s}{dt} = \alpha A_0 \rho_a C_d (u^2 + v^2)^{3/2} - \gamma E_s^{3/2}$
- Stationary Richardson number (Burchard, 2002) may be derived for this case as
  $Ri_{st} = \frac{Pr \Delta c_{\epsilon 21}}{\Delta c_{\epsilon 23} - \nu_0^{-1} Pr C_s \Delta c_{\epsilon 21} (u^2 + v^2)^{3/2}} \approx 0.30$ for typical wind speed

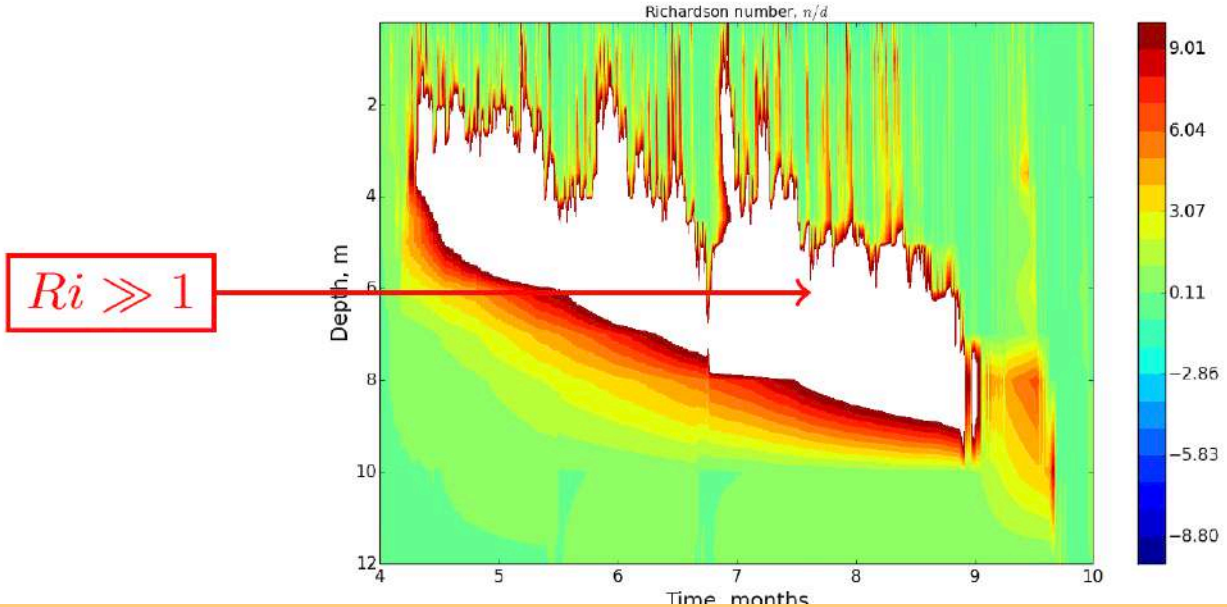

Svensson (1978) representation of barotropic seiches

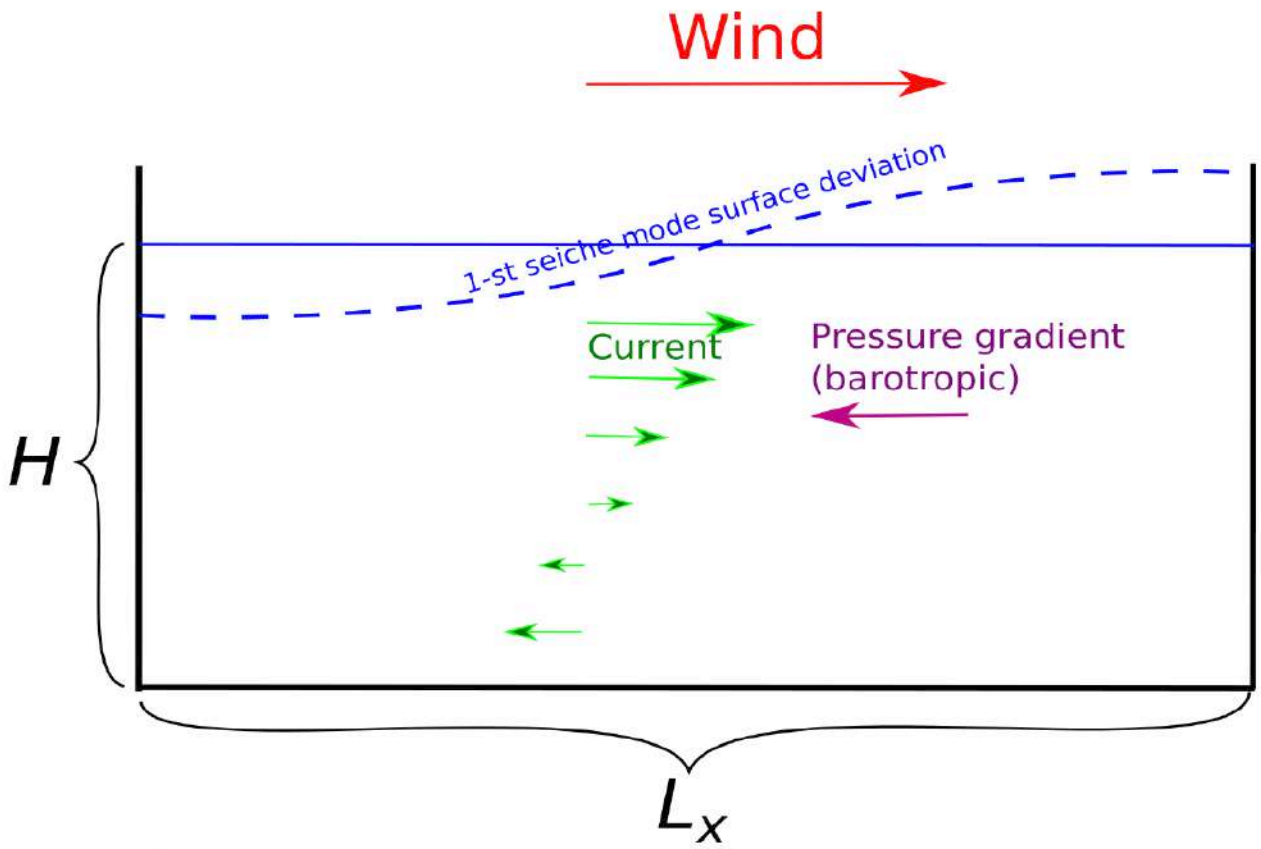

$$\overline{\left(\frac{1}{\rho_w}\frac{\partial p}{\partial x}\right)} = \frac{\rho_w g \pi^2 H}{L_x^2}\int_0^t \overline{u}dt', \quad \overline{\left(\frac{1}{\rho_w}\frac{\partial p}{\partial y}\right)} = \frac{\rho_w g \pi^2 H}{L_y^2}\int_0^t \overline{v}dt' \qquad (4)$$

Water is moved by wind, it changes the water surface elevation. The inclination of surface causes horizontal pressure gradient assuming hydrostatic equilibrium with constant water density – surface seiches.

The basic proposition

Svensson coupled 1D lake model to a single-layer seiche model.

What if coupling 1D lake model to a multilayer seiche model?

Adaptation of multilayer seiche model

Multi-layer seiche model
(Münnich et al., 1992)

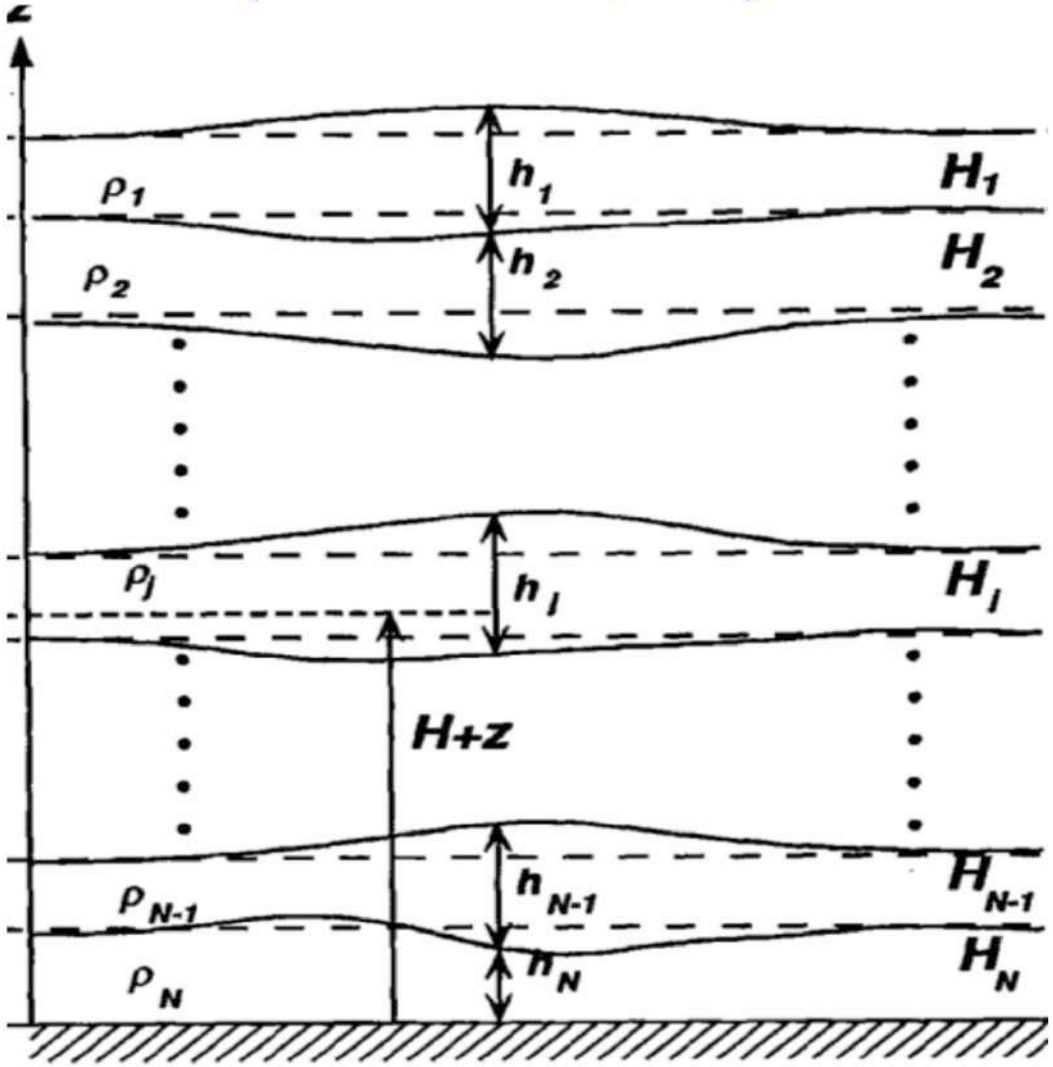

Extension of k-ϵ model

- 1-st horizontal seiche mode is shown in many studies to be the most energetic in lakes
- sssuming only 1-st horizontal mode, equations of multilayer model can be expressed in terms of horizontally-averaged speed:

$$\frac{\partial \overline{u_j}}{\partial t} = -\frac{\pi g}{2L\rho_j} \sum_{k=1}^{N} \rho_{\min(j,k)} \Delta_x \overline{h'_k},$$

pressure gradient

$$\frac{\partial \Delta_x \overline{h'_j}}{\partial t} = \frac{2\pi H_j}{L} \overline{u_j}, \quad j = \overline{1, N}$$

– mass conservation equation.

Coupling of multilayer seiche model with 1D model

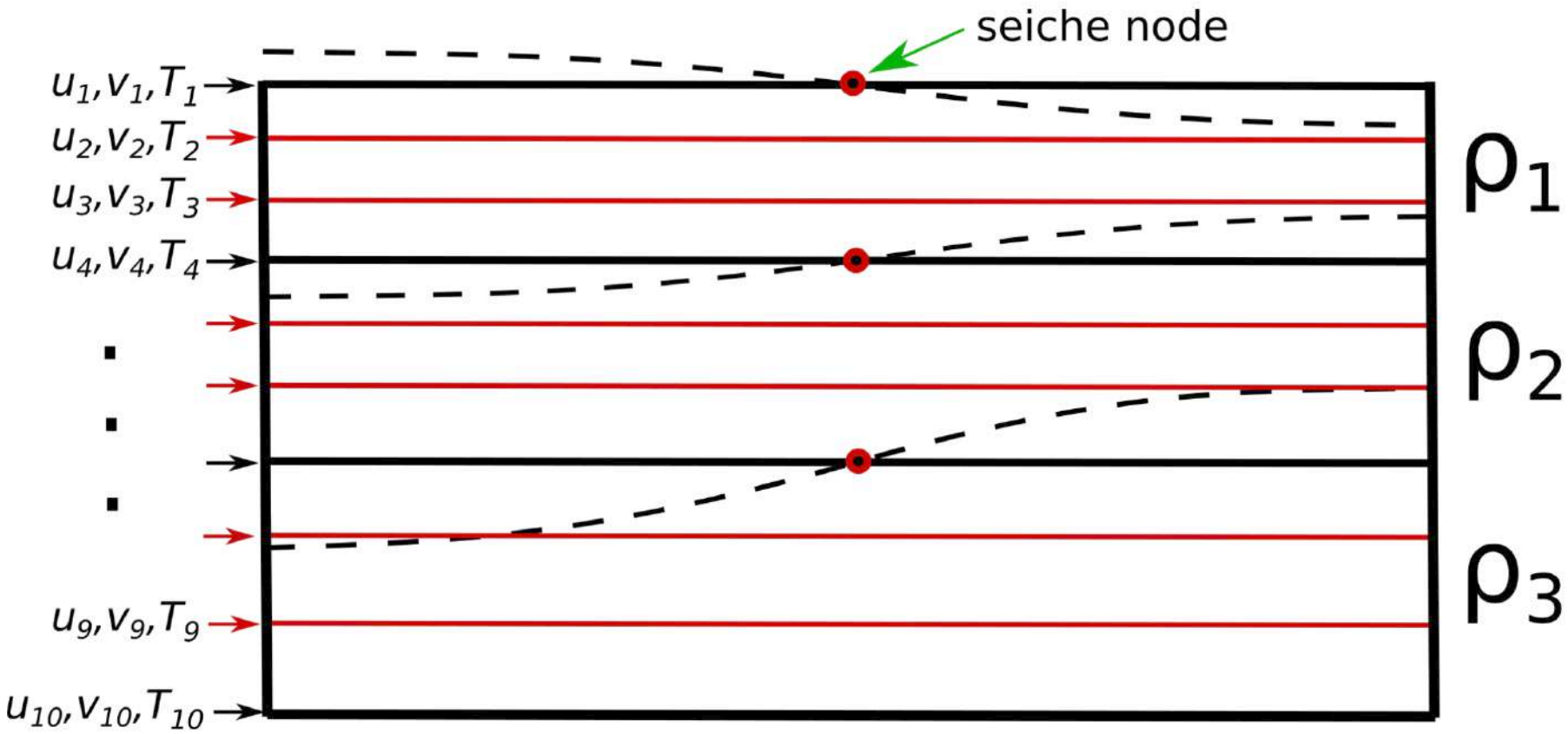

At each time constant-density layers are identified in the 1D model profile. Then, the horizontal pressure gradient in 1D model may be evaluated involving 1-st mode seiche model, as shown at the next slide ...

Momentum equations of the coupled model

$$\frac{\partial u}{\partial t} - \frac{\partial}{\partial z}\nu\frac{\partial u}{\partial z} - lv = -\frac{\pi g}{2L_x\rho_j}\sum_{k=1}^{N}\rho_{\min(j,k)}\Delta_x\overline{h'_k}, \quad j : z \in [z_j, z_{j+1}), \tag{5}$$

$$\frac{\partial v}{\partial t} - \frac{\partial}{\partial z}\nu\frac{\partial v}{\partial z} + lu = -\frac{\pi g}{2L_y\rho_j}\sum_{k=1}^{N}\rho_{\min(j,k)}\Delta_y\overline{h'_k}, \quad j : z \in [z_j, z_{j+1}) \tag{6}$$

$$\frac{d\Delta_x\overline{h'_j}}{dt} = \frac{2\pi H_j}{L_x}\overline{u_j}, \quad j = \overline{1,N}, \tag{7}$$

$$\frac{d\Delta_y\overline{h'_j}}{dt} = \frac{2\pi H_j}{L_y}\overline{v_j}, \quad j = \overline{1,N}. \tag{8}$$

where $(\overline{u_j}, \overline{v_j}) = H_j^{-1}\int_{z_j}^{z_{j+1}}(u,v)dz$.

Highlighted are the new terms to equations of 1D model, representing horizontal pressure gradient of the 1-st seiche mode.

Free baroclinic seiches in the model

Spatio-temporal variability of x-speed component, in the experiment with free gravitational oscillations. The vertical structure corresponds to H1V1 seiche (baroclinic seiche)

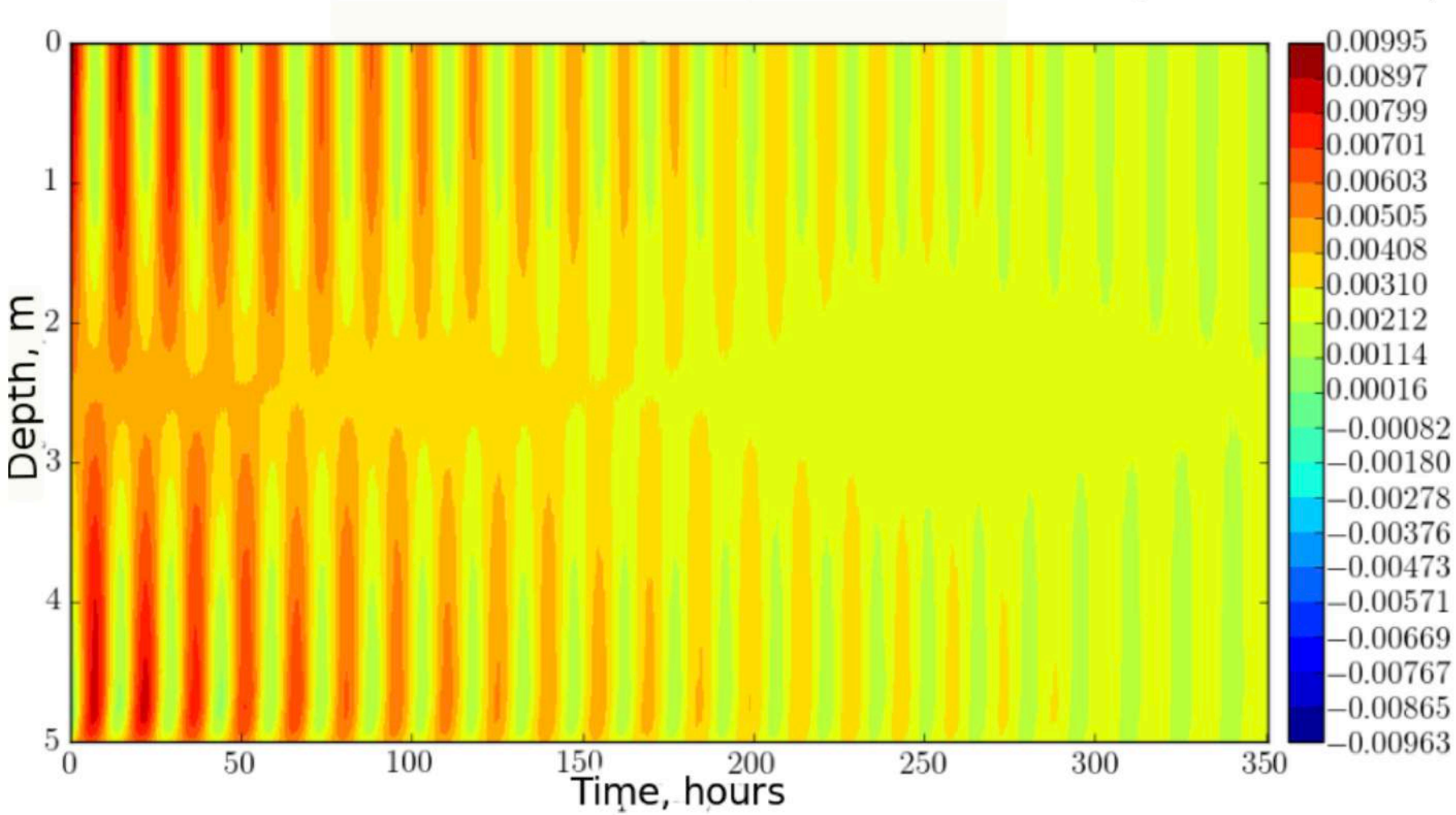

Period ≈ 15.5 hours, solution of Sturm-Liouville problem provides 14.7 hours for H1V1 mode

Barotropic seiches in the model

Spatio-temporal variability of x-speed component, during one period of H1V1 mode. High-frequency oscillations correspond to mode H1V0 (barotropic seiche)

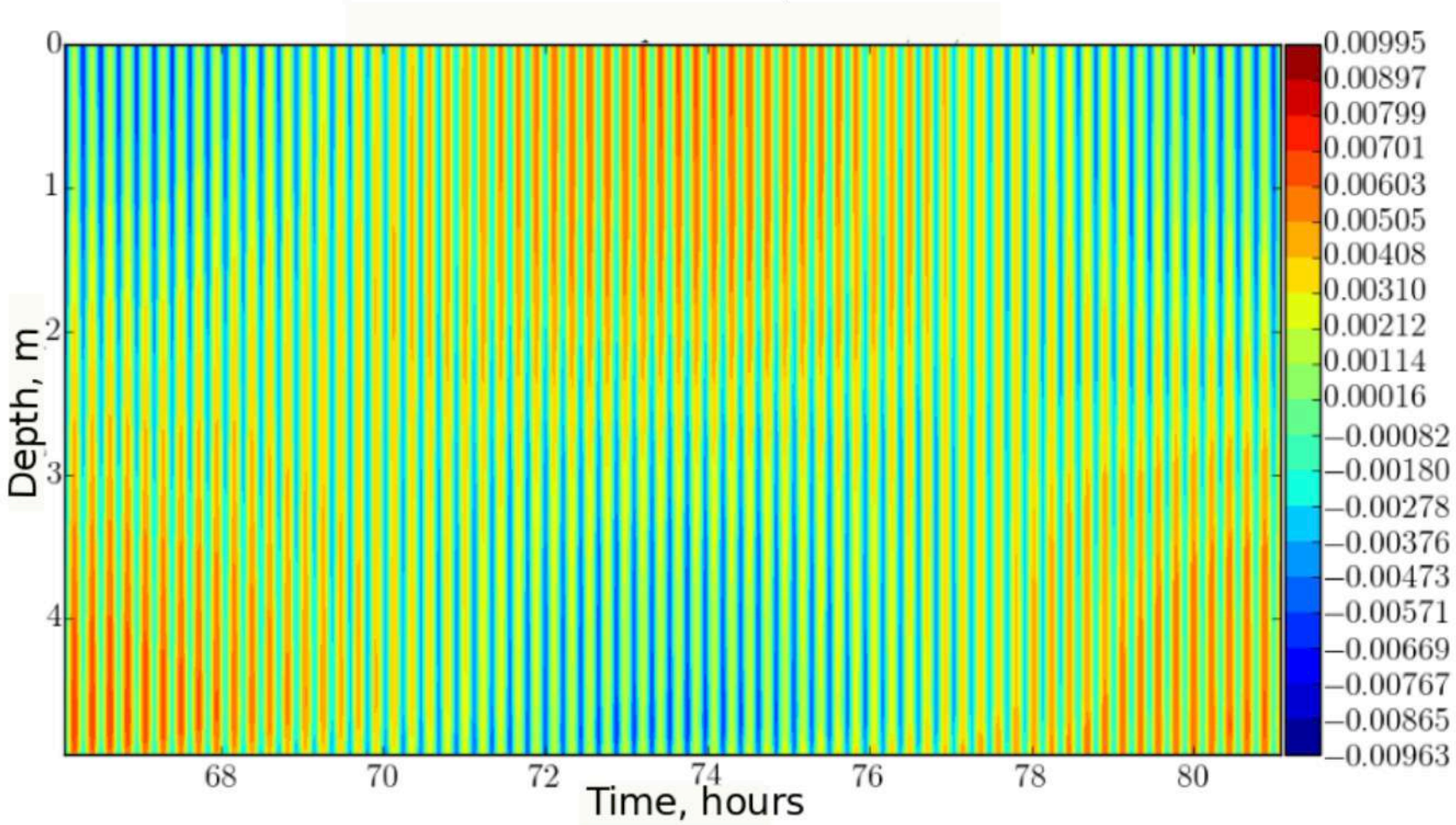

Modelling of seiche-caused temperature fluctuations

Estimating the seiche-induced temperature fluctuations
in the fixed locations of a lake

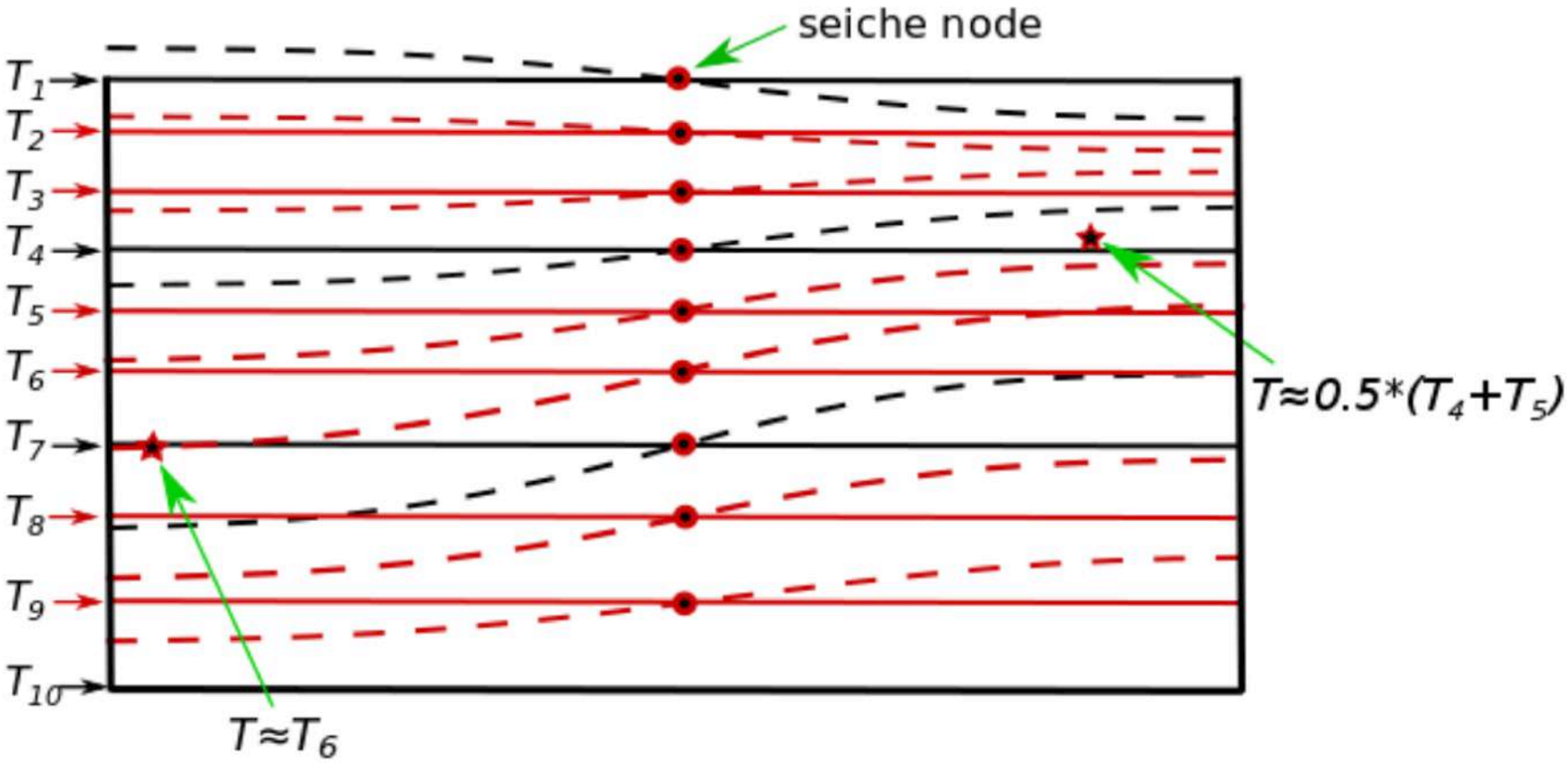

Model levels are treated here as fluctuating material surfaces. Temperature is linearly interpolated between two seiche-displaced levels, to which the measurement point is currently in between

Kato-Phillips experiment as a model benchmark

(Kato and Phillips, 1969)

- no rotation, no horizontal pressure gradient
- linear initial density profile
- constant stress (momentum flux) at the surface
- well-known analytic laws of mixed-layer deepening (Price, 1979)
- widely used benchmark for turbulent closures (Burchard et al., 2002; Reffray et al., 2015):

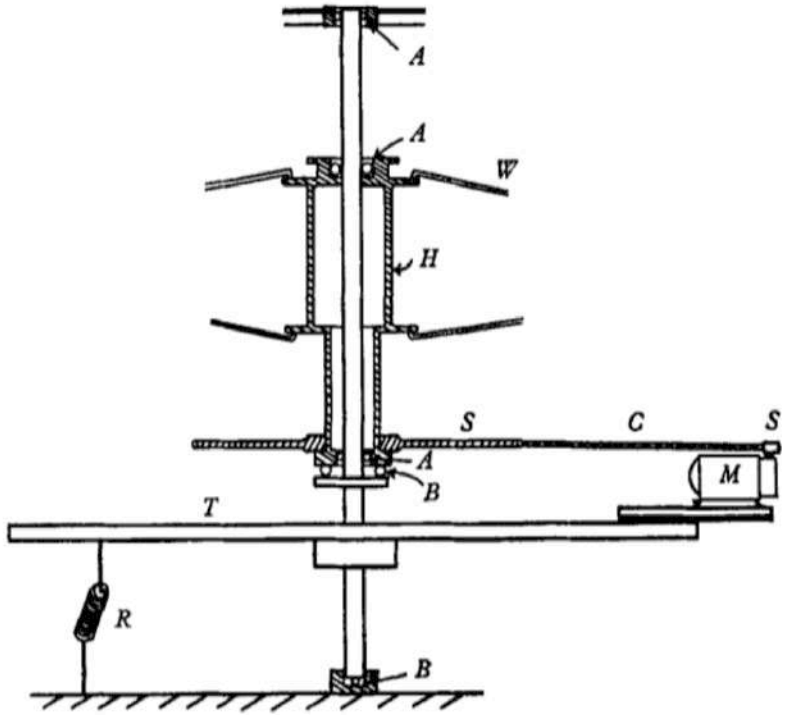

The simplest prototype of summertime mixed-layer penetration into thermocline in lakes

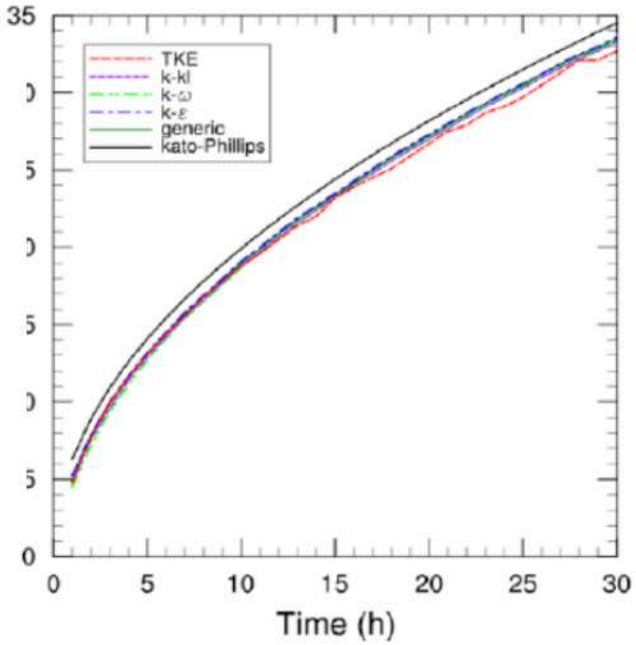

Kato-Phillips experiment

- no heat and radiation flux at the top and bottom boundaries
- constant surface wind stress 0.01 N/m^2
- linear stable initial temperature profile, 2 K/m
- no morphometry
- no rotation
- depth 7 m, 60 vertical computational layers
- 10 days of the model integration

Kato-Phillips experiment extensions

- including Coriolis force
- including horizontal pressure gradient, resulting from boundedness of the basin
- including Coriolis force and horizontal pressure gradient

We conduct extended Kato-Phillips experiments with 1D model including seiches, with typical depth, summer stratification and wind forcing of midlatitude lakes.

Basic presumption: The effect of rotation on mixing should dominate that of seiching at $L \gg L_R$, and vice versa if $L \ll L_R$; in a case $L \sim L_R$ these effects should be comparable.

$L_R \doteq \frac{NH}{l}$ – Rossby internal deformation radius.

Mixed-layer depth

The horizontal dimensions of a lake $L = L_R$

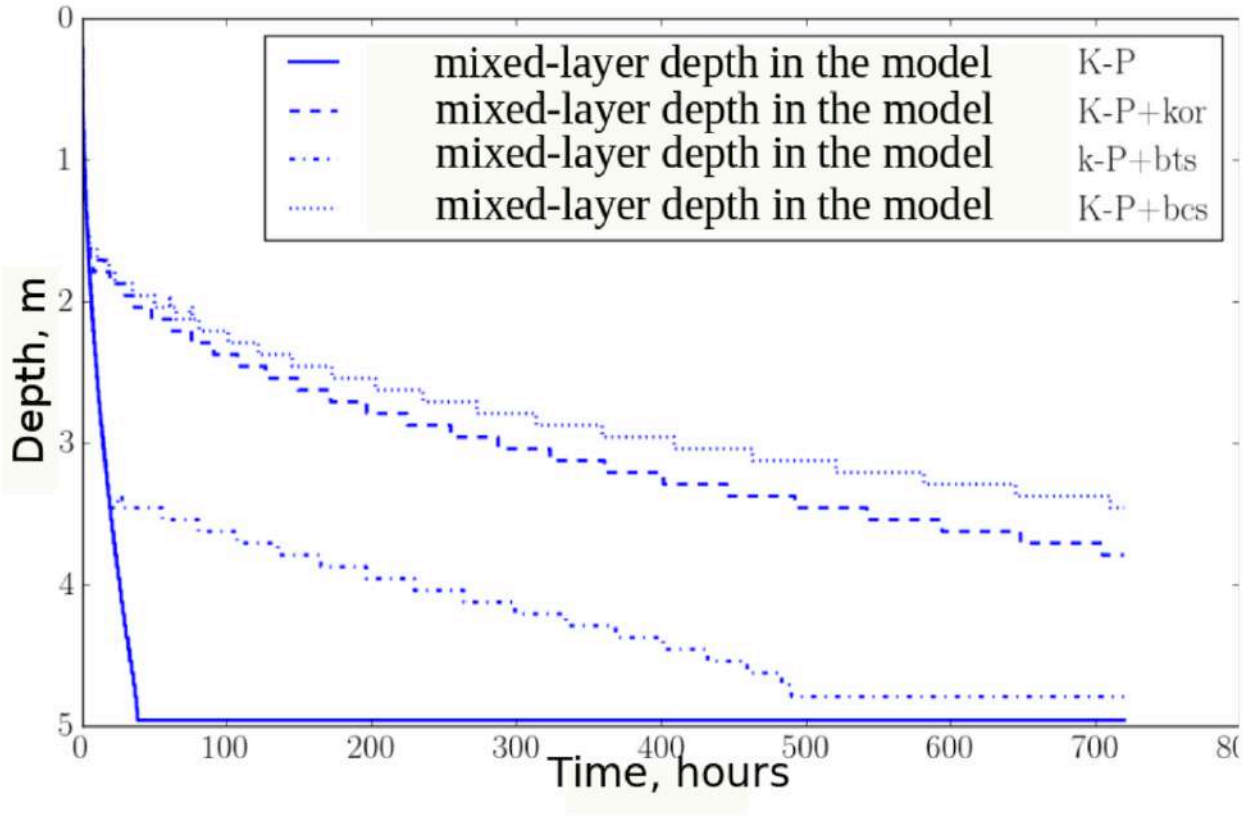

K-P – Kato-Phillips experiment,
K-P+kor – Kato-Phillips experiment with Coriolis force,
K-P+bts – Kato-Phillips experiment with barotropic seiches,
K-P+bts – Kato-Phillips experiment with baroclinic seiches

- The presence of horizontal pressure gradient opposed to surface wind stress limits the speed in the upper mixed layer and thus hinders the penetration of the mixed layer into stratified stratum below
- Rotation and seiching impose similar suppressing effect on vertical mixing
- Svensson (barotropic) seiche parameterization is not sufficient to produce "correct" mixing

Mixed-layer depth

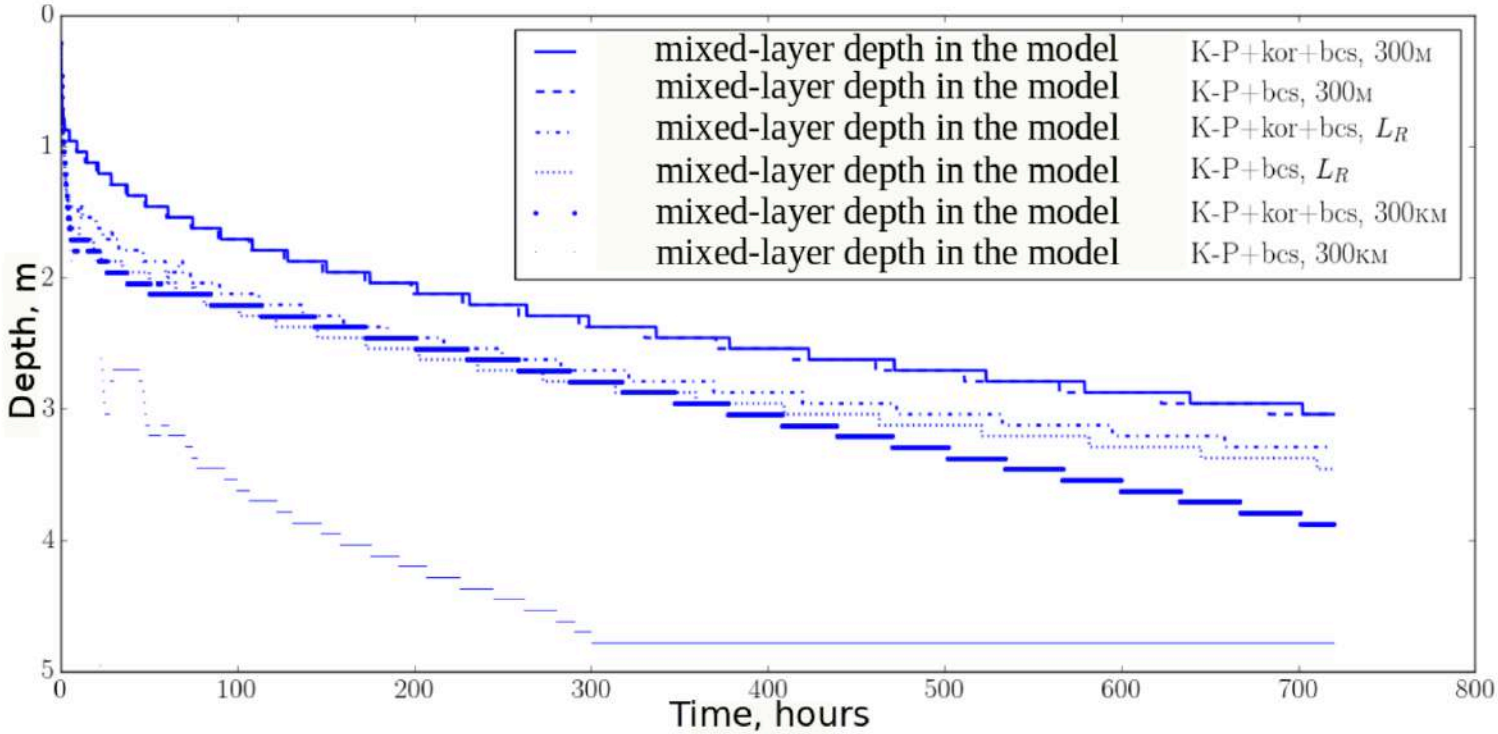

Kato-Phillips experiment with Coriolis force and baroclinic seiches at different lake sizes:
300 m×300 m. $L_R \times L_R$ and 300 km×300 km ($L_R \approx$2.77 km)

- Coriolis force plays overwhelming role in mixing compared to seiching only for the lake size $L \gg L_R$
- For small lakes $L < L_R$, Coriolis force alone causes insufficient damping of seasonal mixed-layer deepening

Kato-Phillips experiment results: Standard k-ϵ model

Time-depth distribution of velocity

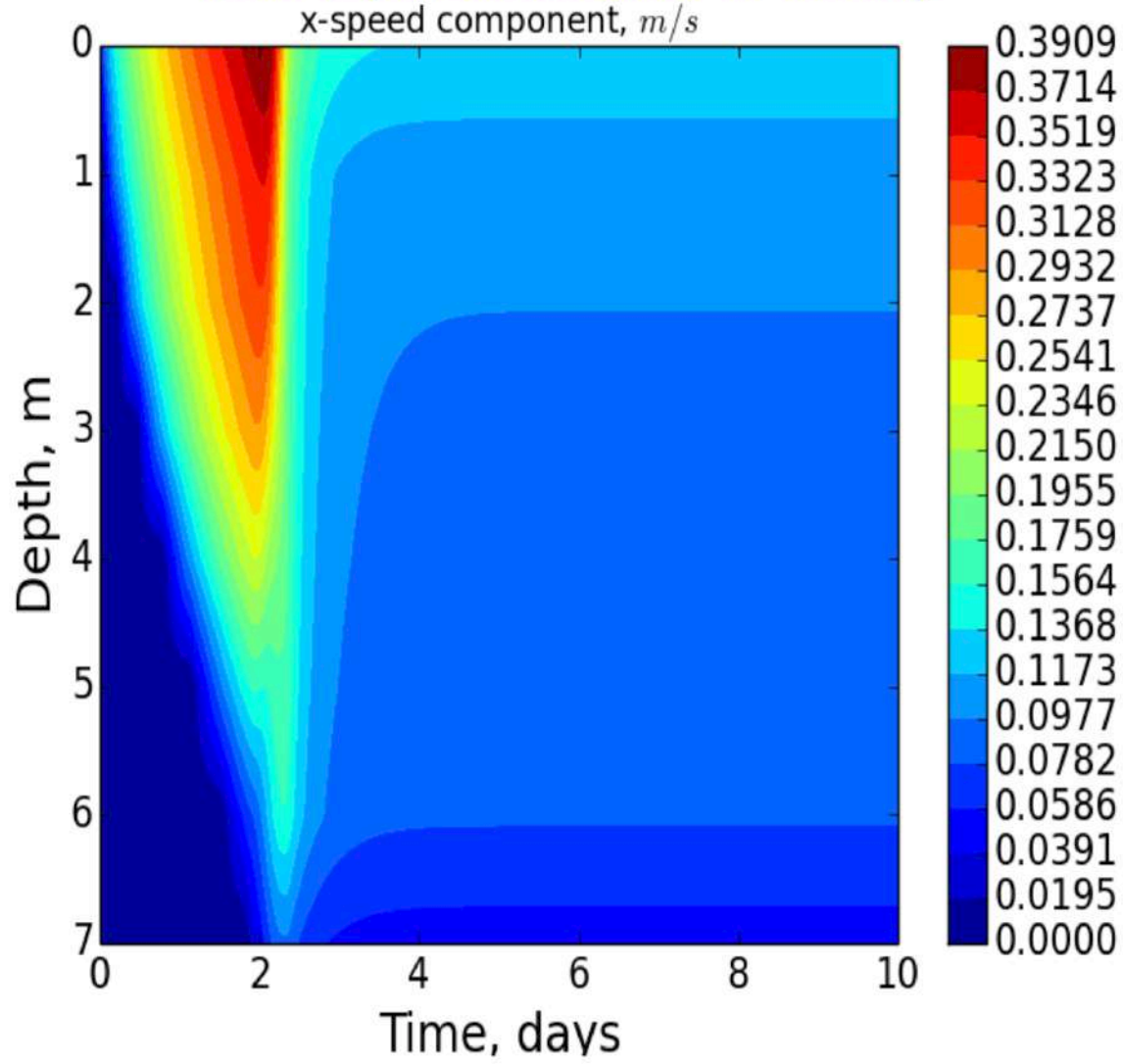

Temperature and eddy conductivity profiles 9-th day

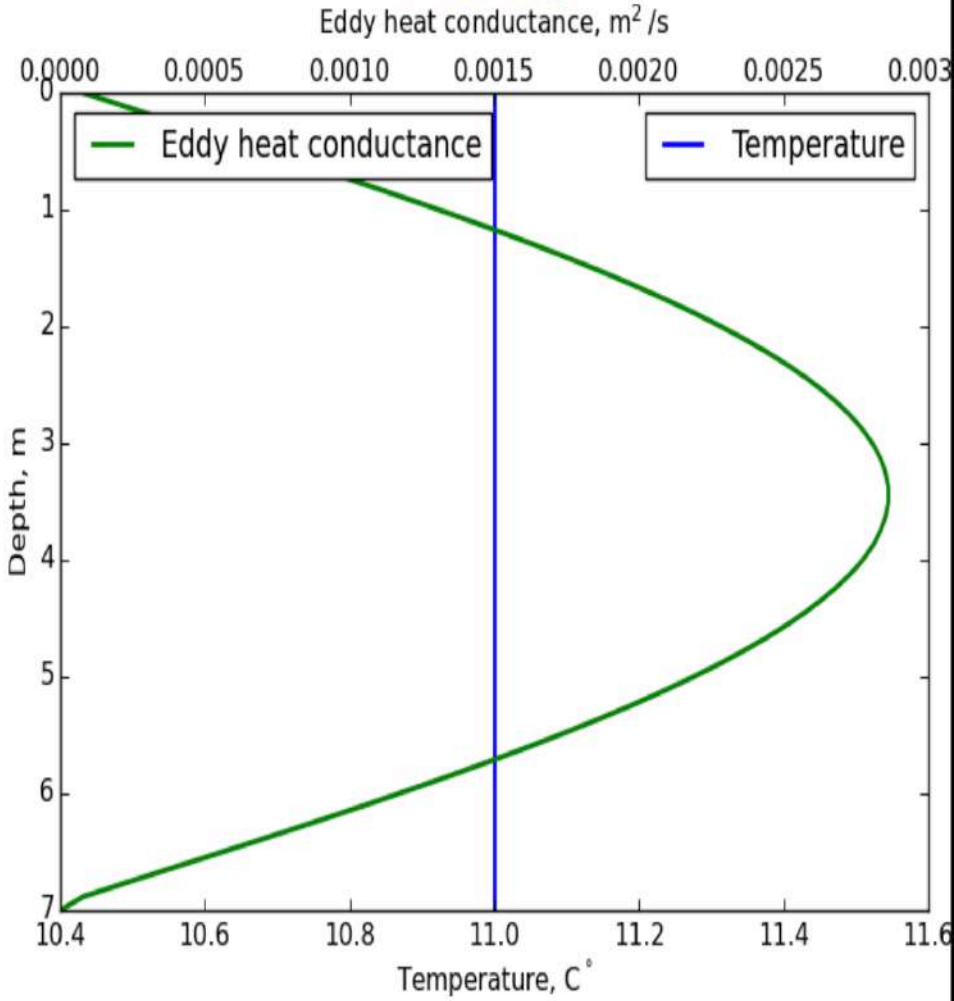

After complete mixing of temperature the flow is classical Cuette flow

he deepening of the mixed layer follows well the know formula $H_{ML} = 1.05 u_{*w} N_0^{-1/2} t^{1/2}$ (Price, 1979)

Kato-Phillips experiment: k-ϵ model + baroclinic seiches

Time-depth distribution of velocity

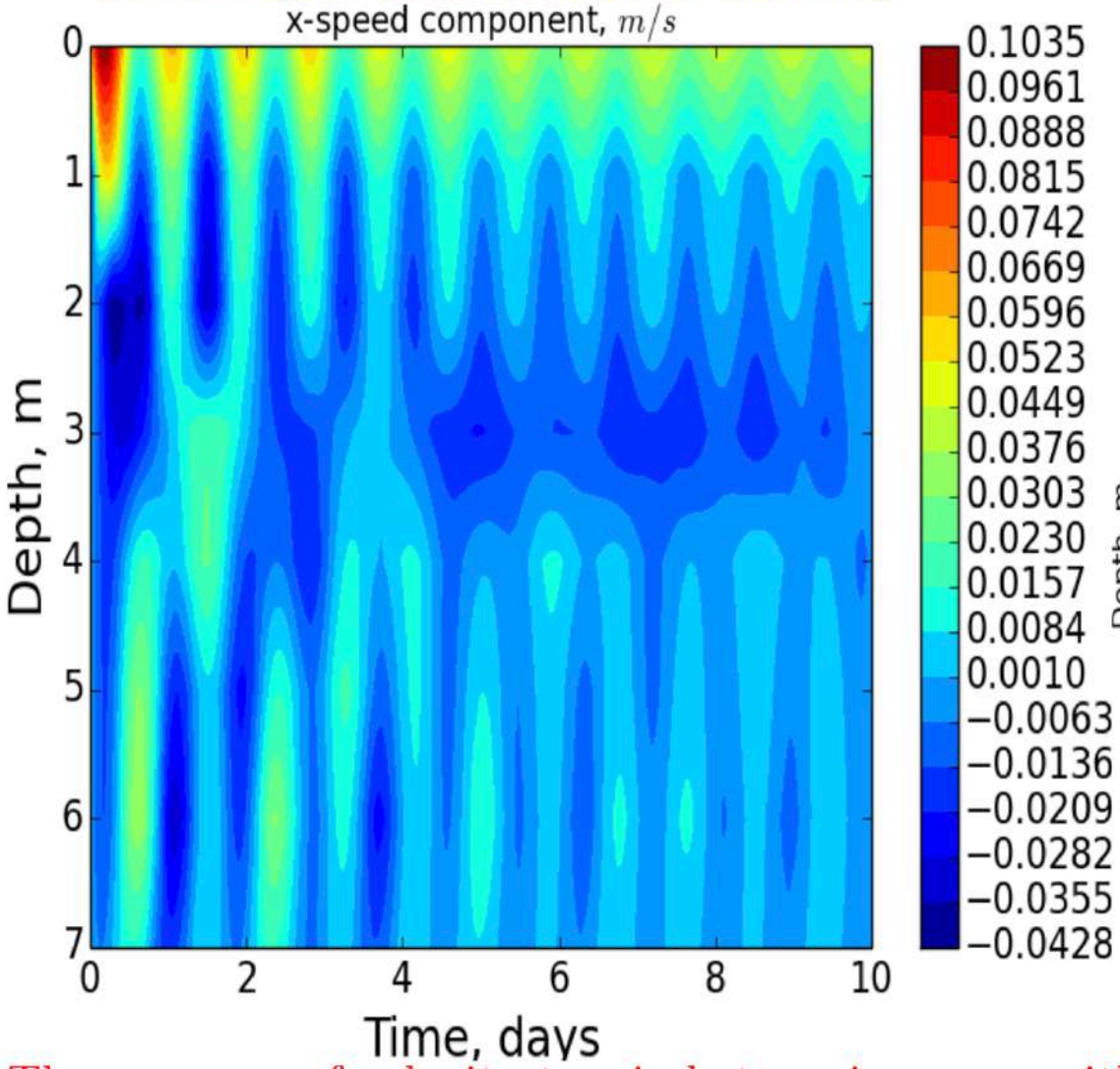

Temperature and eddy conductivity profiles, 9-th day

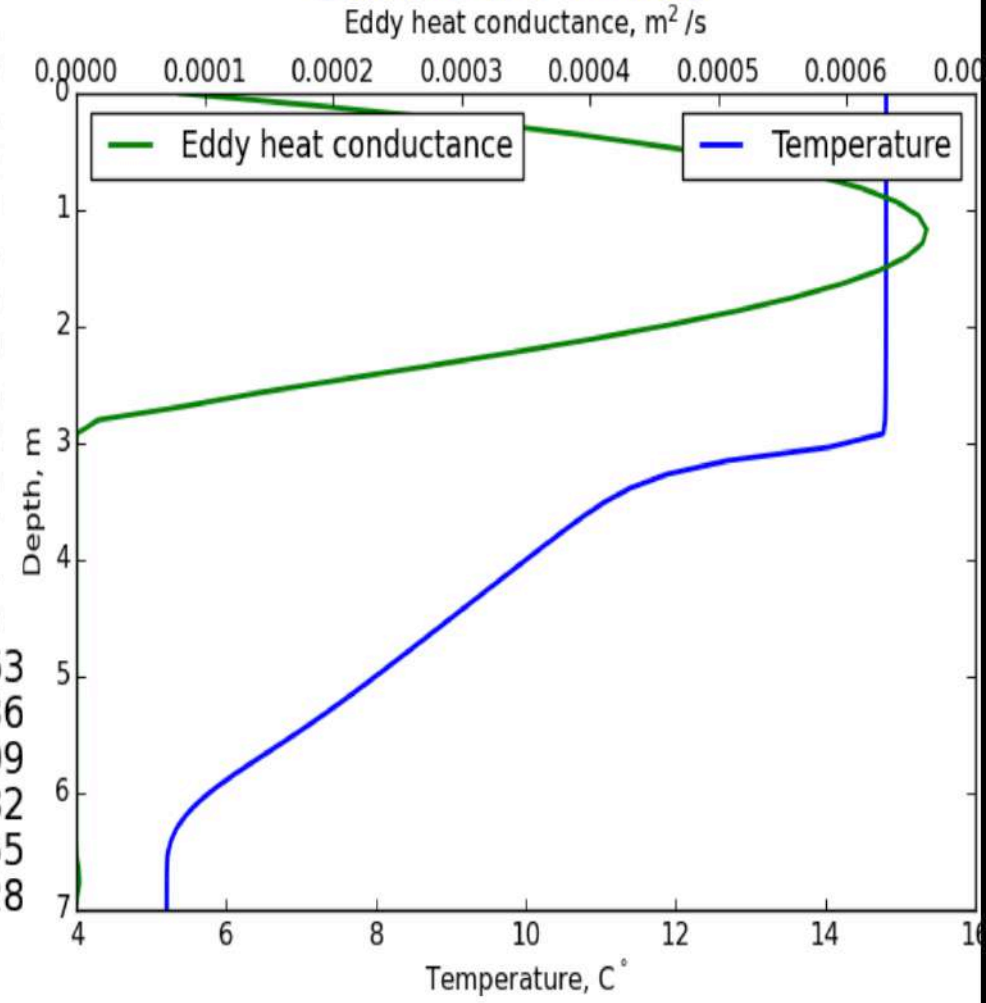

The response of velocity to wind stress is waves, with dominating 1-st vertical mode, ~ 1 day period. The thermocline is preserved, with both surface and bottom mixed layer present.

Implication for conventional 1D models

- Conventional 1D models including Coriolis force are fair in simulation of vertical mixing for lakes with $L \sim L_R$ and larger, due to minor-to-moderate contribution of pressure gradient forces on the lake dynamics. For lakes with $L \sim 0.1 L_R$, 1D models lacking pressure gradient force (seiches) should overestimate vertical mixing
- Only including pressure gradient force in 1D model allows to reproduce bottom boundary layer created by bottom current

The effect of seiches on mixing in Lake Valkea-Kotinen

Coriolis force OFF, seiches OFF

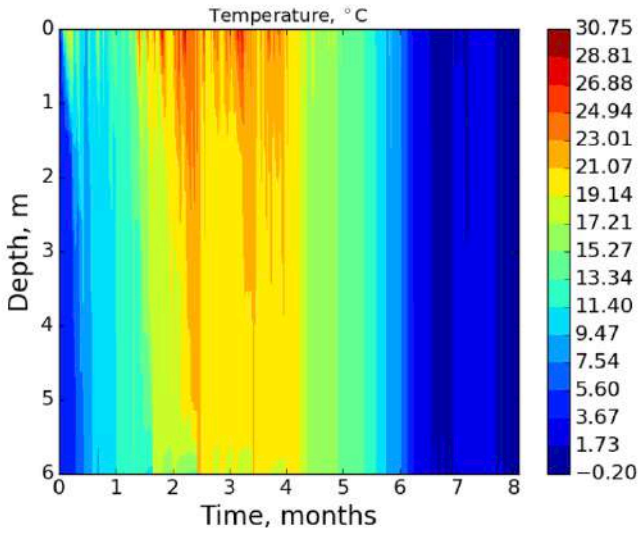

Coriolis force ON, seiches OFF

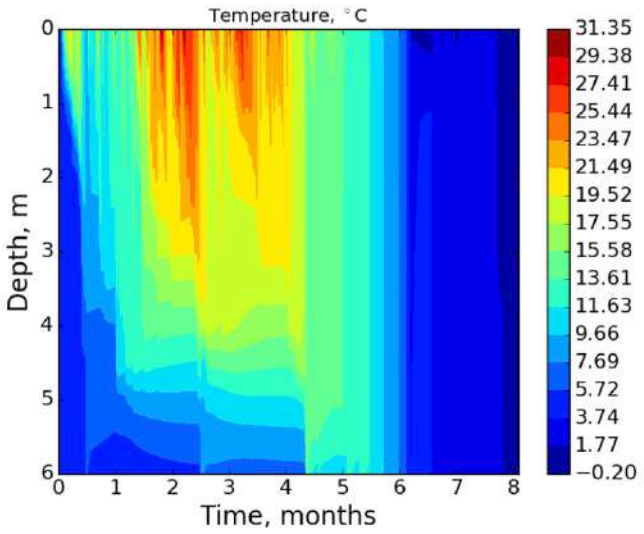

Coriolis force ON, seiches ON

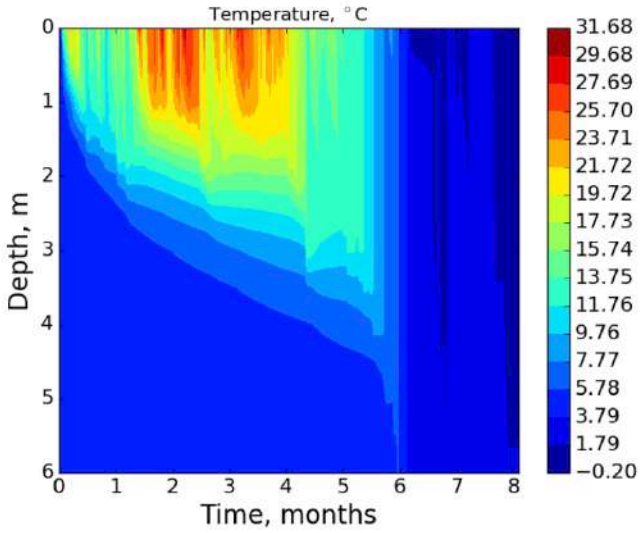

Measurements

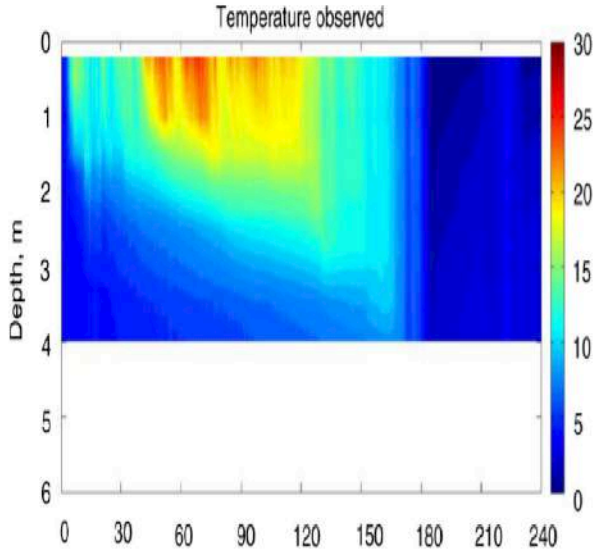

The lake size
≈100 m×400 m

Seiche parameterization makes profound effect on mixed-layer depth, along with mechanisms related to limited wind fetch and presence of forest (Stepanenko et al., Tellus A, 2014)

Why the mixing is suppressed by rotation and seiching?

- In classical Kato-Phillips setup, the friction is zero at the base of mixed layer, leading to continuous increase of total momentum in mixed layer (under constant momentum flux from the atmosphere), the shear production of TKE and mixed-layer deepening until complete mixing of temperature and achieving stationary Cuette flow (where the momentum flux at the top is compensated by friction at the bottom)
- In both cases of rotation and seiching quasi-stationary oscillatory velocity patterns are established where Coriolis and pressure gradient terms (respectively) "consume" the constant momentum flux from the atmosphere

THE KATO-PHILLIPS EXPERIMENT[6] & SEICHE INFLUENCE ON MIXING

$\mathbf{H}$ = 10 m, $\mathbf{t_{max}}$ = 7 days, $\boldsymbol{\partial T/\partial z}$ = 1,5 °C/m, $\boldsymbol{\tau}$ = 10^{-2} N/m^2

(Gladskikh et al., Water Resources, 2021)

$$MLD\,(t) = \frac{1.05\,u_*\sqrt{t}}{\sqrt{N(t=0)}}$$ [7]

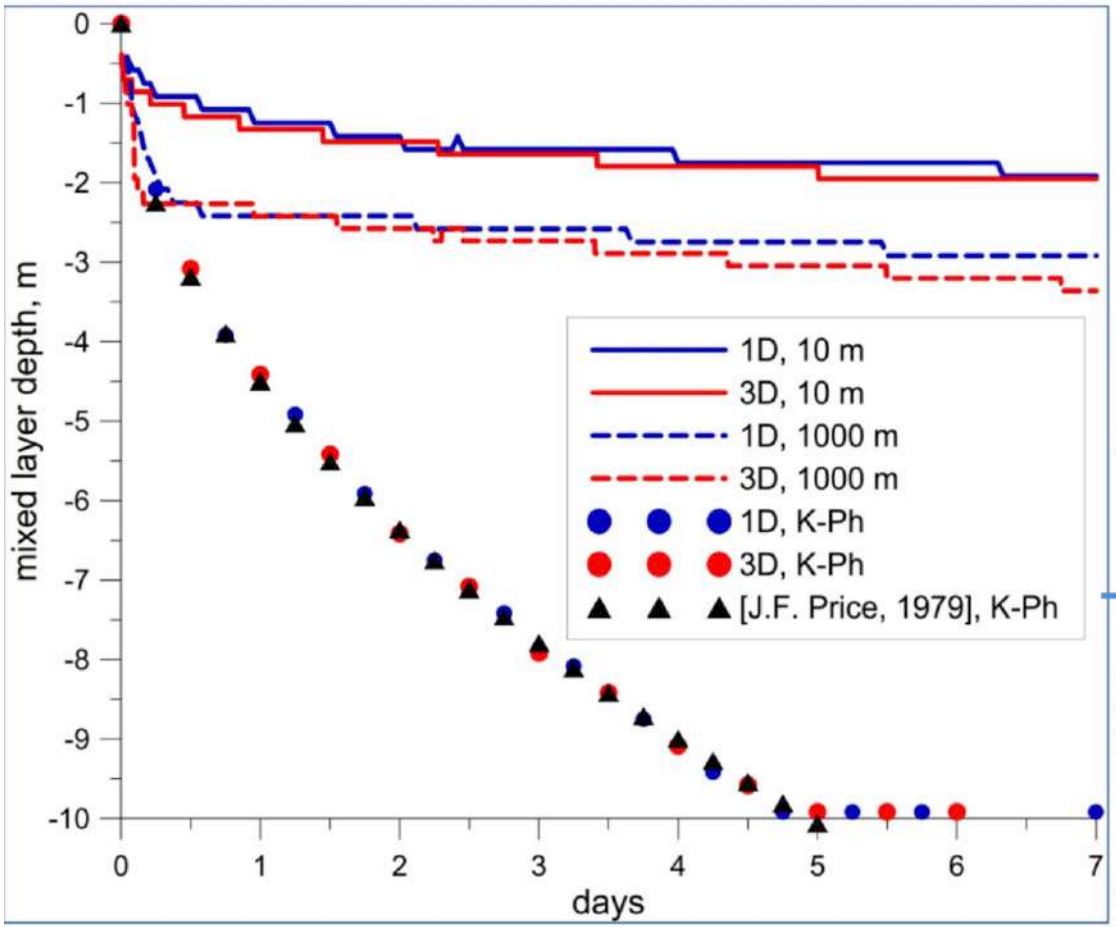

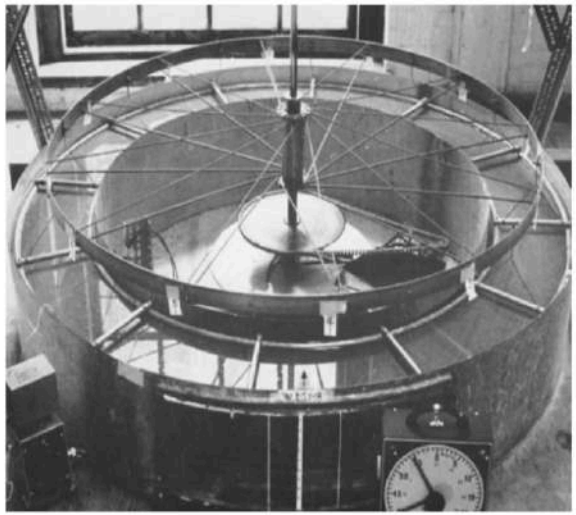

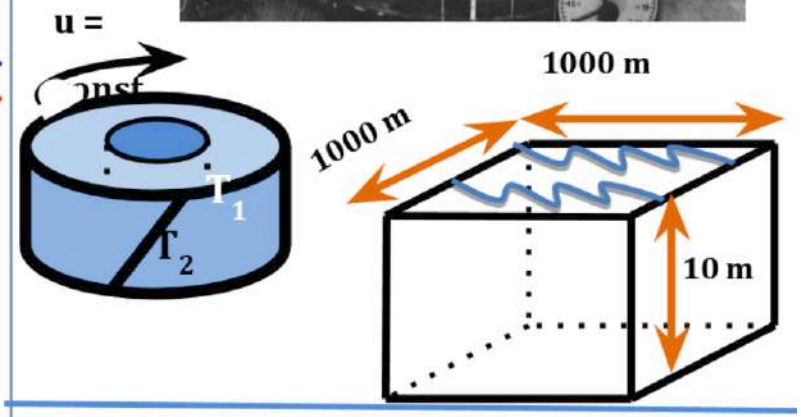

[6] Kato, H., Phillips, O.M., On the penetration of a turbulent layer into stratified fluid // Journal of Fluid Mechanics. 1969V.37, №4. p. 643

[7] Price, J.F., 1979. On the scaling of stress-driven entrainment experiments. Journal of Fluid Mechanics. V.90, №4. p. 509

TEMPERATURE & VELOCITY DISTRIBUTION

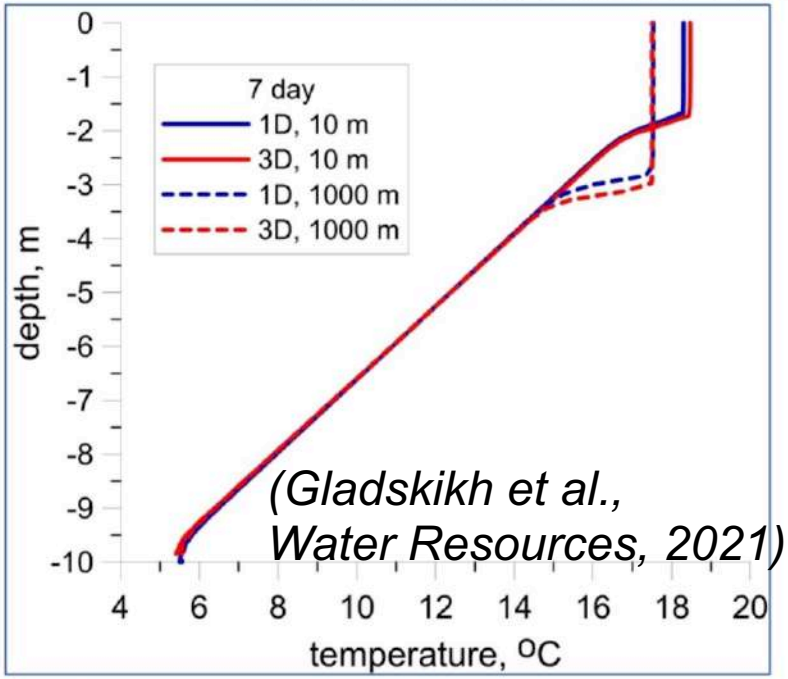

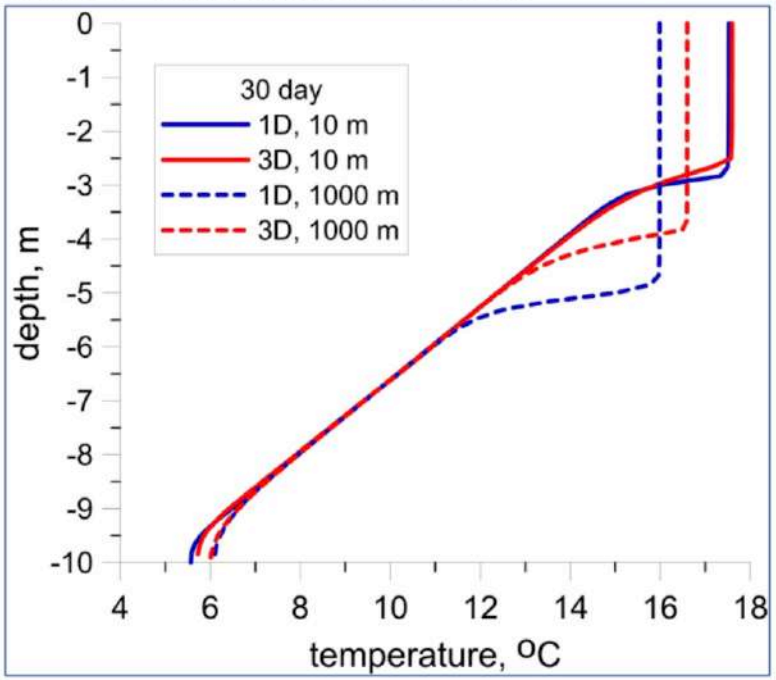

(Gladskikh et al., Water Resources, 2021)

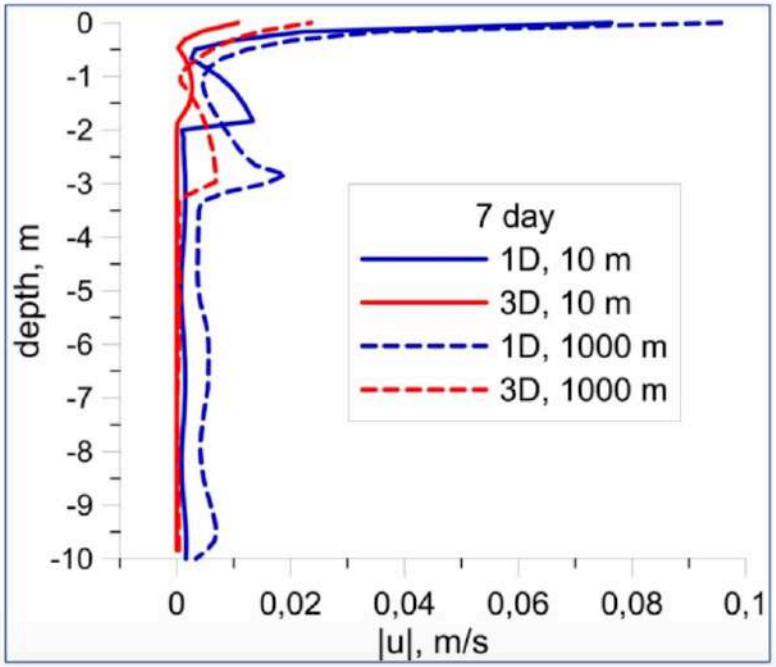

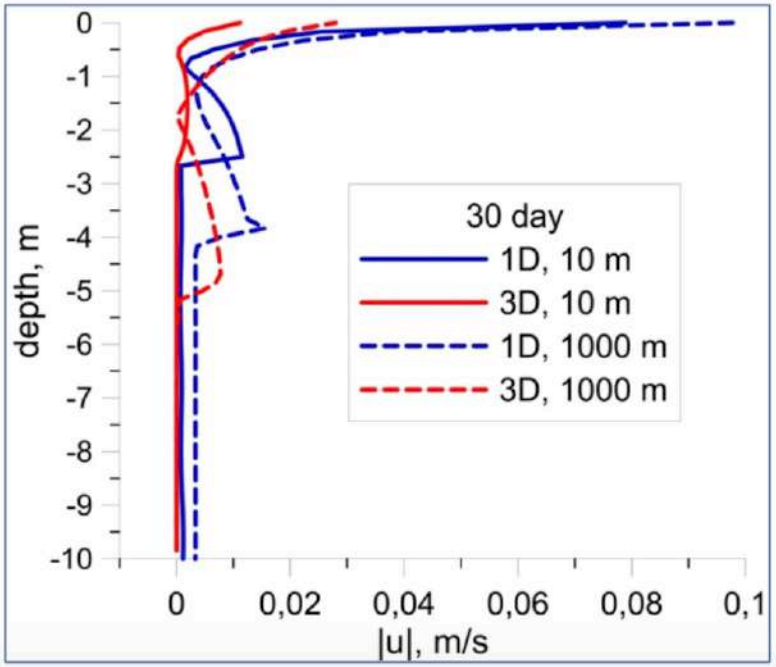

EDDY VISCOSITY

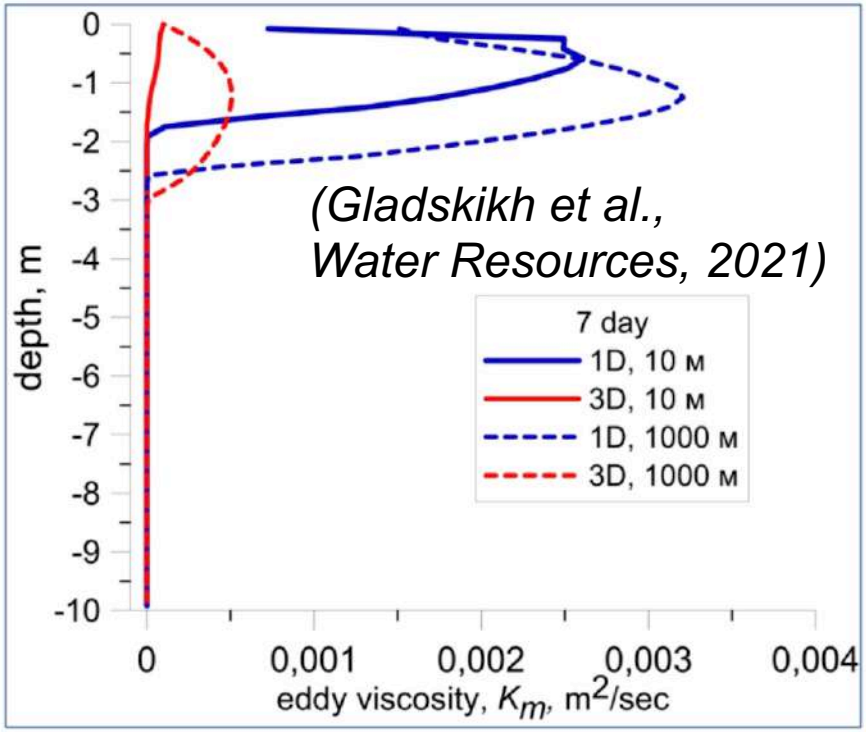

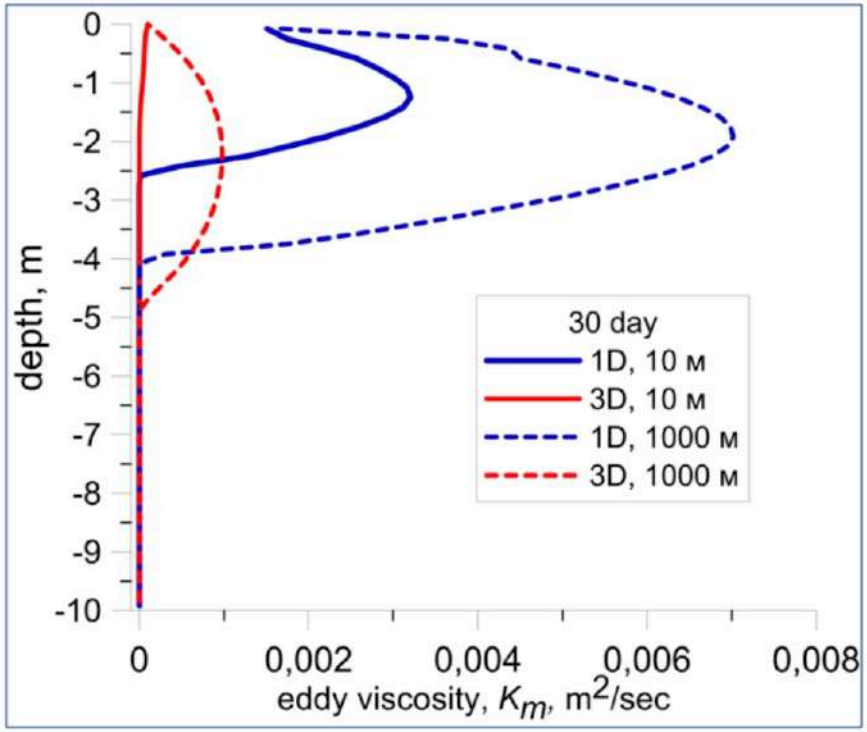

• A series of numerical experiments demonstrates that **the horizontal sizes of a reservoir play a significant role in the dynamics of mixing**: the thickness of the mixed layer increases more slowly in small water objects than in large ones, where internal wave oscillations play insignificant role compared to Coriolis force.

• The LAKE model with the accounting of seiches allows us to correctly reproduce the processes in most real inland water objects.

Barotropic pressure gradient and seiches

Barotropic (surface) seiches are lake surface and related velocity oscillations after strong wind events.

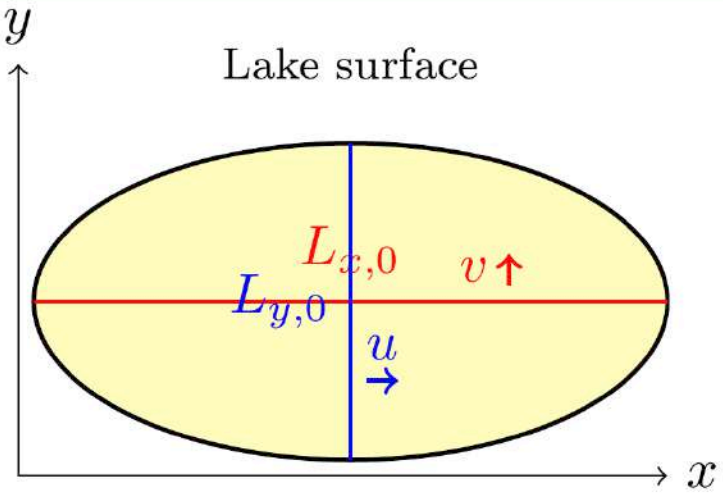

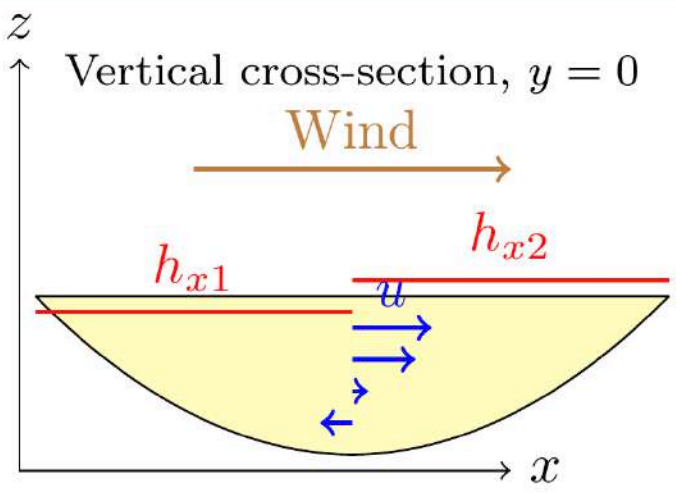

Turbulent kinetic energy profile (modeled), June 2013, Kuivajarvi Lake, seiches produce TKE near bottom

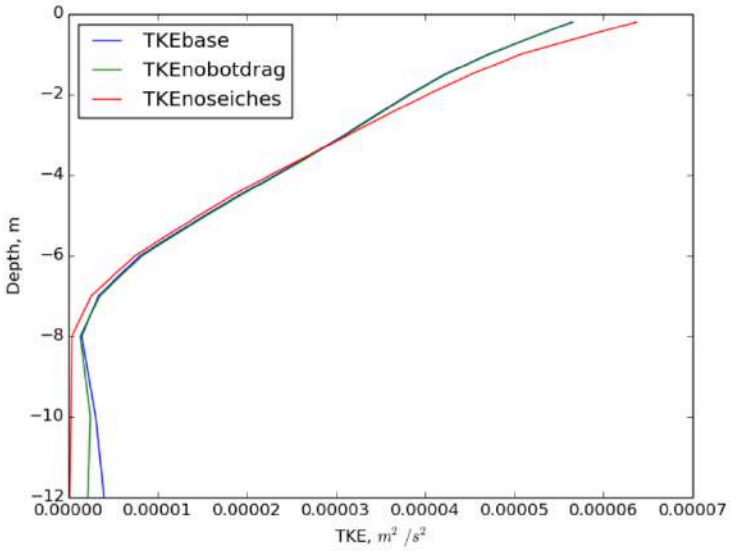

Mass conservation

$$\begin{cases} \frac{dh_N}{dt} A_0(t) = -\frac{dh_S}{dt} A_0(t) = 2\int_0^1 v L_{W-E} h d\xi, \\ \frac{dh_E}{dt} A_0(t) = -\frac{dh_W}{dt} A_0(t) = 2\int_0^1 u L_{S-N} h d\xi, \end{cases}$$

Barotropic pressure gradient force

$$\begin{cases} g\overline{\frac{\partial h_s}{\partial x}} \approx \frac{g\pi^2}{4} \frac{h_E - h_W}{L_{W-E,0}}, \\ g\overline{\frac{\partial h_s}{\partial y}} \approx \frac{g\pi^2}{4} \frac{h_N - h_S}{L_{S-N,0}}. \end{cases}$$

Surface oscillations in the model

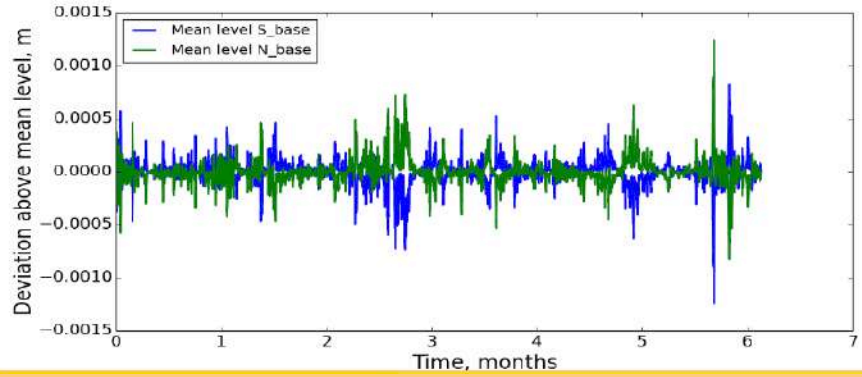

Seiche parameterization

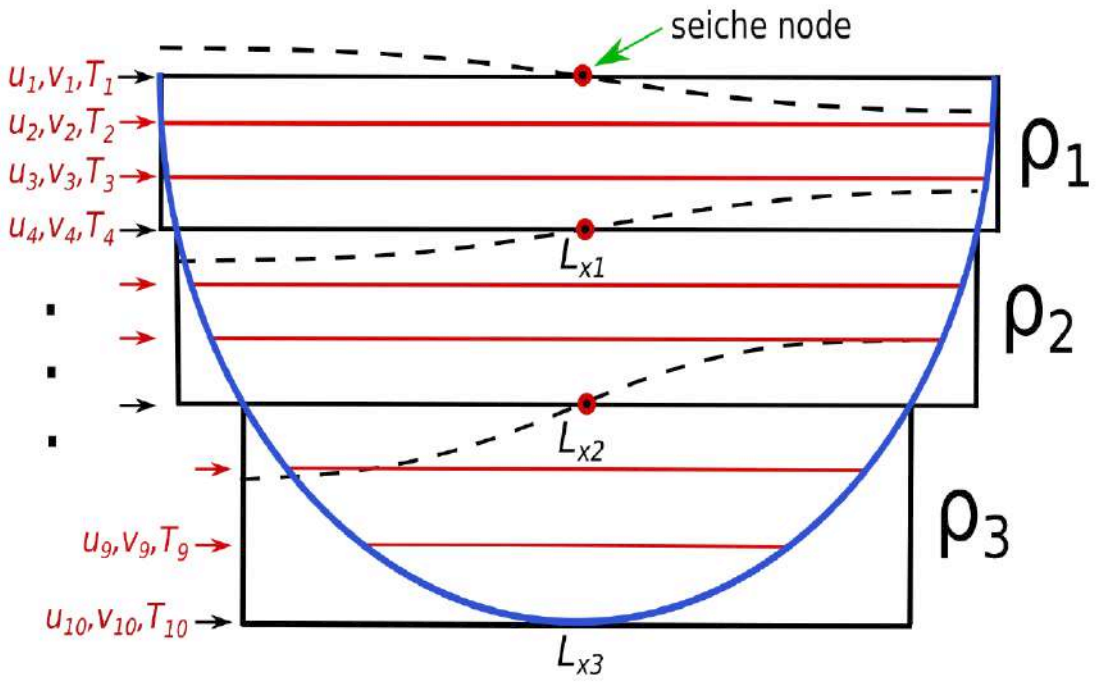

Available potential energy – quadratic from in $\Delta_x h'_k$, $\Delta_y h'_k$,

$$a_{kj} = b_{kj} = \sqrt{\frac{L_{xk} L_{yk}}{L_{xj} L_{yj}}} = \sqrt{\frac{S_k}{S_j}}$$

Multilayer model for the 1-st horizontal mode:

$$\frac{d\overline{u_j}}{dt} = -\frac{\pi g}{2 L_{xj} \rho_j} \sum_{k=1}^{N} \rho_{\min(j,k)} \, a_{kj} \, \Delta_x h'_k + l\overline{v_j},$$

$$\frac{d\overline{v_j}}{dt} = -\frac{\pi g}{2 L_{yj} \rho_j} \sum_{k=1}^{N} \rho_{\min(j,k)} \, b_{kj} \, \Delta_y h'_k - l\overline{u_j},$$

$$\frac{d\Delta_x h'_j}{dt} = \frac{2\pi H_j}{L_{xj}} \overline{u_j},$$

$$\frac{d\Delta_y h'_j}{dt} = \frac{2\pi H_j}{L_{yj}} \overline{v_j}, \quad j = \overline{1, N},$$

Cpefficients a_{kj} and b_{kj} are sought from a condition of mechanical energy conservation.

Lake Iseo (Northern Italy): the site and measurements

Lake parameters

- depth: max 256 m, mean 150 m
- horizontal dimensions ≈20 km×3 km
- radiation extinction coefficient 0.33 m^{-1}

Measurements

- conventional meteorology and energy fluxes
- thermistor chains: Northern point (≈7 km N of center), Southern point (≈8.5 km S of center)

Model parameters

- 120 levels
- Simulation period: August 2011
- area-depth dependence included
- the only calibration parameter: bottom friction coefficient

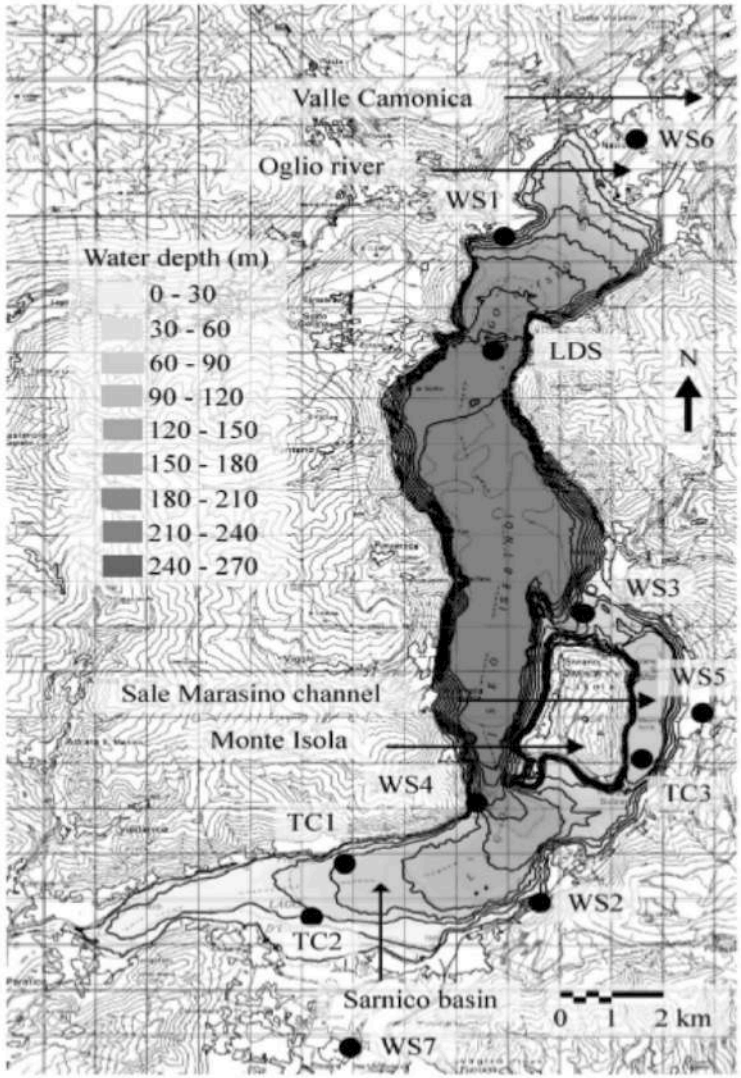

WS – weather stations, LDS – lake diagnostic system, TC – thermistor chains

Results with Iseo Lake

(Stepanenko, Valerio, Pilotti, JAMES, 2020)

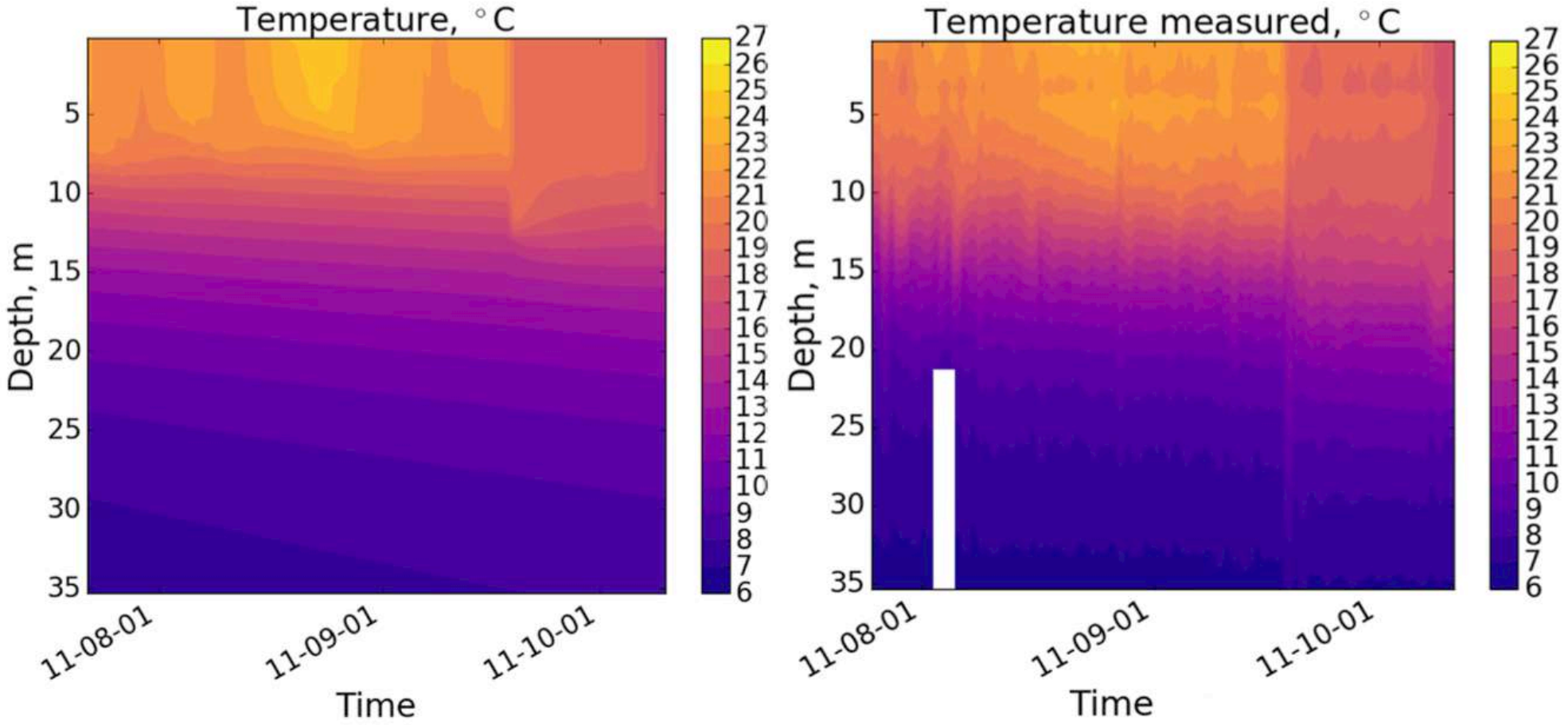

Figure 7. Temperature distribution over depth and time, modeled (left) and observed (right). Observed time series are averaged between series at LDS and TC stations. All data are smoothed by running mean with 1 day window.

Results with Iseo Lake: temperature series

(Stepanenko, Valerio, Pilotti, JAMES, 2020)

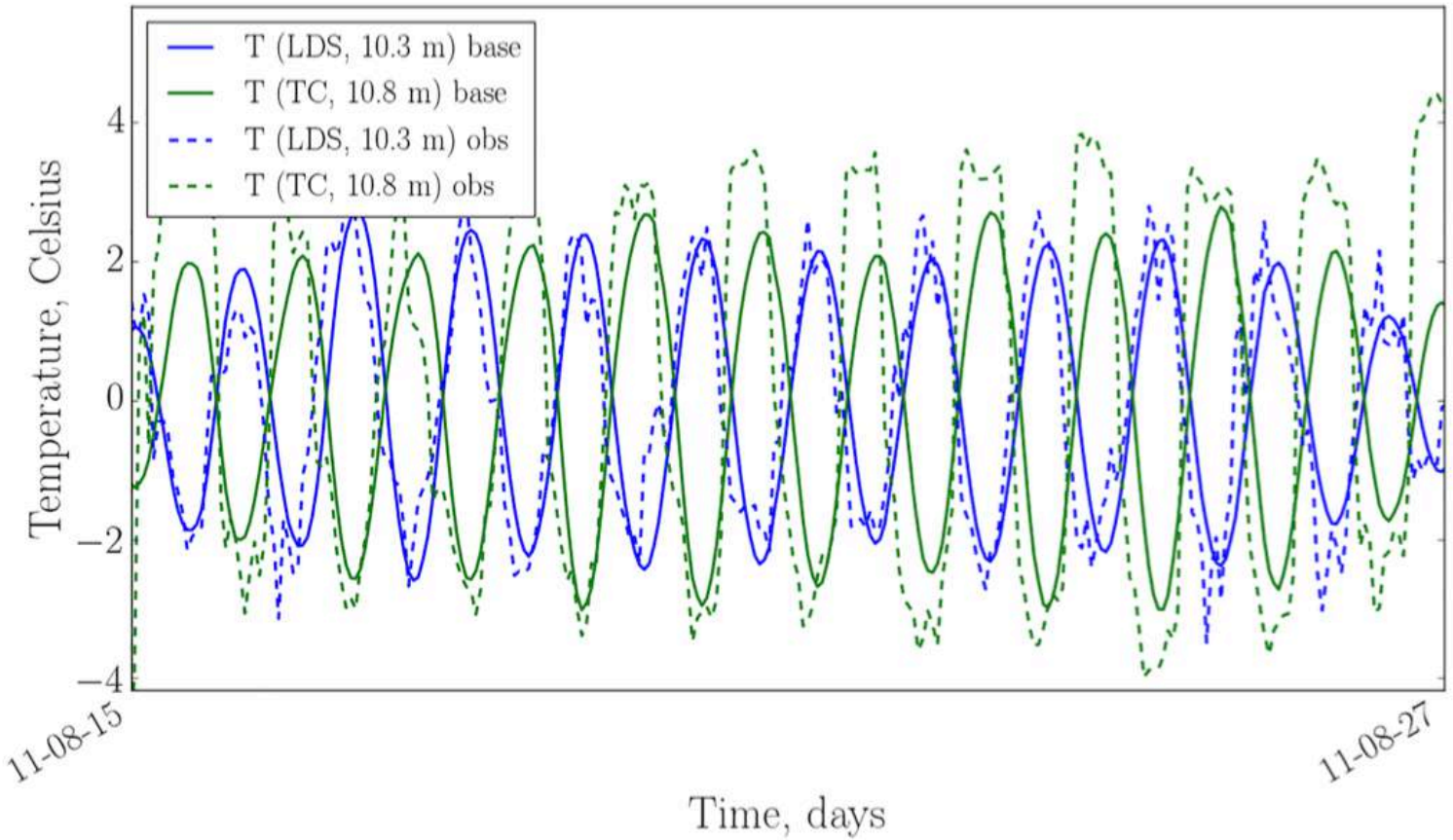

Figure 8. An excerpt of water temperature seiche oscillations T^*, measured ("obs") and simulated ("base") in TC (10.8 m) and LDS (10.3 m) locations.

Results with Iseo Lake : temperature series

(Stepanenko, Valerio, Pilotti, JAMES, 2020)

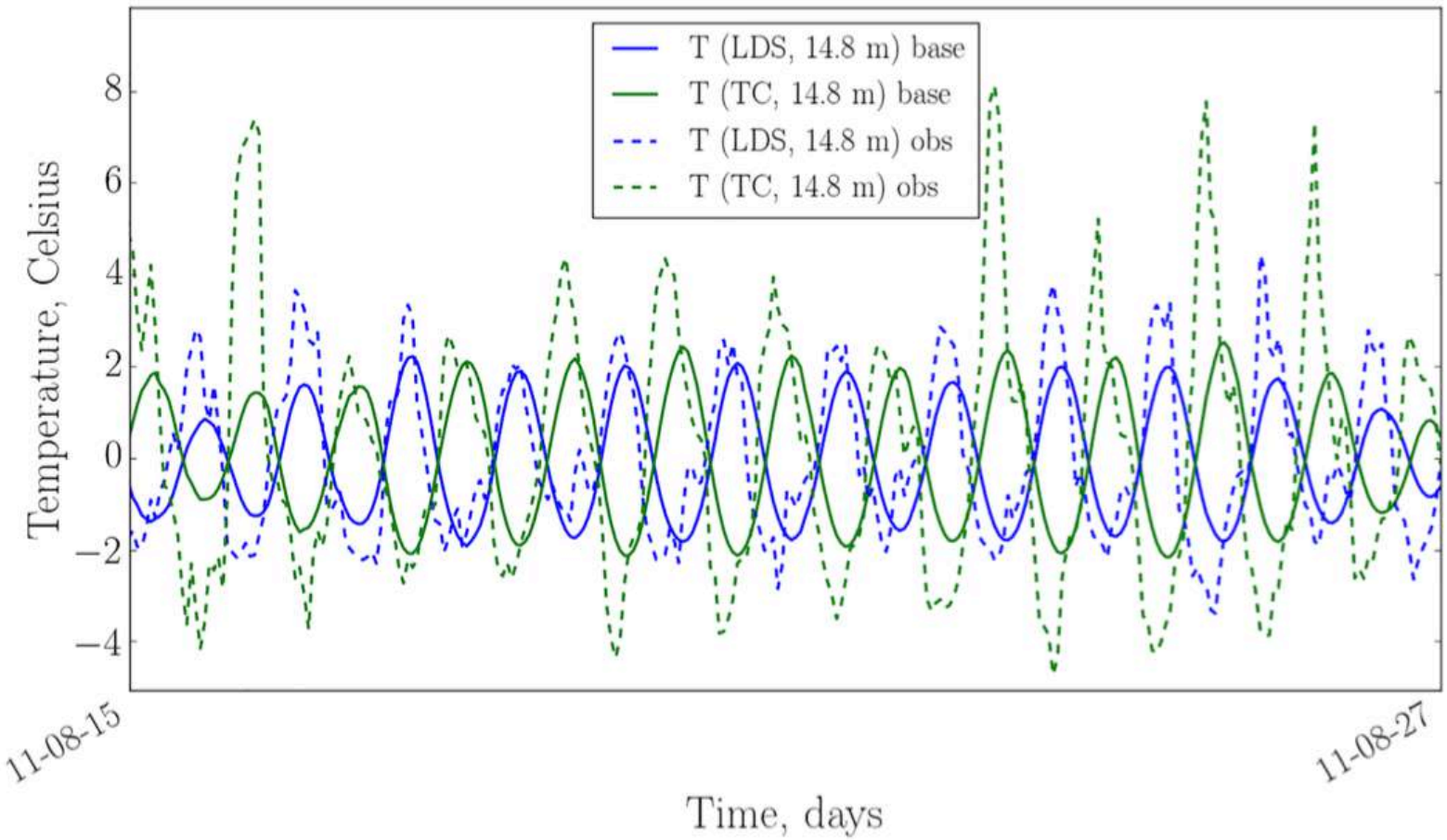

Figure 9. The same as Figure 8 but for TC (14.8 m) and LDS (14.8 m) locations.

Results with Iseo Lake : temperature series

(Stepanenko, Valerio, Pilotti, JAMES, 2020)

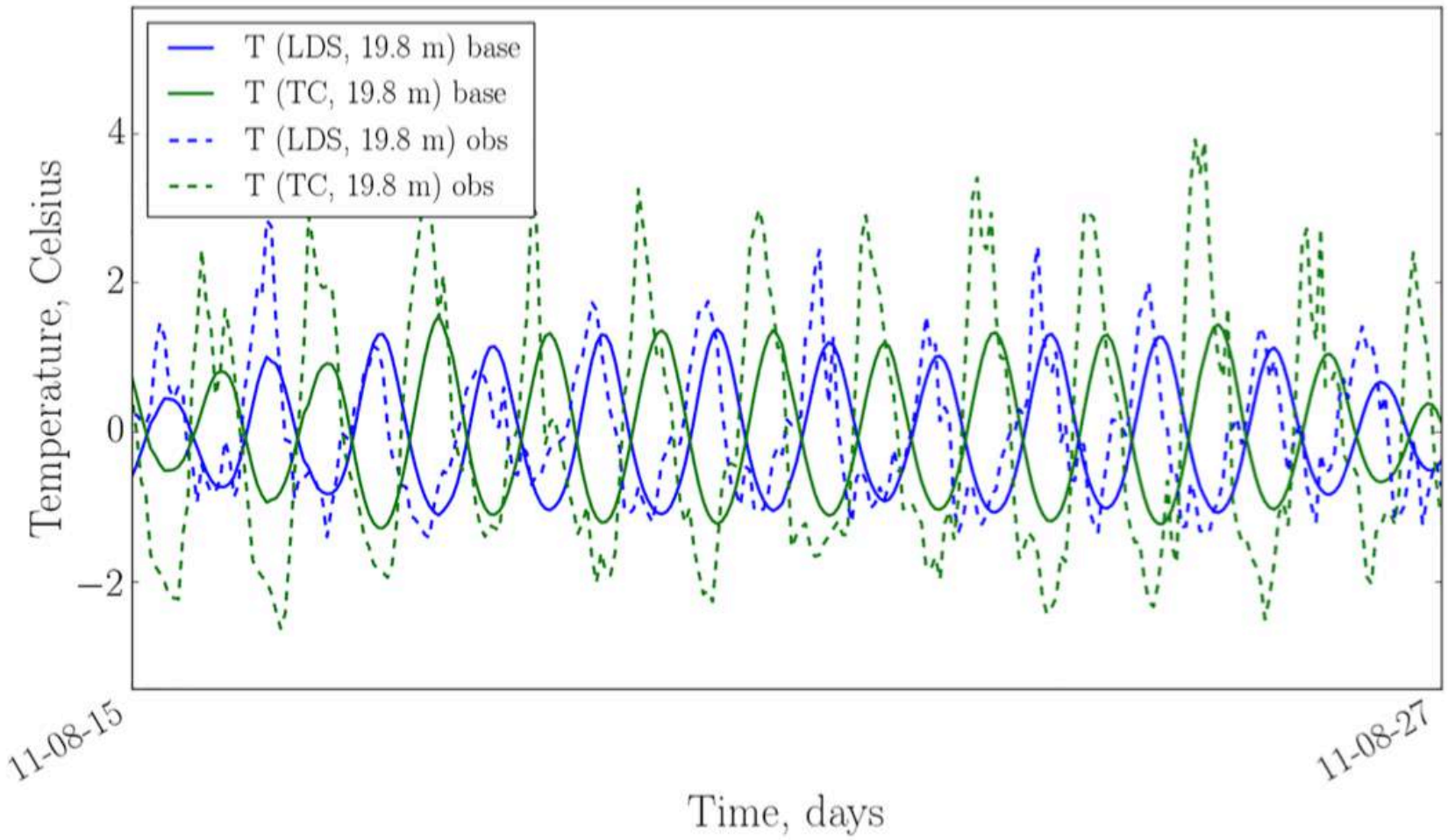

Figure 10. The same as Figure 8 but for TC (19.8 m) and LDS (19.8 m) locations.

Results with Iseo Lake: intensity of temperature fluctuations

(Stepanenko, Valerio, Pilotti, JAMES, 2020)

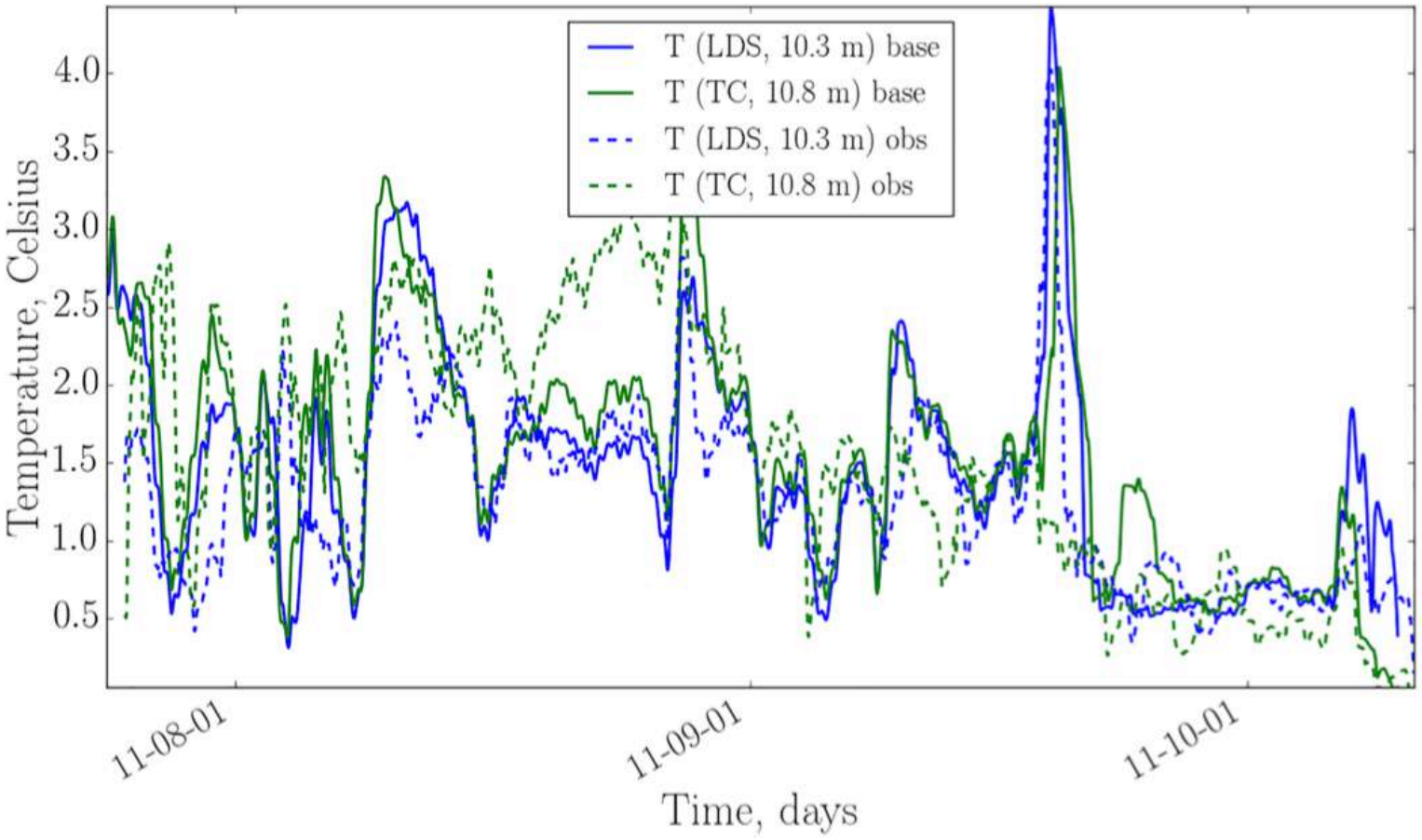

Figure 11. Running root-mean-square deviation of seiche oscillations $\sigma(T^*)$ at LDS (10.3 m) and TC (10.8 m) points for the period 25 July to 10 October 2011, measured ("obs") and modeled ("base"). The running average window is 24 hr.

Results with Iseo Lake: spectra of temperature

(Stepanenko, Valerio, Pilotti, JAMES, 2020)

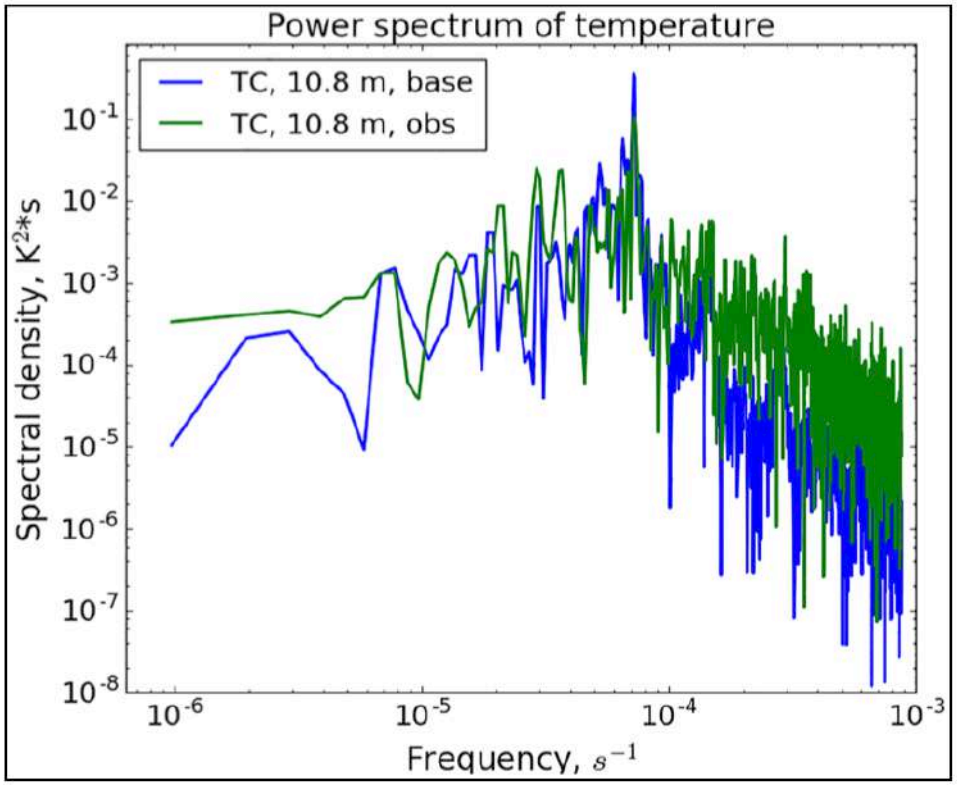

Figure 12. Fourier power spectrum of temperature at TC point (10.8 m) for the period 25 July to 10 October 2011, measured ("obs") and modeled ("base").

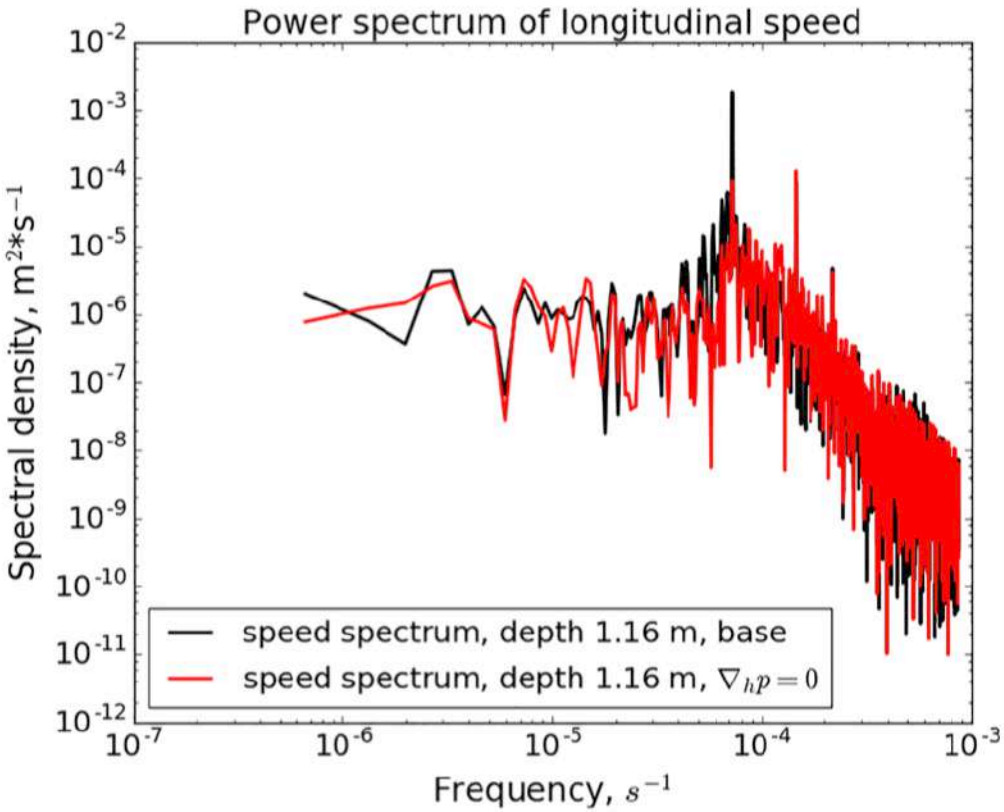

Fourier power spectrum of modeled longitudinal speed at depth 1.16 m for the period 18 June to 10 October 2011. Baseline simulation is represented by **black line**, and **red curve** presents simulation with horizontal pressure gradient parameterization switched off.

Thank you!

A list of validation sites

Lake	Thermodynamics	CH_4	CO_2	Reference
Vendyurskoe (Russia)	+	-	-	Stepanenko, 2007
Shuchi (Siberia)	-	+	-	Stepanenko et al., 2010
Kossenblatter (Germany)	+	-	-	Stepanenko et al., 2013
Valkea-Kotinen (Finland)	+	-	-	Stepanenko et al., 2014
Kuivajarvi (Finland)	+	+	+	Heiskanen et al., 2014; Stepanenko et al., 2016
Kivu (Kongo)	+	-	-	Thiery et al., 2014
Seida (Russia)	+	+	-	Guseva et al., 2016
Bolshoi Vilyui (Russia)	+	-	-	Stepanenko et al., 2018
Uvs Nuur (Mongolia)	+	-	-	Stepanenko et al., 2019
Alqueva (Portugal)	+	-	+	Iakunin et al., 2020
Mozhayskoe (Russia)	+	+	-	Stepanenko et al., 2020a
Suva (Japan)	+	+	-	-
Iseo (Italy)	+	-	-	Stepanenko et al., 2020b

LAKE model website

LAKE model

http://tesla.parallel.ru/Viktor/LAKE/-/wikis/LAKE-model

LAKE is an extended one-dimensional model of thermodynamic, hydrodynamic and biogeochemical processes in the water basin and the bottom sediments (Stepanenko and Lykosov 2005, Stepanenko et al. 2011). The model simulates vertical heat transfer taking into account the penetration of short-wave radiation in water layers (Heiskanen et al., 2015), ice, snow and bottom sediments. The model allows for the evolution of ice layer at the bottom after complete lake freezing in winter. The equations of the model are formulated in terms of quantities averaged over the horizontal section a water body, which leads to an explicit account of the exchange of momentum, heat, and dissolved gases between water and the inclined bottom. In the water column, $k-\epsilon$ parametrization of turbulence is applied. The equations of motion take into account the barotropic (Stepanenko et al., 2016) and baroclinic pressure gradient (Степаненко, 2018). In ice and snow, a coupled transport of heat and liquid water is reproduced (Volodina et al. 2000; Stepanenko et al., 2019). In bottom sediments, water phase changes are simulated. The model also describes vertical diffusion of dissolved gases (CO_2, CH_4, O_2), as well as their bubble transfer, methane oxidation, photosynthesis and processes of oxygen consumption. Parameterization of methane production in sediments is included (Stepanenko et al. 2011), and for the case of thermokarst lakes, an original formulation for the methane production near the lower boundary of "talik" is implemented. Model was tested in respect to thermal and ice regime at a number reservoirs in contrasting climate conditions, specifically, within the LakeMIP project (Lake Model Intercomparison Project, Stepanenko et al., 2010; Stepanenko et al., 2013; Stepanenko et al., 2014; Thiery et al., 2014).

The current **version** of the model is 2.3

The complete **model archive** with sample input data:

- LAKE2.0.zip
- LAKE2.1.zip (salinity dynamics in ice cover is added)
- LAKE2.2.zip (input/output of control point added, minor bugs fixed)
- LAKE2.3.zip (commit `7d016e79` in gitlab repository, which is updated by testing at GNU Fortran 9.3.0 compiler; the model is adapted to simulate artificial reservoirs with high throughflow and water level variations; a model configuration for simulating the vertical structure of river flow is added)
- LAKE2.4.zip (commit `f29fb387` in repository; bugs related to $k-\epsilon$ model fixed, new b.c. options for $k-\epsilon$, Cuette-Poiseuille flow setup and turbulence closure added, methane production parameters are set specific for each sediment column, new output options)

The role of bubbles trapped in sediments

Hypothesis: presence of bubbles in sediments significantly affects total CH_4 emission to atmosphere, because gaseous diffusivity 4 orders large than aqueous one.

The general aqueous and gaseous diffusion equation reduces to:

$$\frac{\partial \theta_g^{n+1}}{\partial z} + \tilde{S} + (z + z_1)\tilde{r}_{eb}(\theta_{g,cr} - \theta_g) = 0,$$

which is solved semi-analytically.

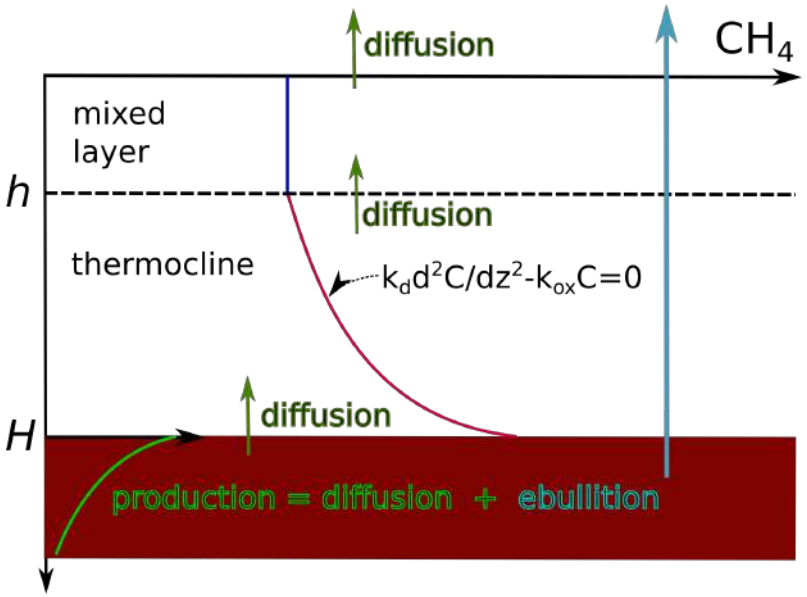

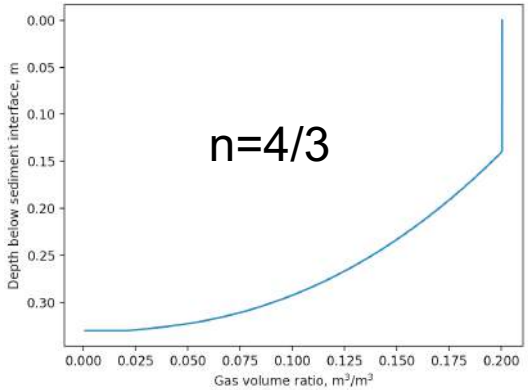

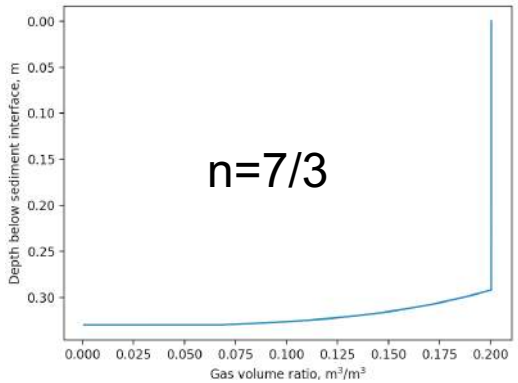

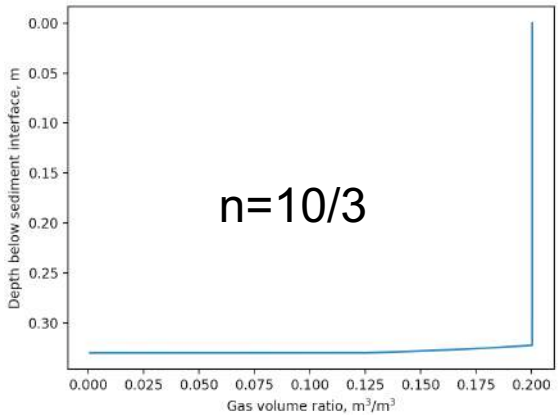

Production	1.08*10^{-6} mol/(m^2*s)	1.08*10^{-6} mol/(m^2*s)	1.08*10^{-6} mol/(m^2*s)
Diffusion	**6.25*10^{-7}**	1.25*10^{-7}	2.51*10^{-8}
Ebullition	4.58*10^{-7}	**9.59*10^{-7}**	**1.05*10^{-6}**

Проект с РусГидро

“Измерение выбросов парниковых газов и оценка поглощающей способности гидроэнергетических объектов”

Задачи исследования:

3.3.1. Проведение измерений выбросов парниковых газов с поверхности водохранилищ ГЭС.

3.3.2. Разработка методики и **математических моделей баланса парниковых газов водохранилищ**;

3.3.3. Придание разработанной методике статуса **национальной методики Российской Федерации**.

Lake Model Intercomparison Experiment

- The motivation is realistic parameterization of lakes in NWP and climate models
- 1D thermodynamic lake models are ran in the unified setup, forced by on-lake measured meteorology
- Focus on simulation of temperature and heat fluxes (Kossenblatter Lake, Valkea-Kotinen Lake, Lake Kivu, ...)
- Ongoing experiment: Harp Lake, focus on gas exchange (CO_2, O_2)

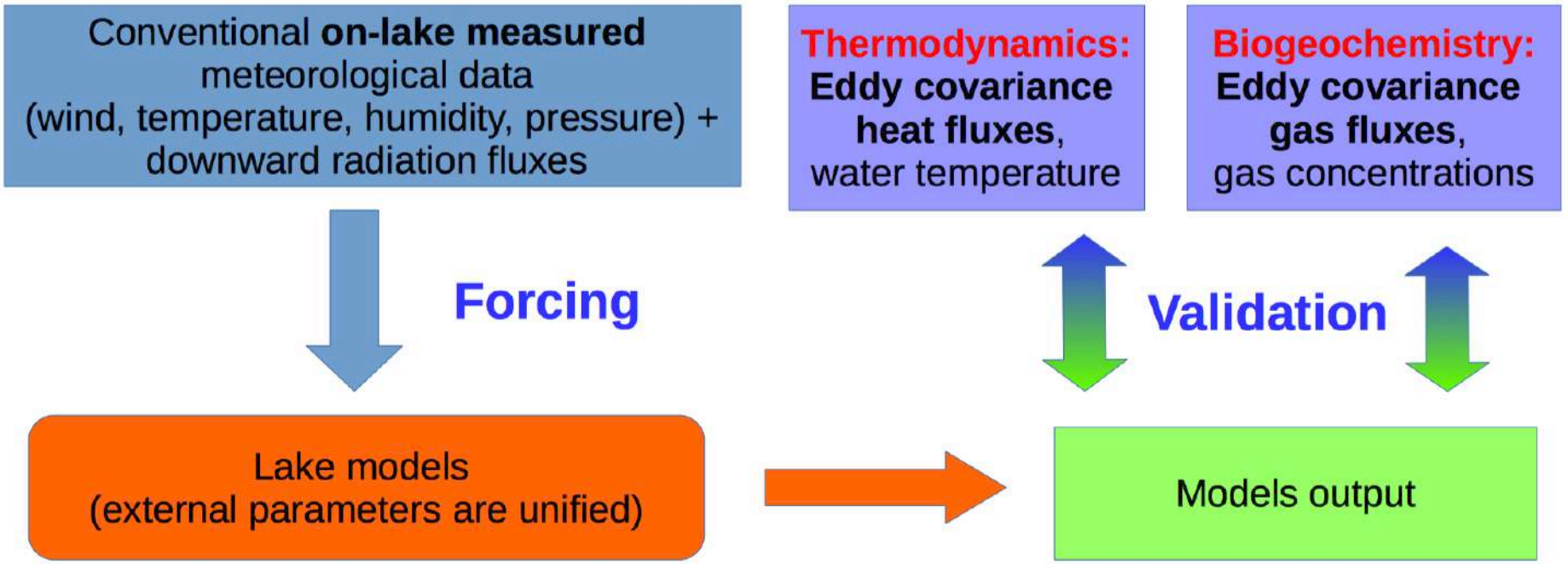

Participating models

ALBM	(Tan et al., 2015)	*CLM4 – LISSS*	(Subin et al., 2012)
LAKE	(Stepanenko et al., 2016)	*FLake*	(Mironov et al., 2008)
LAKEoneD	(Jöhnk et al., 2008)	*Simstrat*	(Goudsmit et al., 2002)
MyLAKE	(Saloranta et al., 2007)	*Hostetler*	(Hostetler et al., 1993)
GLM	(Read et al., 2014)	*MINLAKE2012*	(Fang et al., 2014)
SIWAS	(Wang et al., 2016)	Модель ИВП СО РАН	(Зиновьев, 2014)
DYRESM	(Tanentzap et al., 2007)	StoLAM	(Strauss et al., 2009)
CSLM	(Guerrero et al., 2017)	Lake Erie 1D model	(Rucinski et al., 2010)
PROBE	(Omstedt et al., 2011)		

- -- k-epsilon models
- -- Henderson-Sellers models
- -- models based on TKE balance in the mixed layer
- -- integral (1/2 dimensional) models